CORA Cork Open Research Archive
Cartlann Taighde Oscailte Chorcaí

Title	Nonlinear water wave models with vorticity
Authors	Kluczek, Mateusz
Publication date	2019
Original Citation	Kluczek, M. 2019. Nonlinear water wave models with vorticity. PhD Thesis, University College Cork.
Type of publication	Doctoral thesis
Rights	© 2019, Mateusz Kluczek. - http://creativecommons.org/licenses/by-nc-nd/3.0/
Download date	2026-11-17 08:23:09
Item downloaded from	https://hdl.handle.net/10468/8576

UCC
University College Cork, Ireland
Coláiste na hOllscoile Corcaigh

Nonlinear Water Wave Models with Vorticity

Mateusz Kluczek
MSc
115224100

Thesis submitted for the degree of Doctor of Philosophy



NATIONAL UNIVERSITY OF IRELAND, CORK

Department of Applied Mathematics

September 2019

Head of Department: Prof. Sebastian Wieczorek

Supervisor: Dr David Henry

Research supported by the Science Foundation Ireland (SFI)
research grant 13/CDA/2117.

Contents

Acknowledgments **V**

Abstract **VII**

Introduction **IX**

Equatorial water waves with underlying currents in the f-plane approximation
Mateusz Kluczek,
Applicable Analysis, 97:1867—1880, 2018. **1**

Exact and explicit internal equatorial water waves with underlying currents
Mateusz Kluczek,
Journal of Mathematical Fluid Mechanics, 19:305—314, 2017. **17**

Mean flow properties for equatorially-trapped internal water wave-current interactions
Adrián Rodríguez-Sanjurjo and Mateusz Kluczek,
Applicable Analysis, 96:2333—2345, 2017. **31**

Exact Pollard-like internal water waves
Mateusz Kluczek,
Journal of Nonlinear Mathematical Physics, 26:1–14, 2019. **47**

Physical flow properties for Pollard-like internal water waves
Mateusz Kluczek,
Journal of Mathematical Physics, 59:1–12, 2018. **61**

Nonhydrostatic Pollard-like internal geophysical waves
Mateusz Kluczek,
Discrete & Continuous Dynamical Systems - Series A, 39:5171–5183, 2019. **77**

Dispersion relations for fixed mean-depth flows with two discontinuities in vorticity
Mateusz Kluczek and Calin-Iulian Martin,
Journal of Nonlinear Analysis, 181:62–86, 2019. **91**

Conclusion **121**

Bibliography **123**

I, Mateusz Kluczek, certify that this thesis is my own work and has not been submitted for another degree at University College Cork or elsewhere. All external references and sources are clearly acknowledged and identified within the contents. I have read and understood the regulations of University College Cork concerning plagiarism.

Mateusz Kluczek

Acknowledgments

I would like to express my sincere gratitude to my supervisor Dr David Henry for his guidance and support during these years of my doctoral studies. I am very fortunate to benefit from his mentorship.

I want to heartily thank the Science Foundation of Ireland (SFI) for the opportunity to carry out this doctoral research through a funded PhD program. Also I would like to thanks the School of Mathematical Sciences UCC for providing a great stimulating research atmosphere. Moreover, I want to express my thanks to all of my fellow PhD and MSc students that I had the pleasure to meet in UCC.

On a personal level, I owe a debt of gratitude to my Mom for all her support. Also I would like to gratefully acknowledge support received from my sister Kasia, her husband Michał and their family.

Abstract

The results presented in this thesis consider geophysical nonlinear water waves and small-amplitude gravity waves. New exact and explicit solutions in terms of Lagrangian variables are derived to model geophysical surface and internal water waves and an analysis of small-amplitude waves from the point of view of the dispersion relation is presented. The solutions are Gerstner-like or Pollard-like in their character and prescribe three-dimensional water waves propagating in the horizontal direction. The models presented in this thesis represent various complicated and intricate scenarios which build the dynamics of the ocean. We prove using a rigorous mathematical analysis the validity of these models. In each model a dispersion relation arises as a product of the analysis indicating how the relative wave speed of the wave varies with respect to various physical parameters introduced by a particular model.

Introduction

1 State-of-the-Art

The modelling and description of water waves in general is an extremely difficult endeavour. The governing equations of fluid flow were introduced by Euler in 1757 [45] and they were among the first partial differential equations presented. The equations describe a perfect fluid where the effects of viscosity are neglected and the equations are complemented by the equation of incompressibility of the fluid. The force of gravity is taken to be the only external restoring force acting on the fluid body. The nonlinear equations in this form are complicated and intractable. Despite these difficulties arising in the prescription of the fluid flow by nonlinear partial differential equations, sinusoidal solutions were obtained for linearized Euler equations assuming small steepness of waves [14, 89]. This approach gives solutions describing characteristics of fluid as time-dependent functions for fixed point in the fluid domain. A rather different, but complementary view of the flow is given by the Lagrangian representation which describes flow characteristics as time-dependent functions tracing fixed particles [2].

It is remarkable that there exists an exact and explicit solution, given by Gerstner [136] in 1809 and rediscovered independently by Rankine [124], for the nonlinear Euler equations. The advantage of Gerstner's explicit solution is that it is described in terms of Lagrangian variables and, using a subtle transition between the Eulerian and Lagrangian description of the flow, it shows how to solve the Euler equations. The Eulerian framework has predominated the studies but recent works have shown that the Lagrangian approach is often helpful and it is motivated by the emergence of Lagrangian observing technology. Nevertheless, the Lagrangian formulation is not likely to replace the Eulerian formulation rather to complement.

Although, Gerstner's solution is remarkable, it was discarded for being rotational which means that the wave described by that solution cannot be generated by conservative forces. Despite that, Constantin [5] proved by an rigorous analysis (using an interplay of topological and analytical ideas) that the wave motion described by Gerstner's solution is dynamically possible. This precise analysis was further extended and degree-theoretical methods [54] were used to prove that the Gerstner solution describes a global diffeomorphism and the evolution of the fluid domain under the wave propagation is dynamically conceivable. The work of Constantin triggered further works on the Gerstner solution. This solution was consequently extended to describe more complicated geophysical scenarios where the rotation of Earth plays an important role, which falls into the scope of geophysical fluid dynamics. The Coriolis force introduces additional linear terms to the governing equations, and to simplify the governing equations to some extent, the models are presented in the equatorial region where the effects of Coriolis force are less pronounced. Therefore,

exact and explicit solutions were obtained for equatorially-trapped surface waves [10, 9, 80]. Subsequently, those solutions were generalised to represent water waves in presence of underlying currents [60, 65].

Geophysical fluid dynamics targets not only flows on rotating bodies but also stratified flows, which means that the change in the density of the fluid must be taken into account. As a result, new type of waves, namely internal water waves, are described by a Gerstner-like solution [12, 13, 78, 77] in the equatorial region. In this case the internal water waves represent the oscillation of a thermocline, which is a sharp interface separating two layers of fluid with different temperatures. Some physical observation shows that in the neighbourhood of the equator a strong equatorial undercurrent residues approximately at the same level as the thermocline, thus the solutions were modified to include an underlying current [78, 79].

The existence of exact and explicit solutions for such complicated geophysical scenarios is significant for oceanographical and mathematical reasons, however there was still an open question whether the derived solutions are dynamically possible and describe a valid evolution of the fluid domain. That question was answered in [129] for surface waves and in [125] for internal waves, where both of authors use degree-theoretic methods to show that the equatorially-trapped water waves are described by global diffeomorphic map. This result is very compelling as waves in the equatorial region can be described in the $f-$ or $\beta-$plane [39, 120], where $\beta-$plane captures the sphericity of the Earth and waves are three-dimensional with amplitude decaying as one moves away from the equator. Therefore, it is important to emphasize those solid results proving that such complicated solutions exist.

Together with the studies of exact and explicit solution for geophysical flow, there is a considerable body of research to prove the existence of small and large amplitude steady periodic gravity waves. In this case all the geophysical effects are neglected and inviscid Euler equations are taken into consideration, where flow is assumed to be rotational. The situation here is more complicated, and at the same time more interesting from a physical point of view, as the presence of vorticity describes wave-current interactions [7, 91, 134]. It has been already proven in [33] that small and large amplitude steady periodic water waves with a fixed-mass flux and general regular vorticity exist. It started a series of articles regarding the mathematical analysis of water waves with vorticity in terms of symmetry [15, 16, 71], regularity [18, 42, 56, 58] and the presence of stagnation points and critical layers [32, 41, 112, 119, 137].

The existence of small and large amplitude waves for fixed-mass flux is very interesting, but from the physical point of view, the more desirable situation is when the depth is fixed instead of the mass flux. This situation was addressed in [62, 61] where the flow experiences a general continuous vorticity distribution and has a specified mean-depth $d > 0$ over a flat bed. A novel reformulation of the governing equations, and local and global bifurcation theory was used in the proof. Following those studies a discontinuous distribution of vorticity was considered, which may represent layered models with separated region of flowing current. Similar to the situations above, the discontinuous vorticity was discussed in the fixed mass-flux

regime [36], subsequently being modified for the fixed mean-depth situation [69, 76]. As the vorticity is taken to be piecewise constant it describes models with a vorticity layer adjacent to the free surface [59] and with a layer adjacent to the bed [57], in the fixed mean-depth scenario, with complementary studies in the fixed mass-flux scenario [8, 36, 103, 104, 105, 111]. Piecewise constant vorticity, a particular type of which were considered, is highly relevant to the modeling of wave-current interactions as it may represent different structures of currents.

This doctoral thesis is a publication-based thesis, therefore preliminary contents prescribing the governing equations and physical models overlap to some extent in specific chapters. An extensive introduction is included in each paper taking the form of a review of relevant literature particularly in relation to recent developments and an explanation of the scope and objectives of the work. A combined bibliography is included at the end of the thesis for better readability. The last subsection of this introductory chapter presents a brief outline of the thesis.

2 Geophysical water waves

Geophysical fluid dynamics concerns large-scale flows naturally occurring on any object in the universe, but mostly focuses on flows on the Earth. The oceans and atmosphere are vital to sustain the life on Earth, thus understanding the large-scale flows driving the dynamics of both environments and their interactions is necessary. The scale of the flows is important; geophysical fluid dynamics do not take into consideration river flows or turbulence in the surface of lakes as they fall into the scope of other scientific categories. Moreover, the two physical aspects - rotation and stratification, play a major role in governing the geophysical flows. Generally speaking, geophysical fluid dynamics deals with the stratified fluids on rotating objects [39].

The ambient rotation of Earth around its axis, toward the east, introduces additional terms into the equations of motions. The two new terms are interpreted as forces in the rotating framework and they are the Coriolis force and the centrifugal force [39]. The latter force is to some extent neutralised by the gravitational forces, which results in a small change to the shape of Earth, where Earth is a slightly flattened sphere. Therefore, in the studies presented in this thesis, the centrifugal force is neglected and only the Coriolis force is of interest. The Coriolis force introduces a certain vertical rigidity to the fluid and in fast rotating fluids this effect can be so strong that the fluid moves in vertical columns retaining its vertical alignment [39]. However, this effect is only visible in laboratory experiments, since the angular speed of celestial bodies is not rapid enough and the other additional processes are involved into governing the dynamics of large-scale fluids preventing such strong and limiting behaviour of fluid (in particular the oceans and seas) on Earth.

Fluids tend to arrange themselves into layers of fluid of different densities. The gravitational force is of great importance in this case, since it is responsible for lowering the heavy fluid and rising the light. In a stable stratification the fluids consist of stacked horizontal layers of fluid. In this layout the fluid contains interfaces

separating those horizontal layers of fluid of different densities and any disturbance of this equilibrium leads to generation of internal waves describing the oscillation of the interfaces in the fluid [39, 49]. The "dead water" phenomenon is an excellent example of the internal water waves, which is briefly described here. In a stable stratified fluid without visible surface waves, a ship sailing on the surface can generate the oscillation of the interface inside the fluid. The energy consumed by the generation of the internal wave produces a drag that can be translated into resistance to the forward motion of the ship resulting in gradual decrease of the speed of ship.

This thesis is concerned with waves of wavelengths such that they are affected by the Coriolis force. Moreover, the stratification of the oceans is well-documented along with the existence of currents in the ocean [49, 135], thus it is reasonable to examine the different geophysical internal water waves models, which falls into the scope of this thesis. Therefore, a short description of this physical phenomenons is introduced in the following sections, but first the geophysical governing equations and the Gerstner solution will be introduced.

2.1 Euler equations for geophysical waves

In this section a brief discussion of the geophysical governing equations is introduced. The Euler equations, where the assumption of constant density ρ is made, take the form [1, 7, 39]

$$\frac{D\mathbf{u}}{Dt} = -\frac{1}{\rho}\nabla P + (0, 0, -g).$$

The equations are coupled with the equation for incompressibility

$$\nabla \cdot \mathbf{u} = 0,$$

and the boundary conditions

$$\begin{aligned} w = \eta_t + u\eta_x + v\eta_y \quad &\text{on} \quad z = \eta(x, y, t), \\ w = 0 \quad &\text{on} \quad z = -d, \\ P = P_{atm} \quad &\text{on} \quad z = \eta(x, y, t). \end{aligned}$$

These have to be modified in order to accommodate the distinctive features of the geophysical flows. In the equations above D/Dt is the material derivative [1], $\mathbf{u} = (u, v, w)$ is the velocity field in the directions (x, y, z), g is the gravitational acceleration, ρ is the density of water, P is the function of pressure, P_{atm} is the atmospheric pressure (constant), η is the free surface, $z = -d$ defines the bed. The main difficulty here is to include rotation into the governing equations, in contrast with the stratification, where the density is included already in the equations of motion. Then the equations have to be solved in each layer of fluid by substituting the particular density of layer in the Euler equations. The rotating reference framework of the geophysical flows is considered to be fixed at a point on the Earth's surface

(see Figure 1). A local Cartesian reference frame is set up with x, y, z pointing eastward, northward and upward respectively, with corresponding unit vectors i, j, k. In this setting the absolute acceleration is equal to

$$\frac{D\mathbf{u}}{Dt} + 2\mathbf{\Omega} \times \mathbf{u} + \mathbf{\Omega} \times (\mathbf{\Omega} \times \mathbf{r}),$$

where $\mathbf{u}$ is the velocity vector, $\mathbf{\Omega}$ is the vector rotation and $\mathbf{r}$ is the distance from the origin (cf. [39] for the derivation of the absolute acceleration in rotating systems). The second component of the absolute acceleration is the Coriolis force component, the third one is the centrifugal force component. We neglect the centrifugal component since the centrifugal force is balanced by gravity. Taking the vector of rotation on Earth

$$\mathbf{\Omega} = \Omega \cos\phi \mathbf{j} + \Omega \sin\phi \mathbf{k},$$

where Ω is the angular velocity of rotating Earth, ϕ is the latitude on the surface of Earth, the Euler equations take the form

$$\frac{D\mathbf{u}}{Dt} + 2\mathbf{\Omega} \times \mathbf{u} = -\frac{1}{\rho}\nabla P + (0, 0, -g).$$

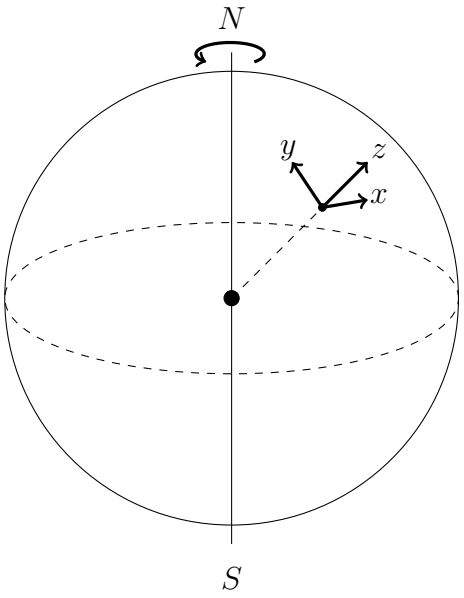


Figure 1: The rotating framework of reference fixed at a point on the Earth's surface.

The decomposition of the Euler equations into the x, y, z momentum equations gives

$$\begin{cases} u_t + uu_x + vu_y + wu_z + 2\Omega\cos\phi w - 2\Omega\sin\phi v = -\frac{1}{\rho}P_x, \\ v_t + uv_x + vv_y + wv_z + 2\Omega\sin\phi u = -\frac{1}{\rho}P_y, \\ w_t + uw_x + vw_y + ww_z + 2\Omega\cos\phi u = -\frac{1}{\rho}P_z - g. \end{cases}$$

The coefficient $f = 2\Omega \sin\phi$ is called the Coriolis parameter and $\hat{f} = 2\Omega\cos\phi$ does not have a specific name but is usually called the reciprocal parameter. In order to simplify the nonlinear geophysical Euler equations, the β- and f-plane approximation is invoked. Now approximate the equations around a fixed latitude ϕ_0, where $\phi = \phi_0 + y/R$ for a local framework with y pointing northward and R being the radius of Earth [39]. Expanding the functions of $\sin\phi$ and $\cos\phi$ in the Taylor series and retaining only the first two components the Coriolis parameters become

$$\begin{aligned} f &= 2\Omega\sin\phi_0 + 2\Omega\tfrac{y}{R}\cos\phi_0 = f_0 + \beta y\cos\phi_0, \\ \hat{f} &= 2\Omega\cos\phi_0 - 2\Omega\tfrac{y}{R}\sin\phi_0 = \hat{f}_0 - \beta y\sin\phi_0, \end{aligned}$$

where $\beta = 2\Omega/R = 2.28\times 10^{-11} m^{-1}s^{-1}$ [39] is the so-called "beta" parameter and this results in the $\beta-$plane approximation, whereas taking only the first component of the Taylor expansion leads to the $f-$plane approximation. In this thesis we consider the $\beta-$plane approximation close to the equator $\phi_0 = 0$ thus the Euler equations become

$$\begin{cases} u_t + uu_x + vu_y + wu_z + 2\Omega w - \beta yv = -\dfrac{1}{\rho}P_x, \\ v_t + uv_x + vv_y + wv_z + \beta yu = -\dfrac{1}{\rho}P_y, \\ w_t + uw_x + vw_y + ww_z - 2\Omega u = -\dfrac{1}{\rho}P_z - g, \end{cases}$$

and the $f-$plane Euler equations for any particular fixed latitude ϕ_0 are

$$\begin{cases} u_t + uu_x + vu_y + wu_z + \hat{f}w - fv = -\dfrac{1}{\rho}P_x, \\ v_t + uv_x + vv_y + wv_z + fu = -\dfrac{1}{\rho}P_y, \\ w_t + uw_x + vw_y + ww_z - \hat{f}u = -\dfrac{1}{\rho}P_z - g, \end{cases}$$

with

$$f = 2\Omega\sin\phi_0, \quad \hat{f} = 2\Omega\cos\phi_0,$$

being the Coriolis parameters. Those approximations capture the most dynamical effects of sphericity of Earth without the complicated geometric effects, which are not essential to describe many phenomena.

2.2 The Gerstner wave

The water wave problem has received considerable attention from the mathematical community (see [66, 84, 90] and the references within). Despite numerous research papers dealing with water waves, the subject of water waves and their aspects still has not been fully explained. However, this situation is somewhat understandable,

since water waves are described by highly nonlinear equations and the free boundary problem has to be treated carefully in the study [1].

Most models employ perturbation methods applied to the governing equations. The governing equations were replaced by approximated models, usually linear models, where the linear analysis results in sinusoidal waves [94]. Nevertheless, the justification itself of these approximations is technically and conceptually very difficult and can lead to vague results. Therefore, the solution or approach, which does not replace the full governing equations with some approximated models and captures the nonlinearity of the equations would be beneficial to the topic of water waves. This was achieved by Gerstner in [136].

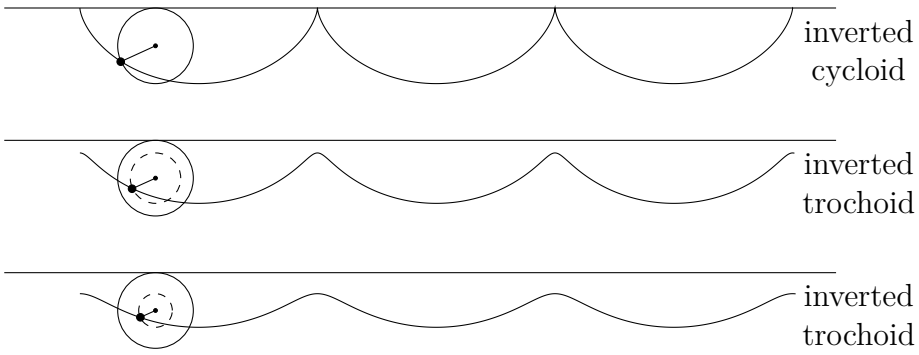


Figure 2: The shape of water waves is represented by an inverted trochoid. The extreme case of cycloid is regarded more as a mathematical curiosity than a physical representation of water waves.

The idea behind Gerstner's solution is to describe the motion of individual water particles using the Lagrangian labelling variables (cf. for a detailed explanation of the advantages of Lagrangian approach [2]).

The solution is constructed by assuming that the particles moves in circular orbits (see Figure 3). The Lagrangian position of the particle in time is given by [136]

$$\begin{cases} x = q - \dfrac{1}{k} e^{kr} \sin(k(q - ct)), \\ z = r + \dfrac{1}{k} e^{kr} \cos(k(q - ct)). \end{cases}$$

The wave passing through the fluid is taken to be a two-dimensional periodic wave travelling zonally. Therefore, the particles move only in the vertical plane XZ and its motion and flow characteristics are independent of the meridional direction Y. The parameters q, r are the Lagrangian labelling variables, the constant $k = 2\pi/L$ is the wavenumber associated with the wavelength L, t denotes the time, where the parameter c is the wave phase speed. The wave phase speed for the Gerstner wave is $c = \sqrt{g/k}$. The parameters q, r may fix the position of a particle in the equilibrium state before passing the wave. However, it cannot be confused with the initial position of the particle. Although, the solution does not deal with the generating mechanism of the wave, it is implied that the creation of wave produces

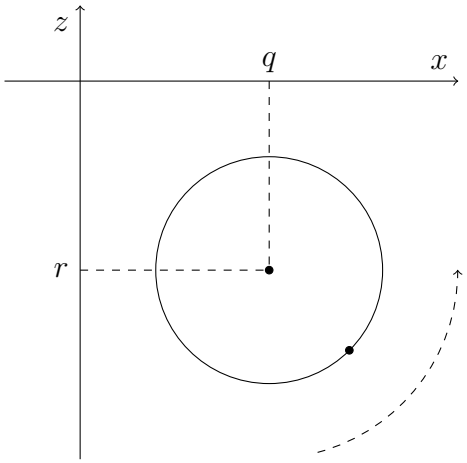


Figure 3: The sketch of the idea behind Gerstner wave and the approach of describing the motion of an individual particle in the fluid domain. The Lagrangian variables (q, r) labels the centre of the circle made by a particle moving on the circumference.

drag moving the particle from its q, r position into the circumference of the circle, where q, r denotes the centre of the circle.

The Gerstner solution captures the salient nonlinear character of the equations by describing waves with a narrow crests and wide troughs which stands in stark contrast to the sinusoidal waves obtained in the linear regime. The Lagrangian labelling variables belongs to the set $(q, r) \in \mathbb{R} \times (-\infty, r^*)$, where $r \leq r^* < 0$. When the variable r takes the value $r = 0$, the inverted trochoid becomes an inverted cycloid with upward cups and this limiting case is regarded more as a mathematical curiosity than a valid physical representation of water waves. Therefore, the Lagrangian labelling variable r has to be negative in the case of surface waves.

It has to be emphasised here that internal water waves are described by a regular trochoid and the Lagrangian labelling variables belongs to the set $(q, r) \in \mathbb{R} \times (r_0, r^*)$, where $r \geq r_0 > 0$, $r^* > r_0$ and r_0 represents the oscillating boundary inside the fluid domain (more detailed explanation of the shape of the internal water waves can be found in the following chapters concerning the models of internal waves).

The wave described by Gerstner's solution is represented by an inverted trochoid (see Figure 2). The trochoid is obtained by tracing a fixed point inside a circle rolling without slipping along a horizontal line and is represented by parametric equations

$$\begin{cases} x(\theta) = a\theta - b\sin(\theta), \\ z(\theta) = a - b\cos(\theta) \end{cases}$$

parameterised by θ, where a is the radius of the circle, b is the distance of a fixed point from the centre of the rolling circle. Tracing a point on the circumference of the circle will result in a cycloid with cusps. Moreover, tracing a point outside the circle will result in a trochoid intersecting itself which is not a realistic representation of water waves. Now introducing new parametrisation

$$\theta = kq,$$

and choosing

$$a = \frac{1}{k}, \quad b = \frac{e^{kr}}{k},$$

moreover taking a symmetry with respect to the horizontal line, the Gerstner solution is recovered by shifting in time by $\sqrt{gk}t$ the sinusoid and by $r - 1/k$ the z-coordinate.

The advantage of this solution is that it can be modified to describe very complicated and compound flows. Moreover, the Lagrangian formulation of solution permits the embedding an underlying current into the solution, which gives an opportunity to study wave-current interactions.

The Gerstner solution is given in terms of predefined labelling variables (in particular, in this thesis by mentioned (q, s, r)). Therefore, the geophysical governing equations can be reexpressed in the Lagrangian description of the flow and take the form

$$\begin{aligned}
(x_{tt} - fx_t + \hat{f}z_t)x_q + (y_{tt} + fx_t)y_q + (z_{tt} - \hat{f}x_t)z_q + P_q/\rho + gz_q = 0,\\
(x_{tt} - fy_t + \hat{f}z_t)x_s + (y_{tt} + fx_t)y_s + (z_{tt} - \hat{f}x_t)z_s + P_s/\rho + gz_s = 0,\\
(x_{tt} - fy_t + \hat{f}z_t)x_r + (y_{tt} + fx_t)y_r + (z_{tt} - \hat{f}x_t)z_r + P_r/\rho + gz_r = 0,
\end{aligned}$$

with the incompressibility condition being expressed as the Jacobi determinant

$$\frac{d}{dt}\left|\frac{\partial(x, y, z)}{\partial(q, s, r)}\right| = 0,$$

for particle labels $q, s,$ and r and positions $x(q, s, r, t), y(q, s, r, t)$ and $z(q, s, r, t)$, respectively. A subtle transition between the two description of the flow is introduced now. In the Eulerian description of the flow the fluid properties are described as functions of fixed position and time t, i.e. the velocity $\mathbf{U}(\mathbf{X}, t)$, where the vector $\mathbf{X}$ is the Eulerian position. As mentioned above, in the Lagrangian description the particles are labelled by some labelling variables (in the cases here (q, s, r)) which results in functions describing the properties of fluid as functions of fixed particles and time t, i.e. the position $\mathbf{x}((q, s, r), t)$. Given those two descriptions, they are linked by the relation [2, 1]

$$\mathbf{U}(\mathbf{x}((q, s, r), t), t) = \frac{\partial \mathbf{x}}{\partial t}((q, s, r), t).$$

Gerstner's solution is rotational, which means in terms of the wave motion that it cannot be generated by the conservative forces. However, recent laboratory experiments prove that such waves cannot be excluded in the description of the water waves

[117, 140]. The generation of the Gerstner wave has not been discussed yet, as the wave is strongly vortical, therefore there is a need to reconcile the different formalism (Lagrangian and Eulerian). Nevertheless, the solution captures the salient character of the nonlinear governing equations by obtaining waves with profiles significantly different to the sinusoidal profiles in the linear theory. Moreover, Gerstner's solution describes waves with the amplitude decreasing exponentially with the depth.

This exact solution was treated more as a curiosity than a result of practical importance. This situation changed when a rigorous mathematical analysis of the Gerstner solution was employed using mixture of topological and analytical methods [5], subsequently also theoretical degree methods were used [54], showing that it is possible to have a motion of the whole fluid body where all particles describe circles with a radius being dependent on the depth and in this general case the meridional distance from the equator. Besides the mathematical aspects, it should be mentioned that also the computer gaming industry influenced a recent interest in this solution by showing that copies of the Gerstner analytical formulation may be used to generate a realistic visualisation of water waves. The remarkable advantage of the Gerstner solution is that it can be modified to describe complicated and compound geophysical water wave models, which is the subject of this thesis. In the following chapters Gerstner's solution is adapted and modified to describe various physical models. It is showed that three-dimensional and internal water waves can be represented by an exact and explicit Gerstner-like solution.

2.3 Currents

The next physical features, that are equally important in driving the dynamics of the oceans and seas, are currents [49, 135]. On Earth two types of currents can be distinguished: the surface currents, which are mostly wind-generated, and the undercurrents. Both types of currents have a very important influence on the Earth's climate, temperature and biological productivity. The surface currents are located in the uppermost 400m of the ocean's surface. Part of the energy generated by the wind acting on the ocean's surface is transferred by the waves to the water by friction. The drag induced by the wind cause mass of water to flow and to form a surface current. As the mass of water starts to move the Coriolis force intervenes and deflects the path of motion of water to the right in the Norther Hemisphere and to the left in the Southern Hemisphere. The direction of the surface currents is also affected by the basin topography and continents surrounding the oceans, which acts as natural boundaries diverting the current's flow [135].

In the equatorial region the surface currents are almost directly beneath the trade winds, which is a situation slightly different to the one encountered in the mid-latitude regions. In the mid-latitude regions the Coriolis force causes the current to turn and the resulting motion of surface water creates the Ekman spiral in which the vertically-averaged transport is perpendicular to the wind stress. This shows that it is unwise to apply equatorial models to the mid-latitude regions and vice versa. Moreover, in the equatorial regions the surface currents are paired with countercurrents, which flow in the opposite direction from the main current and do

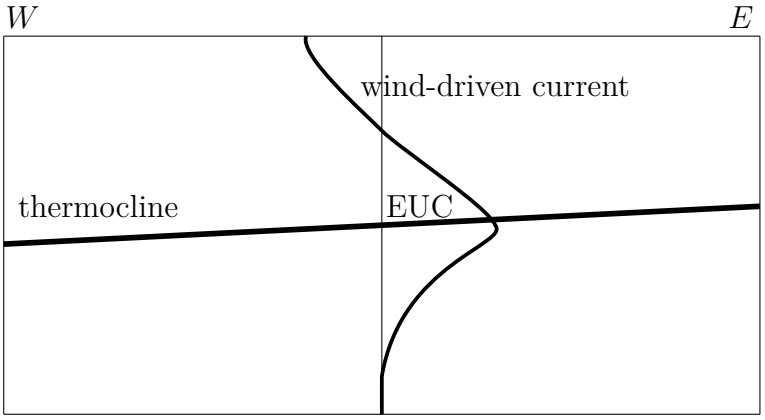


Figure 4: The sketch of the structure of currents in the equatorial Pacific region. In the shallow water layer there is an westward current and beneath the current there is a countercurrent called the Equatorial Undercurrent and its core resides on the thermocline. The depth of the thermocline in the equatorial region decreases in the eastward direction as the result of downwelling and upwelling of water [27, 49].

not necessarily have to be on the surface [49].

The most pronounced currents in the vicinity of the equator in the Pacific Ocean are the North and South Equatorial Currents directed to the west with a return flow governed by the North Equatorial Counter-Current. However, a major part of the return flow is carried by the subsurface current discovered by Cromwell in 1951 [38] and referred as the Equatorial Undercurrent (EUC). Undercurrents have since been discovered under most major currents. They can be vary large and sometimes might approach the volume of the current above them. Nevertheless, the dynamic of the oceans is very complex and varies between oceans. A good example is the equatorial region of the Indian Ocean, where a series of weak but still pronounced alternating jets expanding from the thermocline to nearly the ocean bed was discovered [102]. The structure of oceanic currents is very complicated and compound; the EUC and Antarctic Circumpolar Current (ACC) can be considered to illustrate the complex structure of currents (see Figure 4). The EUC resides approximately at the depth of 100-240m and spans 300km about the Equator in the Pacific Ocean [23]. It is an eastward jet which can be represented in the models as region with constant positive vorticity. The current dies out rapidly with the depths. Moreover, above the EUC in the regions adjacent to the surface there is an eastward wind driven current, which can be described by constant negative vorticity. Another fascinating example is the ACC, which is not a single flow but is composed of a number of jets reaching even the seafloor [26]. The jets are high-speed and surround Antarctica in a closed system of currents parallel to the edge of Antarctica. Therefore, here the ACC can be modelled with vorticity being different but constant in time for different regions with respect to the depth. All those facts supports the idea of constructing mathematical models representing surface as well and internal water waves in the presence of mean background underlying currents.

2.4 Thermoclines and pycnoclines

Density in the ocean depends on salinity, pressure and temperature [49]. Density is defined as the mass per unit volume, where salinity is the amount of salt dissolved in a body of fluid (technically it is dimensionless quantity) [49]. Temperature and salinity shares an inverse relationship, and salinity and density a positive relationship. When one of this quantities changes rapidly, this region is refereed to as a cline (temperature - thermocline, density - pycnocline, salinity - halocline). Following that, the ocean can be divided into three density zones. The surface zone or mixed zone heated by the sun with relatively constant temperature and density, where this steady and uniform state is supported by the actions of currents and waves. The thermocline is a zone where the temperature is rapidly decreasing with depth and hence this results in the change of the density of the water, being more accurate, the density of water starts to increase with depth. We can say that the thermocline separates the layers of ocean water of different densities [39, 49, 135] as the change of density indicates change of temperature and vice versa. Finally, there is the deep zone below the thermocline with constant temperature and water more dense than the water in the surface layer. Therefore, the thermocline is situated at the same level as the pycnocline, and coincide with it. Pycnocline is the correct term for an interface separating layers of fluid of different densities but those two names in terms of the models presented in this thesis can be used interchangeably as they both separate regions of constant density and temperature. However, this difference should be acknowledged to avoid semantic confusion.

The stratification of the ocean water makes the water columns very stable and prevents the mixing of surface and deep water since it is possible only when the density of surface water is similar to the density of deep water. The thermocline is not identical in form in all areas or latitudes. Considering the equatorial cross-section of the thermocline in the Pacific Ocean it is gradually rising toward the eastern edge of ocean at a rate of about 1m over one degree of longitude [27, 47] (see Figure 4). In addition, the surface temperature is proportional to the available sunlight. Therefore, the surface layer is thicker in the tropics and the tropical thermocline is deeper than the thermocline at higher latitudes, because the ocean is heated to the greater depth. Moreover, the polar waters are not stratified by temperature since they receive relatively little solar energy [49]. Generally, the polar surface waters are as cold as the deep water. An important role in the temperature profile of the polar water plays the Antarctic Circumpolar Current, which minimizes salinity differences and the thermocline does not have favourable conditions to exist there [26, 49].

The uneven depth of the thermocline is also driven by the two following effects of wind and diffusion [135]. The strength of wind influences the depth of thermocline because the wind-stress curl forces water to downwell and meet upwelling colder abyssal water. In contrast to the effects caused by the wind, the diffusivity exert an impact on the thickness of the thermocline. Moreover, during the seasons the surface water experiences the seasonal thermocline superimposing the permanent thermocline.

In summary, the thermocline depends on many physical factors. The depth of

the thermocline increases with the latitude moving away from the equator to the tropical zone and then gradually decreases to finally disappear as the polar regions are reached [49, 135]. Therefore, the permanent thermocline is primarily a mid- and low-latitude phenomenon considered at latitudes 66°33′46.9" N − 66°33′46.9 S and it confirms the need of solution in spirit of Gerstner for the internal water waves, which is applicable at all latitudes.

The thermocline is a phenomenon which is very complicated in physical terms, thus a mathematical consideration of the thermocline as the boundary is complicated as on this interface the change of the fluid properties is very abrupt. Across the thermocline density and temperature change their value very quickly with respect to depth, however in the models provided in this thesis a simplified assumption is considered where the density is piecewise constant and at the thermocline there is a sudden jump in the density and the equation of state in this case is omitted. Therefore, a discontinuity of the density is allowed, however it is small and in the overall context of the velocity profile is unimportant. It has to be emphasised that close to the thermocline there is a region of high shear and strong stratification. Therefore, the velocity field is continuous in the normal direction at the thermocline, on the other hand it can be or even is discontinuous in the tangential direction. The thermocline in these models simply provides kinematic and dynamic conditions that are appropriate across any interface in the body of fluid. The kinematic boundary condition ensures that the thermocline is an interface and particles are confined to it

$$w = \eta_t + u\eta_x + v\eta_y \quad \text{on} \quad z = \eta(x, y, t),$$

with η being the profile of the thermocline. On the other hand the dynamic boundary condition expresses the balance of the forces at this internal boundary and is expressed by an unambiguous statement that the pressure is continuous across the thermocline

$$P(x, y, z, t) \quad \text{is continuous on} \quad z = \eta(x, y, t).$$

The assumption of a hydrostatic still water layer under the thermocline is a rather strong assumption in this context. It represents a complex model whereby a nonlinear exact internal geophysical wave solution can be constructed at mid latitudes. It is hoped that future work may result in an exact solution for a more physically realistic nonhydrostatic layered model (as exists for internal equatorial waves in [13]), yet this situation promises to be more complex mathematically due to the fact that flows are not considered to be purely equatorial. Nevertheless, it appears that the simplified models presented in the thesis manage to capture the salient geophysical features of flows.

3 Outline of thesis

In the first chapter a new explicit solution is derived in the Lagrangian formulation describing surface water waves. The model is presented in a narrow equatorial strip,

where the Coriolis force is less pronounced, therefore the f-plane approximation of the geophysical governing equations might be employed [120, 135] and the equations become more tractable but are still nonlinear. Although we work with approximate equations, the model is complicated since we allow for a zonal constant underlying current and variable meridional current representing an intricate physical scenario which is a generalisation of model presented in [65]. The solution represents in this case weakly three-dimensional waves, which can propagate eastward or westward. This result is very interesting from the viewpoint of the geophysical dynamics in the equatorial region [9, 47] as this region is dominated by the existence of eastward-propagating waves. Therefore, the freedom in the direction of propagation of the waves is regarded as a consequence of the f-plane approximation. Remarkably the dispersion relation can be derived describing the exact wave speed which is independent of the meridional current but is dependent on a zonal current and the Coriolis force. The chapter is concluded with the examination of the mean flow physical properties, where the currents play a major role in the evaluation of the mean velocities and mass transport.

In the second chapter a nonhydrostatic model is introduced accommodating the stratification of the equatorial region [39, 47] represented by the existence of a thermocline in the ocean. The thermocline is an interface separating two layers of a fluid of different densities [49]. Moreover, this model incorporates a transitional layer, which is responsible for a transition from a wave motion region to an abyssal deep-water region. In addition to that a constant underlying current in the direction of wave propagation is admitted in the model. The work done here derives a generalised solution for model presented in [13] and allows for a zonal underlying current. A new solution constructed in this chapter represents internal water waves describing the weakly three-dimensional oscillation of the thermocline in the presence of a constant underlying current. The governing equations are prescribed in the β-plane approximation which allow to consider a wider equatorial band than in the f-plane and it captures the sphericity of this region. Unfortunately, this draws consequences and the Coriolis terms vary linearly in space introducing latitudinally-dependent terms in the governing equations. The construction of the solution is troublesome as we consider equatorially-trapped waves, which means that the amplitude of the waves diminishes as we move away from the equator. In addition to that the amplitude of waves decreases as well as we ascend above the thermocline. The decaying factor in the meridional direction is dictated by the β-plane approximation and must be derived as a part of the solution. Moreover, the pressure and the velocity field have to be continuous across each interface in the fluid body. Therefore, this model represents a far more complicated scenario both mathematically and physically than the one presented in the first chapter. The dispersion relation derived for this complicated model is a quadratic equation, however only one solution describing eastward-propagating equatorially-trapped waves is valid and satisfies the physical characteristic of waves.

Both of the solutions presented in the first and second chapter are Gerstner-like, which means that the Gerstner solution can be recovered by neglecting the various additional physical characteristic like currents and the Coriolis force. In order to

complete this section of the thesis, the third chapter is concerned with an analysis of the mean flow velocities and the mass transport for the β-plane model presented in the second chapter along lines [75]. The description of the mean flow physical properties in this model is challenging since the flow is equatorially-trapped, three-dimensional and incorporates an underlying zonal current. All of this physical aspects cause difficulties in determining the mean Eulerian velocities and mass transport. Regardless the complexity of the model, the advantage is that the explicit solution is represented in terms of Lagrangian variables and it allows to present the flow properties without any approximations, which is of great interest from both mathematical and physical perspectives.

The three next chapters are concerned with new Pollard-like exact and explicit solutions for internal water waves. In contrast to the previous solutions, the Pollard-like solutions derived here are fully three-dimensional and non-equatorial. The three-dimensional character of the solutions is a ramification of the effects of the Earth's rotation at an arbitrary latitude and water particles experience a cross-wave tilt to their orbital motion. The models that are presented in this section are the first attempt in description of internal water waves by a Pollard-like solution [121]. In the governing equations the Coriolis force cannot be neglected since we want to prescribe a solution at any fixed latitude, however we employ the f-plane approximation and by working in the close neighbourhood of an arbitrary latitude the Coriolis parameters become constant and the Coriolis acceleration introduced in the equations is no more latitudinally-dependent. In the fourth chapter the aim is to work with a hydrostatic model in order to derive a solution for internal water waves, the model in this context might take a rather strong physical assumptions, however it still represents a complex model whereby a nonlinear geophysical wave solution can be constructed and still captures salient geophysical features of the flow. The dispersion relation is identified in this model and it takes the form of a fourth order polynomial after a non-dimensional change of variables which stands in a stark contrast to the dispersion relations in the equatorial models dealing with quadratic equations. One mode of water waves is obtained as a solution of the polynomial, which is an intriguing fact given the order of the polynomial.

Following the work done in the first section of the thesis, the physical flow properties are presented also for the Pollard-like internal water wave solution as it was similarly presented in [75, 128]. The case of Pollard-like solution is vastly more complex and technical mathematically due to the fact that the flow is not considered to be purely equatorial. Therefore, the physical flow properties and mass transport are presented as three-dimensional vectors. As this model do not include underlying currents we prove that the net mass transport is zero over a wave period. However, there exist a hallmark of an underlying current expressed as the Stokes drift but it is balanced by the Eulerian mean velocity. Subsequently, this model is extended to a nonhydrostatic model in the next chapter.

In contrast to the nonhydrostatic model presented in the second chapter, the model presented in the sixth chapter is described in the f-plane approximation, where the advantage of constant Coriolis parameters is taken into account and it represents a generalisation of models in [13, 127]. Although the f-plane is considered, we show

that the Coriolis parameters have a great influence not only on the cross-wave tilt of the motion of particles but also on the form of the interfaces in the fluid and new fascinating results are obtained. In this model the dispersion relation becomes a polynomial equation of sixth order. The increase in the order of the polynomial is caused by the introduction of a transitional layer in the model. Two types of wave modes arise as a solution of the polynomial representing the dispersion relation. The first fast mode is a standard gravity water wave very slightly modified by the Earth's rotation and the second one slow mode is a nonlinear phenomenon, which is not captured by the linear theory. This second mode is proposed to be called an inertial Gerstner wave as it describes almost inertial circles. This chapter completes the study of exact and explicit solutions derived for various models of the dynamics in the ocean.

The final chapter aims to mathematically analyse a dispersion relation for small-amplitude two-dimensional steady periodic gravity water waves with fixed mean-depth and discontinuous vorticity, which in extensive way complements the works done for the fixed mass-flux scenario [33, 36] as well some work in fixed mean-depth scenario [62, 61, 76]. From the physical point of view, the scenario in which the mean-depth is fixed is more desirable. In this model an isolated layer of constant non-zero vorticity is introduced and the geophysical effects are neglected. This discontinuity of vorticity can be illustrated physically as a layer of a strong underlying current, which does not extend to the surface or to the bed of the ocean. The presence of vorticity highly complicates the mathematical description, however it is extremely interesting from the physical point of view since it describes the wave-current interactions. Piecewise constant vorticity is highly relevant to the modeling of wave-current interactions as it gives an opportunity to represent different types and models of currents [103, 104, 105, 105]. A novel reformulation of the governing equations is used to prove the existence of small-amplitude waves which are prescribed as perturbations of a laminar flow. The problem considered here is made to be equivalent to the existence of a unique solution of a dispersion relation. We show that the dispersion relation in the fixed mean-depth approach coincides with the one from the fixed mass flux [104] and it suggests that the differences in the two frameworks are manifest primarily in larger amplitude waves. Since the small-amplitude waves are considered as a perturbation of a laminar solution, a stability analysis of the laminar flow solutions is presented based on a variational formulation [31].

Equatorial water waves with underlying currents in the f-plane approximation

Mateusz Kluczek

Applicable Analysis, 97:1867–1880, 2018.

Abstract We present an exact solution to the governing equations for equatorial geophysical water waves which admits a constant underlying zonal current and a variable meridional current in the f-plane approximation. The solution is three-dimensional, nonlinear and explicit in the Lagrangian formulation. We provide an analysis of the mean flow velocities and the related mass transport.

1 Introduction

The aim of this paper is to present an exact and explicit solution in terms of Lagrangian labelling variables for the geophysical water waves problem. We study the existence of water waves in the presence of a constant underlying zonal current and a variable meridional current. The model we examine represents three-dimensional, nonlinear water waves. We construct our solution in a region within 2° from the equator which allows us to adopt the f-plane approximation of the governing equations [39, 120, 135]. Previous investigations show that by means of the f-plane approximation a variable meridional current can be admitted [63, 65] for the exact and explicit solutions representing both surface and internal water waves. The aim of this paper is to develop [63] further to present a new solution for waves admitting an additional constant zonal current in a fully three-dimensional setting. The solution represents a free surface wave travelling either eastward or westward, exposing one of the differences between the f-plane and β-plane approximations. We consider the three-dimensional model, although the f-plane approximation is closer to the two-dimensional wave motion near the equator than the β-plane approximation. This approach is caused by a variable latitudinally-independent meridional velocity of water particle, which represents a transverse equatorial current. Another distinctive feature in contrast to the β-plane setting is that the waves are not equatorially-trapped – the amplitude of waves does not diminish with increasing distance from the equator. Despite the fact that the solution does not prescribe equatorially-trapped waves, it is valid for restricted latitudes where the f-plane approximation is justified.

Our solution generalises the famous Gerstner solution [5, 136, 54]. Recently, a variety

of exact and explicit Gerstner-like solutions were derived and analysed in various papers for the nonlinear equatorial flows [5, 9, 19, 25, 64, 68, 67, 77, 106, 108, 115]. The Gerstner solution can be modified to describe the edge-waves propagating over a sloping bed [4, 81, 114, 132] and the internal waves generated by an oscillation of the thermocline [12, 13, 63, 68, 77]. However, the advantage of this paper is that it models wave motion in the f-plane approximation, which does not impose restrictions on the magnitude of current and direction of waves. On the contrary, the β-plane setting together with the assumption of diminishing amplitude of waves with increasing distance from the equator force on us eastward propagation of waves and the solution is valid only for restricted values of the current. This restriction on the magnitude of admissible currents was rectified in [64] where one modifies the β-plane model to incorporate centripetal force terms.

The presence of strong currents in the equatorial Pacific region is well documented [39, 135]. Large scale currents such as the Equatorial Undercurrent (EUC) and the wave-current interactions play a major role in the dynamics of the equatorial region [23, 27, 39, 47, 87]. The incorporation of a constant underlying mean zonal current for geophysical Gerstner-like waves was achieved in [60] and this solution was subsequently subjected to a stability analysis and an examination of physical characteristics such as mean flow velocities in [50, 75]. Interesting is the fact that the constant underlying current can be admitted also to the internal water waves model in β-plane [95] and in f-plane [127] setting with the internal wave-current interactions being examined in [128] for the β-plane approximation. Furthermore, it has been proved using degree-theoretic methods that the three-dimensional nonlinear water wave and internal wave solutions are dynamically possible [125, 129]. The precise research carried out on the mean flow properties for surface and internal water waves [75, 128] highlights the importance of currents in a geophysical flow. Following the same path we present in this paper the mean flow properties which are intriguing in their character due to them being three-dimensional. It is hoped that the physical complexity of our solution will broaden the knowledge of water waves having a potential for further generalisation in the geophysical flows [24].

2 Governing equations

The flow pattern we investigate is described in a rotating frame with the origin at a fixed point on the Earth's surface. Let (x, y, z) be the Cartesian coordinates representing the directions of the longitude, latitude and local vertical, respectively. The governing equations for the geophysical ocean waves [39] are the Euler equations

$$\begin{cases} u_t + uu_x + vu_y + wu_z + 2\Omega w\cos\phi - 2\Omega v\sin\phi = -\dfrac{1}{\rho}P_x, \\ v_t + uv_x + vv_y + wv_z + 2\Omega u\sin\phi = -\dfrac{1}{\rho}P_y, \\ w_t + uw_x + vw_y + ww_z - 2\Omega u\cos\phi = -\dfrac{1}{\rho}P_z - g, \end{cases}$$

coupled with the equation of mass conservation

$$\rho_t + (u \cdot \nabla)\rho + \rho(\nabla \cdot u) = 0,$$

and the resulting equation for incompressibility

$$u_x + v_y + w_z = 0. \tag{1}$$

Here t is time, ϕ represents the latitude, $g = 9.81\mathrm{m}s^{-2}$ is the constant gravitational acceleration at the Earth's surface, ρ is the water's density, and P is the pressure, while u, v and w are the respective fluid velocity components. The Earth is taken to be a sphere of a radius $R = 6371$ km, rotating with a constant rotational speed $\Omega = 7.29 \times 10^{-5}\mathrm{rad}\ s^{-1}$ round the polar axis towards the east. Under the assumption that the meridional distance to the equator is relatively small, the approximation $\sin\phi \approx \phi$ and $\cos\phi \approx 1$ can be used to the governing equations [39]. This approximation captures the dynamical effect of the Earth's sphericity and is called β-plane approximation. It approximates the Coriolis force in terms of a planar model with $\beta = 2\Omega/R = 2.28 \times 10^{-11} m^{-1}s^{-1}$ [39]. Wherefore the Euler equations reduce to

$$\begin{cases} u_t + uu_x + vu_y + wu_z + 2\Omega w - \beta yv = -\dfrac{1}{\rho}P_x, \\ v_t + uv_x + vv_y + wv_z + \beta yu = -\dfrac{1}{\rho}P_y, \\ w_t + uw_x + vw_y + ww_z - 2\Omega u = -\dfrac{1}{\rho}P_z - g. \end{cases}$$

The advantage of the β-plane approximation is that it does not contribute nonlinear terms to the Euler equations. Furthermore the variation of the Coriolis term can be ignored and the value of Coriolis parameter appropriate for a particular latitude can be used in the whole domain. In this case we obtain the f-plane approximation [39, 10, 23]. In our study of the water waves we work essentially at a constant latitude and we focus our attention to the purely equatorial waves (which means to take β=0), therefore the Euler equations take the form

$$\begin{cases} u_t + uu_x + vu_y + wu_z + 2\Omega w = -\dfrac{1}{\rho}P_x, \\ v_t + uv_x + vv_y + wv_z = -\dfrac{1}{\rho}P_y, \\ w_t + uw_x + vw_y + ww_z - 2\Omega u = -\dfrac{1}{\rho}P_z - g. \end{cases} \tag{2}$$

The set of equations (2) is coupled with the boundary conditions for the fluid on the free surface $z = \eta(x, y, t)$

$$\begin{aligned} &w = \eta_t + u\eta_x + v\eta_y \text{ on } z = \eta(x, y, t), \\ &P = P_0 \text{ on } z = \eta(x, y, t), \end{aligned} \tag{3}$$

where P_0 is the constant atmospheric pressure. We note that the boundary kinematic condition means that there is no flux of particles on a macroscopic scale, and so a particle initially on the boundary will remain on the boundary for all time. Moreover, we impose that the fluid domain is infinitely deep and the flow approaches a variable meridional current and an uniform zonal current rapidly with depth, that is

$$(u, v, w) \to (-c_0, \psi, 0) \text{ as } z \to -\infty.$$

3 Exact solution

This section presents an exact solution of (2), which represents waves travelling in the zonal direction at a constant speed of propagation c, in the presence of a constant zonal underlying current of strength c_0 and a variable meridional current ψ. The depiction of the three-dimensional flow examined in this paper is presented in Figure 1. It is convenient to use the Lagrangian framework for the description of the flow [2]. The Lagrangian positions (x, y, z) of the fluid particles are given as functions of the labelling variables (q, r, s) and time t by

$$\begin{cases} x = q - c_0 t - \dfrac{1}{k} e^{kr} \sin[k(q - ct)], \\ y = s + \psi(q, r)t, \\ z = r + \dfrac{1}{k} e^{kr} \cos[k(q - ct)]. \end{cases} \tag{4}$$

We show that (4) is exactly the solution of (2) and (3). The parameter $k = 2\pi/L$ is the wavenumber corresponding to the wavelength $L > 0$, while c is the phase speed of wave determined by the dispersion relation (10). The dispersion relation will be derived later on. The parameter q covers the real line. The labelling variable r belongs to the interval $(-\infty, r_0)$, where $r_0 < 0$ represents the streamline for the free surface $z = \eta(x, y, t)$. By its nature, the solution is valid for restricted latitudes of 2° from the equator corresponding to $s \in [-s_0, s_0]$, although the solution (4) in f-plane is not equatorially-trapped in contrast to the β-plane solution in absence of meridional velocity $\psi = 0$. We construct the solution for the geophysical waves which amplitude is diminishing with depth. We note that in (4), the x component of the particle position incorporate a constant underlying current c_0, which expands the model from [65]. Furthermore, in contrast to the model presented in [60], our solution assumes that the particles can move in the meridional direction. The current term $\psi(q, r)$ represents latitudinally-independent meridional velocity of fluid. We consider ψ to be a smooth function of the variables q, r. The resulting flow (4) is three-dimensional if $\psi \neq 0$, which distinguishes it from the purely two-dimensional flow in β-plane approximation. In Figure 2 we present the sketch of the flow for $\psi = 0$ which particularises to the two-dimensional flow.

We introduce here a brief discussion on the trajectories of the particle paths. The vorticity plays a key role in the particle paths. In general the assumption of irrotational flow ensures that the particle paths are open loops. In flows with zero

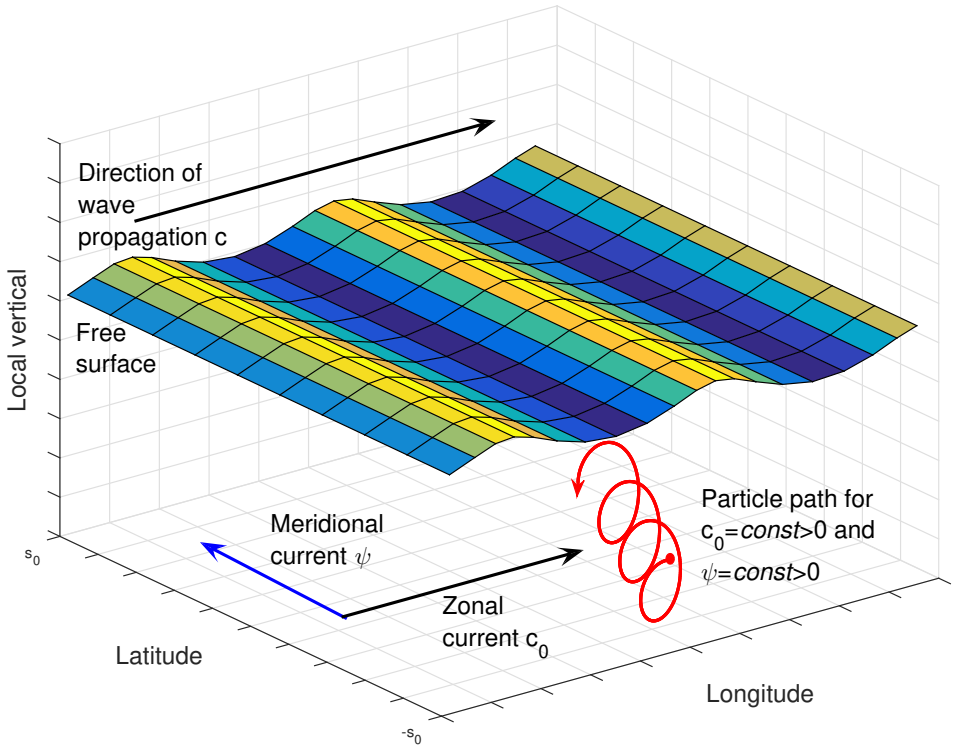


Figure 1: 3-D model. The picture presents the three-dimensional model of the geophysical water waves propagating in the presence of a zonal and a meridional current. The figure presents eastward moving waves $c > 0$ admitting the constant positive underlying current $c_0 > 0$ and the constant positive meridional current $\psi(q, r) = const > 0$. The path of the water particle is represented as clockwise, three-dimensional spiral.

vorticity, such like Stokes wave, the closed particle path is encountered very rarely. If the closed path appears in the irrotational Stokes wave it is at isolated and specific depths [6, 55]. For Gerstner-like rotational flows in the absence of a constant underlying current $c_0 = 0$ the free surface is an inverted trochoid [5, 7, 9, 54] and furthermore, if the meridional current disappears that is, $\psi = 0$, the particle trajectories take the form of closed circles. For the waves travelling eastward the circles made by particle are clockwise and for westward-propagating waves they are counterclockwise. In the contrast to the deep water waves, in the flow with sloping bed the particle paths are closed ellipses instead of closed circles [4, 132]. From Gerstner-like rotational flows we can distinguish the one with a constant underlying current. We prove later on in section 3.1 that indeed the flow described by (4) has non-zero vorticity. In the presence of a constant underlying current and absence of meridional current in the Gerstner-like rotational flow the particle path becomes a more or less stretched trochoid or inverted trochoid (see Figure 2). The fact that the particle path is common (or inverted) trochoid depends on the direction of wave propagation and the direction of a constant underlying current. If we expand the model by transverse equatorial current the particle path becomes intractable to de-

scription, because of the variable character of transverse equatorial current. We note that the appearance of currents takes a simple form in the Lagrangian setting, but mathematically and physically it highly complicates the properties of the underlying flow (cf.[75, 128]).

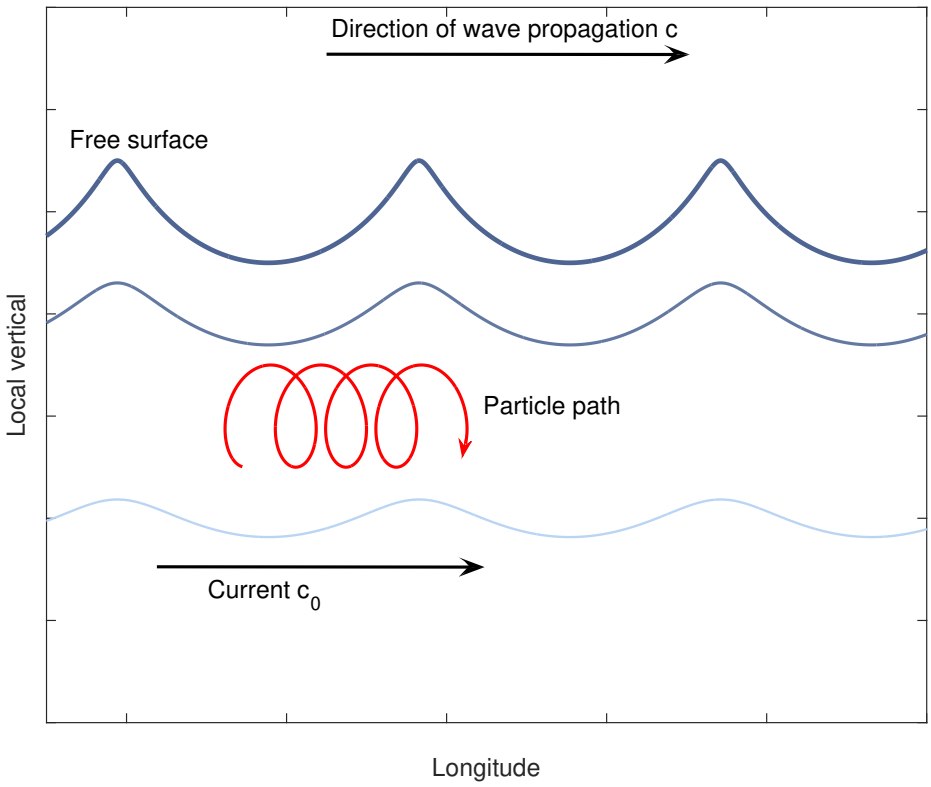


Figure 2: 2-D model. The figure presents the two-dimensional model of waves propagating eastward $c > 0$ in the presence of a constant underlying current $c_0 > 0$, where we assume that the meridional current vanishes $\psi = 0$. The particles move only in the vertical and horizontal direction. For eastward-propagating wave and in the presence of a constant positive zonal current the path of marked fluid particles is a clockwise trochoid. The amplitude of the waves diminishes with depth.

For notational convenience, we set

$$\xi = kr, \quad \theta = k(q - ct).$$

The Jacobian matrix of the map relating the particle positions to the Lagrangian labelling variables is given by

$$\begin{pmatrix} \frac{\partial x}{\partial q} & \frac{\partial y}{\partial q} & \frac{\partial z}{\partial q} \\ \frac{\partial x}{\partial s} & \frac{\partial y}{\partial s} & \frac{\partial z}{\partial s} \\ \frac{\partial x}{\partial r} & \frac{\partial y}{\partial r} & \frac{\partial z}{\partial r} \end{pmatrix} = \begin{pmatrix} 1 - e^{\xi}\cos\theta & \psi_q(q,r)t & -e^{\xi}\sin\theta \\ 0 & 1 & 0 \\ -e^{\xi}\sin\theta & \psi_r(q,r)t & 1 + e^{\xi}\cos\theta \end{pmatrix}. \tag{5}$$

The determinant of (5) is time-independent quantity $1 - e^{2\xi}$. Since $r \leq r_0 < 0$, the determinant is non-zero, thereby the flow is volume preserving and the condition of incompressibility (1) holds in the Eulerian setting. We can rewrite the governing equation (2) in the form

$$\begin{cases} \frac{Du}{Dt} + 2\Omega w = -\frac{1}{\rho} P_x, \\ \frac{Dv}{Dt} = -\frac{1}{\rho} P_y, \\ \frac{Dw}{Dt} - 2\Omega u = -\frac{1}{\rho} P_z - g, \end{cases} \tag{6}$$

where D/Dt is the material derivative. The direct differentiation of the system of coordinates in (4) gives us the velocity of the fluid particle

$$\begin{cases} u = \frac{Dx}{Dt} = ce^{\xi} \cos\theta - c_0, \\ v = \frac{Dy}{Dt} = \psi(q, r), \\ w = \frac{Dz}{Dt} = ce^{\xi} \sin\theta, \end{cases} \tag{7}$$

and the acceleration

$$\begin{cases} \frac{Du}{Dt} = c^2 e^{\xi} \sin\theta, \\ \frac{Dv}{Dt} = 0, \\ \frac{Dw}{Dt} = -kc^2 e^{\xi} \cos\theta. \end{cases}$$

The form of velocity (7) clearly states that the explicit solution (4) comprehends a wave-like term in zonal direction modified by the presence of an underlying current c_0. Due to all above statements, we can write (6) as

$$\begin{aligned} P_x &= -\rho \left[kc^2 + 2\Omega c \right] e^{\xi} \sin\theta, \\ P_y &= 0, \\ P_z &= -\rho \left[-(kc^2 + 2\Omega c) e^{\xi} \cos\theta + 2\Omega c_0 + g \right]. \end{aligned}$$

Since

$$\begin{pmatrix} P_q \\ P_s \\ P_r \end{pmatrix} = \begin{pmatrix} \frac{\partial x}{\partial q} & \frac{\partial y}{\partial q} & \frac{\partial z}{\partial q} \\ \frac{\partial x}{\partial s} & \frac{\partial y}{\partial s} & \frac{\partial z}{\partial s} \\ \frac{\partial x}{\partial r} & \frac{\partial y}{\partial r} & \frac{\partial z}{\partial r} \end{pmatrix} \cdot \begin{pmatrix} P_x \\ P_y \\ P_z \end{pmatrix},$$

we have

$$\begin{aligned} P_q &= -\rho \left[kc^2 + 2\Omega c - 2\Omega c_0 - g \right] e^{\xi} \sin\theta, \\ P_s &= 0, \\ P_r &= -\rho \left[-\left(kc^2 + 2\Omega c \right) e^{2\xi} - \left(kc^2 + 2\Omega c - 2\Omega c_0 - g \right) e^{\xi} \cos\theta + 2\Omega c_0 + g \right]. \end{aligned} \tag{8}$$

Now, the gradient of the expression

$$\tilde{P} = \rho\frac{kc^2 + 2\Omega c - 2\Omega c_0 - g}{k}e^{\xi}\cos\theta + \rho\frac{kc^2 + 2\Omega c}{2k}e^{2\xi} - \rho(2\Omega c_0 + g)r + P_0, \quad (9)$$

with respect to the labelling variables is precisely the right-hand side of (8). The function of pressure must be time independent on the surface, hence we need to eliminate the terms containing time t. Thereby, we take

$$kc^2 + 2\Omega c - 2\Omega c_0 - g = 0.$$

Solving the quadratic for c leads us directly to the dispersion relation

$$c = \frac{\pm\sqrt{\Omega^2 + k(2\Omega c_0 + g)} - \Omega}{k}. \quad (10)$$

This plus or minus choice is not allowed in the β-plane [9, 60] where we must choose $c > 0$ and we obtain eastward-propagating waves. Taking the minus sign in (10) we get a phase speed of wave propagating westward. On the other hand, taking the plus we obtain waves propagating eastward. Furthermore, to avoid a complex solution and moreover, to avoid $c = 0$ in the case of eastward-propagating wave, which is physically implausible, we consider $c_0 \geq -\frac{g}{2\Omega}$. The freedom in the phase speed and hence in the eastward or westward direction of the wave is a consequence of the f-plane approximation. We note that the underlying current c_0 affects the dispersion relation, while interesting is that the transverse current term $\psi(q, r)$ does not appear in the dispersion relation. The last step in our study is to match the pressure (9) and (3) at the surface. Whereby, the pressure (9) takes the form

$$P(q, s, r) = \rho\left(2\Omega c_0 + g\right)\left(\frac{e^{2\xi}}{2k} - r\right) + P_0 - \rho\left(2\Omega c_0 + g\right)\left(\frac{e^{2kr_0}}{2k} - r_0\right).$$

Therefore, the flow determined by (4) satisfies the governing equations (2) and (3) proving the validity of the solution.

3.1 Vorticity

The reason why we investigate vorticity is because it has a major influence on the path of the water particles, which is discussed in section 3. We calculate the vorticity ω of flow prescribed by (4). According to the definition the vorticity is

$$\omega = \nabla \times u = [w_y - v_z, u_z - w_x, v_x - u_y]. \quad (11)$$

The explicit form of the Jacobian (5) easily yields the inverse

$$\begin{pmatrix} \frac{\partial q}{\partial x} & \frac{\partial s}{\partial x} & \frac{\partial r}{\partial x} \\ \frac{\partial q}{\partial y} & \frac{\partial s}{\partial y} & \frac{\partial r}{\partial y} \\ \frac{\partial q}{\partial z} & \frac{\partial s}{\partial z} & \frac{\partial r}{\partial z} \end{pmatrix} =$$
$$= \frac{1}{1-e^{2\xi}} \begin{pmatrix} 1+e^{\xi}\cos\theta & -t\left(\psi_q\left(1+e^{\xi}\cos\theta\right)+\psi_r e^{\xi}\sin\theta\right) & e^{\xi}\sin\theta \\ 0 & 1-e^{2\xi} & 0 \\ e^{\xi}\sin\theta & -t\left(\psi_r\left(1-e^{\xi}\cos\theta\right)+\psi_q e^{\xi}\sin\theta\right) & 1-e^{\xi}\cos\theta \end{pmatrix}.$$

Thereby, we can find the derivative of the velocity of the flow with respect to the position variables (x, y, z)

$$\begin{pmatrix} \frac{\partial u}{\partial x} & \frac{\partial v}{\partial x} & \frac{\partial w}{\partial x} \\ \frac{\partial u}{\partial y} & \frac{\partial v}{\partial y} & \frac{\partial w}{\partial y} \\ \frac{\partial u}{\partial z} & \frac{\partial v}{\partial z} & \frac{\partial w}{\partial z} \end{pmatrix} = \begin{pmatrix} \frac{\partial q}{\partial x} & \frac{\partial s}{\partial x} & \frac{\partial r}{\partial x} \\ \frac{\partial q}{\partial y} & \frac{\partial s}{\partial y} & \frac{\partial r}{\partial y} \\ \frac{\partial q}{\partial z} & \frac{\partial s}{\partial z} & \frac{\partial r}{\partial z} \end{pmatrix} \cdot \begin{pmatrix} \frac{\partial u}{\partial q} & \frac{\partial v}{\partial q} & \frac{\partial w}{\partial q} \\ \frac{\partial u}{\partial s} & \frac{\partial v}{\partial s} & \frac{\partial w}{\partial s} \\ \frac{\partial u}{\partial r} & \frac{\partial v}{\partial r} & \frac{\partial w}{\partial r} \end{pmatrix} =$$
$$= \frac{1}{1-e^{2\xi}} \begin{pmatrix} 1+e^{\xi}\cos\theta & -t\left(\psi_q\left(1+e^{\xi}\cos\theta\right)+\psi_r e^{\xi}\sin\theta\right) & e^{\xi}\sin\theta \\ 0 & 1-e^{2\xi} & 0 \\ e^{\xi}\sin\theta & -t\left(\psi_r\left(1-e^{\xi}\cos\theta\right)+\psi_q e^{\xi}\sin\theta\right) & 1-e^{\xi}\cos\theta \end{pmatrix}$$
$$\times \begin{pmatrix} -kce^{\xi}\sin\theta & \psi_q(q,r) & kce^{\xi}\cos\theta \\ 0 & 0 & 0 \\ kce^{\xi}\cos\theta & \psi_r(q,r) & kce^{\xi}\sin\theta \end{pmatrix} =$$
$$= \frac{1}{1-e^{2\xi}} \begin{pmatrix} -kce^{\xi}\sin\theta & \psi_q\left(1+e^{\xi}\cos\theta\right)+\psi_r e^{\xi}\sin\theta & kce^{\xi}\left(\cos\theta+e^{\xi}\right) \\ 0 & 0 & 0 \\ kce^{\xi}\left(\cos\theta-e^{\xi}\right) & \psi_q e^{\xi}\sin\theta+\psi_r\left(1-e^{\xi}\cos\theta\right) & kce^{\xi}\cos\theta \end{pmatrix}.$$

Hence, the vorticity (11) is

$$\omega = \frac{1}{1-e^{2\xi}}\left[-\psi_q e^{\xi}\sin\theta-\psi_r\left(1-e^{\xi}\cos\theta\right), -2kce^{2\xi}, \psi_q\left(1+e^{\xi}\cos\theta\right)+\psi_r e^{\xi}\sin\theta\right].$$

We note that the vorticity matches that of [65] since the underlying current is constant. We can clearly see that the constant zonal current does not affect the vorticity in contrast to the additional meridional current. If we consider the additional current ψ to be non-constant and dependent on the variables q, r, then the vorticity is three-dimensional and time-dependent (the term θ will not disappear). If we assume that the current in the latitudinal direction is constant $\psi \equiv const$ or vanishes $\psi \equiv 0$, then the flow is still rotational, because the second term in the vorticity does not vanish. Thereupon, the flow described by (4) is rotational for all the time. Hence, the particle paths are closed circles as is the case for Gerstner's wave [5, 9, 55].

4 Flow properties

We conclude the paper with a discussion on the mean flow properties. In this section we analyse the mean Lagrangian and Eulerian velocity of the flow with respect to

the constant underlying current c_0 and the variable meridional current ψ. We also present the Stokes drift $\mathbf{U}^S$, which can be seen as a difference between the mean Lagrangian $\langle \mathbf{u} \rangle_L$ and Eulerian $\langle \mathbf{u} \rangle_E$ velocities [100, 101]

$$\mathbf{U}^S = \langle \mathbf{u} \rangle_L - \langle \mathbf{u} \rangle_E , \tag{12}$$

where $\mathbf{u} = (u, v, w)$ is a vector with the components u in the longitudinal direction, v in the latitudinal direction and w in the vertical direction. Although this emphasises that we deal with three-dimensional motion, we will focus our attention on the first two components of the mean velocities and Stokes drift.

4.1 Mean Lagrangian velocity

The Lagrangian approach indicates the velocity, as a function of time, for each individual fluid element. In our case we will consider the mean Lagrangian velocity $\langle \mathbf{u} \rangle_L = (\langle u \rangle_L , \langle v \rangle_L)$ in the longitudinal $\langle u \rangle_L$ and in the latitudinal $\langle v \rangle_L$ direction. From the exact solution (4) we were able to calculate the velocity of the particle, which now can be used to find the mean velocity. Taking the average of the velocity over a wave period $T = \frac{L}{c}$ for the zonal velocity we get

$$\begin{aligned} \langle u \rangle_L &= \frac{1}{T} \int_0^T u(q - ct, s, r) dt = \frac{1}{T} \int_0^T \left(-c_0 + c e^{\xi} \cos\theta \right) dt \\ &= \frac{-c_0}{T} \int_0^T dt + \frac{c e^{\xi}}{T} \int_0^T \cos[k(q - ct)] dt = -c_0, \end{aligned}$$

and respectively for the meridional velocity we get

$$\langle v \rangle_L = \frac{1}{T} \int_0^T v(q - ct, s, r) \, dt = \frac{1}{T} \int_0^T \left(\psi(q, r) \right) dt = \psi(q, r).$$

Unambiguously, the mean Lagrangian velocity in the zonal direction depends on the sign of the underlying current c_0. Thus, the mean velocity can be eastward or westward. For $c_0 = 0$ it is clear that the mean velocity is zero. Similarly, the mean Lagrangian velocity in the meridional direction depends only on the additional current term $\psi(q, r)$ and for $\psi(q, r) = 0$ the mean meridional velocity is zero. Moreover, if $\psi(q, r) = 0$ then the solution particularises to the two-dimensional case in the β-plane setting [75].

4.2 Mean Eulerian velocity

The presence of a constant underlying current greatly complicate the mean Eulerian velocity $\langle \mathbf{u} \rangle_E = (\langle u \rangle_E , \langle v \rangle_E)$. The mean Eulerian velocity is computed by taking the average over a wave period of the velocity at any fixed depth beneath the wave trough. We proceed as follow, first we fix the depth beneath the wave trough $z = z_0 < z_-(s)$, where $z_-(s)$ describes the level of the wave trough. The fixed depth can be characterised by

$$z_0 = R + \frac{1}{k} e^{kR} \cos\theta, \tag{13}$$

where $r = R(q, z_0, t)$ represents a functional relationship between otherwise independent variables q, r, t. Taking the derivative of (13) with respect to q we obtain

$$R_q = \frac{e^{\xi} \sin\theta}{1 + e^{\xi} \cos\theta}.$$

From this point onward we consider the two components of the mean Eulerian velocity $\langle \mathbf{u} \rangle_E$, $\langle u \rangle_E$ in the longitudinal direction and $\langle v \rangle_E$ in the latitudinal direction. The mean Eulerian velocity $\langle u \rangle_E$ in the longitudinal direction can be computed from

$$\begin{aligned} c + \langle u \rangle_E (z_0) &= \frac{1}{T} \int_0^T [c + u(x - ct, y, z_0)] dt = \frac{1}{L} \int_0^L [c + u(x - ct, y, z_0)] dx \\ &= \frac{1}{L} \int_0^L [c + u(q - ct, z_0)] \frac{\partial x}{\partial q} dq. \end{aligned}$$

Thus, the mean zonal Eulerian velocity is

$$\langle u \rangle_E (z_0) = -\frac{c}{L} \int_0^L e^{2kR} dq - \frac{c_0}{L} \int_0^L \frac{1 - e^{2kR}}{1 + e^{kR} \cos\theta} dq.$$

The constant current c_0 significantly influence the value of the mean Eulerian flow. It is analytically highly complicated to evaluate the exact value of the mean flow. Hence, the mean zonal Eulerian velocity can be eastward or westward, because we do not have any restriction imposed on the current c_0. However, for certain cases we can deduce some characteristic of the flow. It is straightforward that for case $c_0 > 0, c > 0$ and case $c_0 \leq 0, c < 0$ we obtain the westward and eastward mean Eulerian flow respectively. Now we need to consider the opposite signs of the current and the phase speed. We use the relations

$$-1 \leq \cos\theta \leq 1 \text{ and } L \min_{q \in [0,L]} f(q) \leq \int_0^L f(q) dq \leq L \max_{q \in [0,L]} f(q).$$

For $c_0 \leq 0$ and $c > 0$ the mean Eulerian flow is westward $\langle u \rangle_E < 0$, if inequality

$$c_0 > -c \min_{q \in [0,L]} \frac{e^{2kR} \left(1 - e^{kR}\right)}{1 - e^{2kR}}$$

holds, and accordingly the mean flow is eastward $\langle u \rangle_E > 0$ if

$$c_0 < -c \max_{q \in [0,L]} \frac{e^{2kR} \left(1 + e^{kR}\right)}{1 - e^{2kR}}. \tag{14}$$

Finally, we have to consider the case $c_0 > 0$ and $c < 0$. The mean Eulerian flow is westward $\langle u \rangle_E < 0$ if

$$c_0 > -c \max_{q\in[0,L]} \frac{e^{2kR}\left(1+e^{kR}\right)}{1-e^{2kR}}, \tag{15}$$

whereas it is eastward $\langle u\rangle_E > 0$ if

$$c_0 < -c \min_{q\in[0,L]} \frac{e^{2kR}\left(1-e^{kR}\right)}{1-e^{2kR}}.$$

Subsequently, we compute the mean Eulerian flow in the latitudinal direction. Proceeding in the same manner as in the mean zonal velocity we get

$$\begin{aligned}\langle v\rangle_E(z_0) &= \frac{1}{T}\int_0^T v(x-ct,y,z_0)dt = \frac{1}{L}\int_0^L v(x-ct,y,z_0)dx \\ &= \frac{1}{L}\int_0^L v(q-ct,z_0)\frac{\partial x}{\partial q}dq = \frac{1}{L}\int_0^L \psi(q,r)\frac{1-e^{2kR}}{1+e^{kR}\cos\theta}dq.\end{aligned}$$

The mean meridional Eulerian velocity depends entirely on the magnitude and sign of the function $\psi(q,r)$. It is self-evident that for $\psi(q,r)=0$ the mean Eulerian velocity is zero. Furthermore, when $\psi(q,r)=0$ the formula for the mean zonal Eulerian velocity is similar to the solution for the two-dimensional flow obtained in [75]. The difference is that in the β-plane the exponential in the mean Eulerian velocity implicitly depends on fixed latitude s and the phase speed is strictly positive. In our case the exponential in the mean zonal Eulerian velocity $\langle u\rangle_E$ is independent of s and we have complications caused by the wave phase speed c, which can be positive or negative.

4.3 Stokes drift

Finally, we are able to compute the Stokes drift $\mathbf{U}^S$ (12). As before we will consider two components of Stokes drift $\mathbf{U}^S = [U^S, V^S]$, U^S in the longitudinal direction and V^S in the latitudinal direction. The drift in the longitudinal direction U^S is expressed as

$$\begin{aligned}U^S(z_0) &= -c_0 + \frac{c}{L}\int_0^L e^{2kR}\,dq + \frac{c_0}{L}\int_0^L \frac{1-e^{2kR}}{1+e^{kR}\cos\theta}\,dq = \\ &= \frac{1}{L}\int_0^L (-c_0 + ce^{2kR})\,dq + \frac{c_0}{L}\int_0^L \frac{1-e^{2kR}}{1+e^{kR}\cos\theta}\,dq.\end{aligned} \tag{16}$$

For $c_0>0, c>0$, the Stokes drift is eastward $U^S>0$ when the current satisfies the inequality $c_0 < ce^{2kR}$. In the case $c_0\le 0, c<0$ the Stokes drift is westward $U^S<0$ when $c_0 > ce^{2kR}$ holds. On the other hand, for $c_0\le 0, c>0$ we can clearly state that the drift is westward if (14) is satisfied. In like manner, for $c_0>0, c<0$ when inequality (15) holds the zonal Stokes drift is eastward. In any other cases the Stokes

drift is much more complex and the f-plane approximation does not introduce any conditions, which could be used to estimate precisely and analytically the drift.

Now we consider the Stokes drift in the latitudinal direction which is

$$V^S(z_0) = \psi(q,r) - \frac{1}{L}\int_0^L \psi(q,r)\frac{1-e^{2kR}}{1+e^{kR}\cos\theta}\,dq.$$

For $\psi(q,r) = 0$ the difference between our solution and solution in β-plane is that we do not have any dependence on the latitude s in the component U^S, and we have to keep in mind that the current c_0 and the phase speed of the wave c can be positive or negative.

4.4 Mass flux

We present here a discussion on the mass flux $\mathbf{m}$ for the flow represented by (4) with the additional complexity of a three-dimensional model. In this case we consider mass flux through two fixed planes, which are parallel to the planes YZ and XZ, respectively we will get the components of the mass flux $\mathbf{m} = [m^{zonal}, m^{meridional}]$ in zonal and meridional direction. In general the mass flux through any plane S can be written as [122]

$$m = \int\limits_S \rho\mathbf{u}\cdot\mathbf{n}dS,$$

which is an integral over the surface S and $\mathbf{n}$ is the normal vector to the surface S. We introduce the parametrisation of surface S

$$\begin{cases} x = q - c_0 t - \dfrac{1}{k}e^{\xi}\sin\theta, \\ y = s + \psi(q,r), \\ z = r + \dfrac{1}{k}e^{\xi}\cos\theta. \end{cases} \tag{17}$$

If either of the current terms, c_0 or ψ, are not zero the mass flux is infinite since the domain of our model is infinitely deep $r \in (-\infty, r_0)$. Therefore, we focus our attention to mass flux between two streamlines η and η_1, where r_0 represents the streamline of free surface η and $r_1 < r_0$ represents the streamline of wave profile η_1 beneath the free surface.

Zonal mass flux

We start by fixing a equation $x = x_0$ of a plane $S = [\eta_1, \eta] \times [-y_0, y_0]$, where η is the profile of the free surface wave and η_1 the profile of a wave beneath the free surface. For $\mathbf{u} = (u, v, w)$ and $\mathbf{n} = (1, 0, 0)$ the zonal mass flux is

$$m^{zonal} = \iint\limits_{[\eta_1,\eta]\times[-y_0,y_0]} u(x_0 - ct, y, z)dydz. \tag{18}$$

It is convenient for us to change the expression (18) to the Lagrangian labelling variables. As a result, we have

$$m^{zonal} = \int_{r_1}^{r_0} \int_{-s_0}^{s_0} (u(x(q,r,t), y(q,s,r), z(q,r,t))) \begin{vmatrix} \frac{\partial y}{\partial s} & \frac{\partial y}{\partial r} \\ \frac{\partial z}{\partial s} & \frac{\partial z}{\partial r} \end{vmatrix} dsdr. \tag{19}$$

Here, from (17) we get that $\frac{\partial y}{\partial s} = 1$ and $\frac{\partial z}{\partial s} = 0$. To find the $\frac{\partial z}{\partial r}$ we use the fixed point $x = x_0$. From the fixed point x_0 we imply the existence of a functional relationship between the variables q, r, t, where $q = \gamma(x_0, r, t)$ and the derivative of γ with respect to r is exactly

$$\gamma_r = \frac{e^{\xi} \sin\theta}{1 - e^{\xi} \cos\theta}. \tag{20}$$

Using (20) we can find the derivative of z with respect to r

$$\frac{\partial z}{\partial r} = \frac{1 - e^{2\xi}}{1 - e^{\xi} \cos\theta}.$$

It remains to find $\frac{\partial y}{\partial r}$, where using the relationship $q = \gamma(x_0, r, t)$ we get

$$\frac{\partial y}{\partial r} = \gamma_r \psi_r(\gamma(x_0, r, t), r)t.$$

The determinant of the jacobian of mapping (17) is equal

$$\begin{vmatrix} \frac{\partial y}{\partial s} & \frac{\partial y}{\partial r} \\ \frac{\partial z}{\partial s} & \frac{\partial z}{\partial r} \end{vmatrix} = \begin{vmatrix} 1 & \gamma_r \psi_r(\gamma(x_0, r, t), r)t \\ 0 & \frac{\partial z}{\partial r} \end{vmatrix} = \frac{\partial z}{\partial r}$$

Thus, the mass flux (19) per unit width is

$$m^{zonal} = \frac{1}{2s_0} \int_{r_1}^{r_0} \int_{-s_0}^{s_0} (-c_0 + ce^{\xi} \cos\theta) \frac{\partial z}{\partial r} dsdr = \int_{r_1}^{r_0} (-c_0 + ce^{\xi} \cos\theta) \frac{\partial z}{\partial r} dr =$$
$$= \int_{r_1}^{r_0} (-c_0 + ce^{\xi} \cos\theta) \frac{1 - e^{2\xi}}{1 - e^{\xi} \cos\theta} dr$$

as a consequence of the vertical velocity u and the derivative $\frac{\partial z}{\partial r}$ being independent of variable s. In the absence of an underlying current c_0 we can state that the function γ is T-periodic. Furthermore, this implies that the integrand in the mass flux expression is T-periodic and it follows that the average mass flux over a wave period vanishes when $c_0 = 0$. We note that for $\cos\theta = 1$ and $\cos\theta = -1$ the wave profile has a crest and trough respectively and the mass flux takes the form

$$
\begin{aligned}
m^{zonal} &= \int_{r_1}^{r_0} (-c_0 + ce^{\xi})(1 + e^{\xi}) dr \text{ on the crest,} \\
m^{zonal} &= \int_{r_1}^{r_0} (c_0 + ce^{\xi})(1 - e^{\xi}) dr \text{ on the trough.}
\end{aligned} \tag{21}
$$

Evidently, the mass flux between the streamlines prescribed by r_0 and r_1 is finite and depends on the magnitude, the sign of the current and the wave phase speed. We highlight that the meridional current $\psi(q, r)$ does not interfere in mass flux in the direction of wave propagation as expected, since it is purely transverse.

Meridional mass flux

In the next case we consider a plane $S = [\eta_1, \eta] \times [0, L]$ determined by the equation $y = y_0$. Now $\mathbf{u} = (u, v, w)$, $\mathbf{n} = (0, 1, 0)$ and the meridional mass flux has the form

$$
m^{meridional} = \iint\limits_{[\eta_1, \eta] \times [0, L]} v(x - ct, y_0, z) dx dz.
$$

The functions of particle position x and z do not depend on the variable s, this is the reason why we do not consider from $y = y_0$ any functional relationship between variables. After performing the change of variables, we have

$$
m^{meridional} = \int_{\eta_1}^{\eta} \int_{0}^{L} v dx dz = \int_{r_1}^{r_0} \int_{0}^{L} v \begin{vmatrix} \frac{\partial x}{\partial q} & \frac{\partial x}{\partial r} \\ \frac{\partial z}{\partial q} & \frac{\partial z}{\partial r} \end{vmatrix} dq dr.
$$

Where

$$
\begin{vmatrix} \frac{\partial x}{\partial q} & \frac{\partial x}{\partial r} \\ \frac{\partial z}{\partial q} & \frac{\partial z}{\partial r} \end{vmatrix} = \begin{vmatrix} 1 - e^{\xi} \cos\theta & -e^{\xi} \sin\theta \\ -e^{\xi} \sin\theta & 1 + e^{\xi} \cos\theta \end{vmatrix} = 1 - e^{2\xi}.
$$

The meridional mass flux per unit length is

$$
m^{meridional} = \frac{1}{L} \int_{r_1}^{r_0} \int_{0}^{L} \psi(q, r)(1 - e^{2\xi}) dq dr. \tag{22}
$$

When the meridional current is equal to zero it is straightforward that (22) is equal to zero. Finally, we consider two simple cases of a meridional current. Let us assume that the current ψ is constant or depends only on the variable q, which can be written as

$$
\psi = const \text{ or } \psi = \psi(q).
$$

We recall that $\xi = kr$. Therefore, we can separate the integrals in the mass flux (22) and we get

$$m^{meridional} = \frac{1}{L}\int_0^L \psi dq \int_{r_1}^{r_0}(1-e^{2\xi})dr = \Psi \int_{r_1}^{r_0}(1-e^{2\xi})dr \text{ where } \Psi = \frac{1}{L}\int_0^L \psi dq. \quad (23)$$

Assuming the finiteness of Ψ we easily can say that the mass flux (23) is finite. In this case the meridional mass flux depends solely on the magnitude of meridional velocity and in consequence on the value Ψ. The cases $\psi = \psi(r)$ or $\psi = \psi(q, r)$ are intractable and can be considered in further study where the form of variable meridional current is explicitly known. As anticipated the zonal current does not impact on the meridional mass flux.

Exact and explicit internal equatorial water waves with underlying currents

Mateusz Kluczek

Journal of Mathematical Fluid Mechanics, 19:305–314, 2017.

Abstract In this paper we present an exact and explicit solution to the geophysical governing equations in the equatorial region, which represents internal oceanic waves in the presence of a constant underlying current.

1 Introduction

In this paper we present an exact solution to the β-plane governing equations representing internal equatorially-trapped water waves in the presence of an underlying current. The dynamics in the Pacific Ocean near the equator has certain specific features [39, 47, 48] which are of great interest. The equatorial region is characterised by a thin, permanent, shallow layer of warm and less dense water overlying a deeper layer of cold water, both of constant densities. The two layers are separated by an interface called a thermocline [39]. Our aim is to investigate the flow induced by the motion of the thermocline by presenting an exact and explicit solution which models internal waves propagating in the presence of an underlying current.

In 1809 Gerstner [136] found an explicit solution in Lagrangian variables for the full water wave equations. This is one of only a handful of explicit solutions to the governing equations which have been constructed. Gerstner's wave is a two-dimensional gravity wave, where Coriolis effects are neglected and where the motion is identical in all planes parallel to a fixed vertical plane. This exact and explicit solution was analysed in [5, 7, 54], and was extended in [4, 132] to describe three-dimensional edge-waves propagating over a sloping bed. Recently, in [9] an exact and explicit solution for geophysical water waves incorporating the Coriolis effect was successfully achieved. This solution is Gerstner-like in the sense that setting Coriolis terms to zero recovers the Gerstner wave solution. However, the wave solution derived in [9] is a significant extension of Gerstner's wave for a number of reasons, for example it is three-dimensional and equatorially-trapped, whereby Coriolis terms play a vital role in the decay of wave oscillations away from the equator. Subsequently a variety of exact and explicit solutions were derived and analysed in various papers [12, 13, 19, 50, 136, 129, 60, 63, 65, 68, 67, 78, 77, 81, 114, 115, 125] including solutions with underlying background currents [50, 60, 78].

This article is motivated by the recent papers [12, 13], where Constantin presented explicit nonlinear solutions for geophysical internal waves propagating eastward in the layer above the thermocline and beneath the near-surface layer in which wind effects are predominant.

In [12] it was assumed that beneath the thermocline lay an abyssal region of still water, whereas in [13] a more physically plausible model was achieved whereby the region beneath the thermocline has been divided into three layers, which transition from the internal wave at the thermocline to an abyssal zone of purely motionless fluid. In this paper we extend the model and solution in [13] to admit a constant underlying current. This was successfully achieved for geophysical surface waves in [60], and for internal waves in [78] whereby the approach of [60] was implemented for the physically restricted first model of [12]. We note that adding an underlying current to the model introduced in [13], which is the aim of this paper, represents a far more complicated scenario, both mathematically and physically, as we must match the solution in the various transitional layers. We note that the presence of strong currents in the equatorial Pacific is well-documented and they feature significantly in the geophysical dynamics of the equatorial region [39, 10, 23, 25].

It has recently been rigorously shown in [125] that the internal wave solution considered in [13] is dynamically possible. These considerations are also applicable to the model incorporating a constant underlying current which we present in this paper. In this paper we assumed that the model describes the fluid with a motionless deep-water layer of fluid. However, it is possible to further adapt our model to have underlying currents in this deep-water expanse.

2 Governing equations

The flow pattern we investigate is symmetric about the equator, being confined to a region of overall width of about 200 km, centered on the equator. The Earth is taken to be a sphere of a radius $R = 6371$ km, rotating with a constant rotational speed $\Omega = 7.29 \times 10^{-5}$ rad s^{-1} round the polar axis towards the east. The flow will be described in a rotating frame with the origin at a point on the Earth's surface. Therefore the Cartesian coordinates (x, y, z) represent the directions of the longitude, latitude and local vertical, respectively. The governing equations for geophysical ocean waves [39] are the Euler equations

$$\begin{cases} u_t + uu_x + vu_y + wu_z + 2\Omega w\cos\phi - 2\Omega v\sin\phi = -\dfrac{1}{\rho}P_x, \\ v_t + uv_x + vv_y + wv_z + 2\Omega u\sin\phi = -\dfrac{1}{\rho}P_y, \\ w_t + uw_x + vw_y + ww_z - 2\Omega u\cos\phi = -\dfrac{1}{\rho}P_z - g, \end{cases}$$

coupled with the equation of mass conservation

$$\rho_t + (u\cdot\nabla)\rho + \rho(\nabla\cdot u) = 0,$$

and the resulting equation for incompressibility

$$u_x + v_y + w_z = 0.$$

Here t is the time, ϕ is the latitude, $g = 9.81$ m s^{-1} is the constant gravitational acceleration at the Earth's surface, ρ is the water's density, and P is the pressure, while u, v and w are the respective fluid velocity components. Under the assumption that the meridional distance to the equator is moderate, the approximation $\sin\phi \approx \phi$ and $\cos\phi \approx 1$ can be used [39]. This approximation captures the dynamical effect of the Earth's sphericity and is called β-plane approximation. It approximates the Coriolis force

$$2\Omega \begin{pmatrix} w\cos\phi - v\sin\phi \\ u\sin\phi \\ -u\cos\phi \end{pmatrix}$$

by the expression

$$\begin{pmatrix} 2\Omega w - \beta y u \\ \beta y u \\ -2\Omega u \end{pmatrix}$$

with $\beta = 2\Omega/R = 2.28 \times 10^{-11} m^{-1} s^{-1}$ [39]. Thus the Euler equation is replaced by (cf. [39])

$$\begin{cases} u_t + uu_x + vu_y + wu_z + 2\Omega w - \beta y v = -\dfrac{1}{\rho}P_x, \\ v_t + uv_x + vv_y + wv_z + \beta y u = -\dfrac{1}{\rho}P_y, \\ w_t + uw_x + vw_y + ww_z - 2\Omega u = -\dfrac{1}{\rho}P_z - g. \end{cases} \tag{1}$$

3 Discussion of the model

The principle aim of this paper is to present an exact and explicit solution to (1) which prescribes eastward-propagating equatorially-trapped waves (with constant wavespeed $c > 0$) in the presence of a constant underlying current c_0, which for the present time may be either positive or negative. A schematic for our model is given in Figure 1, and it may be described as follows.

The upper near-surface region of the ocean where wind effects are important is denoted $\mathcal{L}(t)$, and we assume that the wave motion there is a small perturbation of the ocean dynamics which are dominated by wind waves. Therefore, the internal geophysical wave motions we consider do not play a major role in the flow characteristics of the fluid in $\mathcal{L}(t)$, and so for the purpose of this model we will not address the interaction of the geophysical waves and wind waves in the $\mathcal{L}(t)$ region.

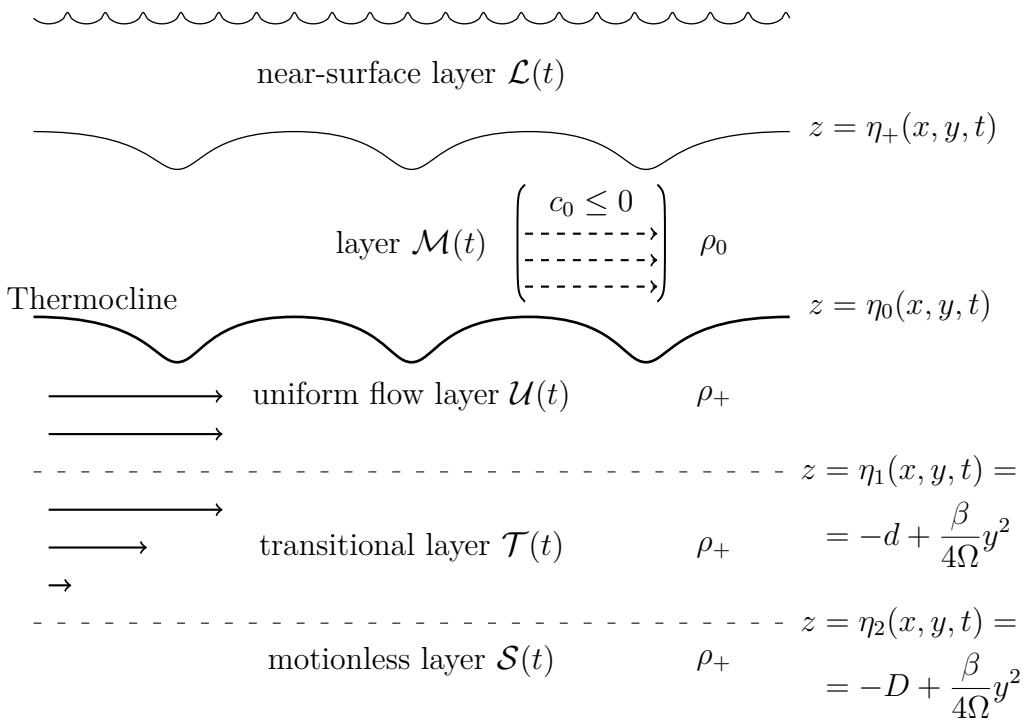


Figure 1: Depiction of the main flow regions at fixed latitude y. The thermocline is described by a trochoid propagating eastward at constant speed. The thermocline separates two layers of different densities $\rho_0 < \rho_+$ in a stable stratification (with the denser fluid below).

Beneath $\mathcal{L}(t)$, whose lower-boundary we label $z = \eta_+(x, y, t)$, we assume that the fluid motion is due primarily to the wave motion resulting from the propagation of the thermocline, which we denote $z = \eta_0(x, y, t)$, interacting with a uniform underlying current c_0. We label this region between the interfaces η_+ and η_0 as $\mathcal{M}(t)$. The appearance of the constant current in our model takes an apparently simple form in the Lagrangian setting, but both mathematically and physically it leads to highly complex modifications in the underlying flow — a detailed exposition of such complications can be found in [75] for the (relatively simpler) setting of surface water waves. Next, we assume that the fluid has a constant density ρ_0 in the region above the thermocline η_0, whereas the fluid has constant density $\rho_+ > \rho_0$ beneath the thermocline — indicative values for the density difference are given by $(\rho_+ - \rho_0)/\rho_0 \approx 4 \times 10^{-3}$ [13] for oceanic Equatorial waves.

We divide the fluid domain of greater density, which lies beneath the thermocline, into three separate regions, which transitions the fluid motion from that induced by the propagation of the thermocline to a motionless abyssal deep-water region. In the region bounded above by the thermocline and below by the interface $z = \eta_1(x, y, t)$ the flow is uniform with velocity $(c - c_0, 0, 0)$, where $c > 0$ is the propagation speed of the oscillations of the thermocline. The region between $z = \eta_1(x, y, t)$ and $z = \eta_2(x, y, t)$ is a transitional layer where the fluid motion decreases until we reach the deep-water layer beneath the interface $z = \eta_2(x, y, t)$ where it is completely still. Now we present the form of the governing equations (1) which are relevant to each layer, and then we derive an exact and explicit solution to these equations.

The layer $\mathcal{M}(t)$

In the region $\eta_0(x,y,t) < z < \eta_+(x,y,t)$ we seek a solution of the governing equations (1) which take the form

$$\begin{cases} u_t + uu_x + wu_z + 2\Omega w = -\dfrac{1}{\rho_0}P_x, \\ \beta yu = -\dfrac{1}{\rho_0}P_y, \\ w_t + uw_x + ww_z - 2\Omega u = -\dfrac{1}{\rho_0}P_z - g, \end{cases} \tag{2}$$

together with the incompressibility condition

$$u_x + w_z = 0, \tag{3}$$

and the kinematic boundary condition

$$w = (\eta_0)_t + u(\eta_0)_x \text{ on } z = \eta_0(x,y,t). \tag{4}$$

The layer of uniform flow $\mathcal{U}(t)$

Between the boundary $\eta_1(x,y,t) < z < \eta_0(x,y,t)$ we seek a solution of

$$\begin{cases} u_t + uu_x + wu_z + 2\Omega w = -\dfrac{1}{\rho_+}P_x, \\ \beta yu = -\dfrac{1}{\rho_+}P_y, \\ w_t + uw_x + ww_z - 2\Omega u = -\dfrac{1}{\rho_+}P_z - g, \end{cases}$$

together with the incompressibility condition

$$u_x + w_z = 0,$$

and the kinematic boundary condition

$$w = (\eta_1)_t + u(\eta_1)_x \text{ on } z = \eta_1(x,y,t).$$

The transitional layer $\mathcal{T}(t)$

In the region $\eta_2(x,y,t) < z < \eta_1(x,y,t)$ the governing equations are in the same form as above:

$$\begin{cases} u_t + uu_x + wu_z + 2\Omega w = -\dfrac{1}{\rho_+}P_x, \\ \beta yu = -\dfrac{1}{\rho_+}P_y, \\ w_t + uw_x + ww_z - 2\Omega u = -\dfrac{1}{\rho_+}P_z - g, \end{cases} \tag{5}$$

with the incompressibility condition

$$u_x + w_z = 0,$$

and with the kinematic boundary condition

$$w = (\eta_2)_t + u(\eta_2)_x \text{ on } z = \eta_2(x, y, t).$$

The motionless deep-water layer $\mathcal{S}(t)$

In the region $z < \eta_2(x, y, t)$ the governing equations are again in the same form as above:

$$\begin{cases} u_t + uu_x + wu_z + 2\Omega w = -\dfrac{1}{\rho_+}P_x, \\ \beta yu = -\dfrac{1}{\rho_+}P_y, \\ w_t + uw_x + ww_z - 2\Omega u = -\dfrac{1}{\rho_+}P_z - g, \end{cases}$$

and we are assuming that the water is still, thus

$$u = v = w = 0.$$

In order to successfully implement the multi-layered model described above, each set of equations must be coupled with the continuity of the pressure across each interface. We also note that the boundary kinematic conditions $w = (\eta_i)_t + u(\eta_i)_x$ on $z = \eta_i(x, y, t)$ with $i = 0, 1, 2$ means that there is no flux of particles on a macroscopic scale, and a particle initially on the boundary will remain on the boundary at all times.

3.1 Exact and explicit solution

We present now the exact and explicit solutions which satisfy the multi-layered model described above. Due to the vastly differing nature of the flow characteristics of the respective solutions, for ease of presentation we describe the solutions layer-by-layer, working from the bottom upwards.

The motionless deep-water layer $\mathcal{S}(t)$

For some fixed equatorial depth $D > 0$ we set $\eta_2(x, y, t) = -D + \frac{\beta}{4\Omega} y^2$. In the region below the surface $\eta_2(x, y, t)$, the fluid is in the hydrostatic state $u = v = w = 0$ with the pressure given by

$$P(x, y, z, t) = P_0 - \rho_+ g z, \tag{6}$$

for $z \leq -D + (\frac{\beta}{4\Omega} y^2)$, where P_0 and D are some constants that we will discuss in greater detail later.

The transitional layer $\mathcal{T}(t)$

We set $\eta_1(x, y, t) = -d + \frac{\beta}{4\Omega} y^2$ for some fixed equatorial depth $d < D$. In the region between $z = \eta_2(x, y, t)$ and $z = \eta_1(x, y, t)$ we define the horizontal component of particle velocity u to be growing linearly from $u = 0$ on $z = \eta_2(x, y, t)$ to $u = c - c_0$ on $z = \eta_1(x, y, t)$, thus

$$u(x, y, z, t) = \frac{c - c_0}{D - d} \left(z - \frac{\beta}{4\Omega} y^2 + D \right).$$

The set of equations (5) is then simplified to $\beta y u = -\frac{1}{\rho_+} P_y$, $-2\Omega u = -\frac{1}{\rho_+} P_z - g$, which yields

$$P(x, y, z, t) = P_0 - \rho_+ g z + \frac{\rho_+ \Omega (c - c_0)}{D - d} \left(z - \frac{\beta}{4\Omega} y^2 + D \right)^2. \tag{7}$$

Note that the pressure P and the velocity u are continuous across the interface $z = \eta_2(x, y, t)$.

The layer of uniform flow $\mathcal{U}(t)$

The interface $z = \eta_0(x, y, t)$ represents the oscillating thermocline, and for each latitude y it takes the form of an eastward-propagating travelling wave. In the region $\eta_1(x, y, t) < z < \eta_0(x, y, t)$ we set the flow to be uniform with $u = c - c_0$ and $v = w = 0$. The simplified vertical momentum equation says

$$-2\Omega u = -\frac{1}{\rho_+} P_z - g,$$

and there is also the $y-$momentum equation

$$\beta y u = -\frac{1}{\rho_+} P_y.$$

We require the continuity of pressure across the interface $z = \eta_1(x, y, t)$. Evaluating the pressure on $z = -d + \frac{\beta}{4\Omega} y^2$ we obtain

$$P(x,y,z,t) = P_0 - \rho_+ gz + \rho_+ \Omega(c-c_0)\,(D+d) + 2\rho_+ \Omega\,(c-c_0)\left(z - \frac{\beta}{4\Omega}y^2\right). \quad (8)$$

The layer $\mathcal{M}(t)$

In this section we present an exact solution in the $\mathcal{M}(t)$ layer which represents waves travelling in the longitudinal direction at a constant speed of propagation $c > 0$, in the presence of a constant underlying current of strength c_0. For the explicit description of this flow it is convenient to use the Lagrangian framework. The Lagrangian positions (x, y, z) of a fluid particle are given as functions of the labelling variables (q, r, s) and time t by

$$\begin{cases} x = q - c_0 t - \dfrac{1}{k} e^{-k[r+f(s)]} \sin[k(q-ct)], \\ y = s, \\ z = r - d_0 - \dfrac{1}{k} e^{-k[r+f(s)]} \cos[k(q-ct)]. \end{cases} \quad (9)$$

Here, $k = 2\pi/L$ is the wavenumber corresponding to the wavelength L. The parameter q covers the real line, while $s \in [-s_0, s_0]$, where s_0 is not in excess of 250 km (the equatorial radius of deformation [12]). For each fixed value of $s \in [-s_0, s_0]$, we require $r \in [r_0(s), r_+(s)]$, where the choice $r = r_0(s) > 0$ represents the thermocline $z = \eta_0(x, y, t)$ at a latitude $y = s$, while $r = r_+(s) > r_0(s)$ prescribes the interface $z = \eta_+(x, y, t)$ separating $L(t)$ and $\mathcal{M}(t)$ at the same latitude. An indicative value for $(r_+ - r_0)$ is 60 m [47]. We will prove the existence of such functions $r_0(s), r_+(s)$ below. The parameter $d_0 > 0$ is determined by specifying that $[d_0 - r_0(0)]$ is the mean depth of the thermocline at the equator, where $r_0(0) > 0$ is the unique choice of r which prescribes the thermocline at the equator. The wave speed c is obtained from the dispersion relation (16), giving us

$$c = \frac{\rho_+ - \rho_0}{\rho_0} \frac{\sqrt{\Omega^2 + \dfrac{\rho_0 k(2\Omega c_0 + g)}{\rho_+ - \rho_0}} - \Omega}{k} > 0, \quad (10)$$

for the speed of an eastward-propagating wave, while

$$c = -\frac{\rho_+ - \rho_0}{\rho_0} \frac{\sqrt{\Omega^2 + \dfrac{\rho_0 k(2\Omega c_0 + g)}{\rho_+ - \rho_0}} + \Omega}{k} < 0,$$

would be the speed of a westward-propagating wave. As we explain below, the only physically acceptable values of the wave speed for the solution (9) are positive, and so $c > 0$ (given by (10)). Furthermore, we note that the underlying current term c_0 plays a role in the dispersion relation which is dependent on the Coriolis terms

as well. The wave motion in $\mathcal{M}(t)$ induced by the propagation of the thermocline, as described by the solution (9), is equatorially-trapped (that is, there is a marked decay in the particle's oscillations moving in the meridional direction away from the equator) if we make a suitable choice for the function $f(s)$. We see below that the structure of the wave motion forces a natural choice

$$f(s) = \frac{\beta}{2(kc - 2\Omega)} s^2. \tag{11}$$

Note that in Gerstner's wave the amplitude of wave oscillations decreases as we descend into fluid, which is the reverse of the present setting whereby the amplitude decreases exponentially as we ascend above the thermocline. Let us now verify that (9) is indeed an exact solution of (2) and (3) representing internal water waves travelling in the presence of a constant underlying current. For notational convenience we set

$$\xi = k[r + f(s)], \quad \theta = k(q - ct).$$

We require

$$r \geq r^* = \min_{s \in [-s_0, s_0]} \{r_0(s)\} > 0, \tag{12}$$

so that $e^{-\xi} < 1$ throughout the $\mathcal{M}(t)$ layer, since $\xi \geq kr^* > 0$. The Jacobian of the map relating the particle's positions to the Lagrangian labelling variables

$$\begin{pmatrix} \frac{\partial x}{\partial q} & \frac{\partial y}{\partial q} & \frac{\partial z}{\partial q} \\ \frac{\partial x}{\partial s} & \frac{\partial y}{\partial s} & \frac{\partial z}{\partial s} \\ \frac{\partial x}{\partial r} & \frac{\partial y}{\partial r} & \frac{\partial z}{\partial r} \end{pmatrix} = \begin{pmatrix} 1 - e^{-\xi}\cos\theta & 0 & e^{-\xi}\sin\theta \\ f_s e^{-\xi}\sin\theta & 1 & f_s e^{-\xi}\cos\theta \\ e^{-\xi}\sin\theta & 0 & 1 + e^{-\xi}\cos\theta \end{pmatrix}$$

is time independent, equaling $1 - e^{-2\xi}$, thus the flow is volume preserving and the condition of incompressibility (3) holds in this layer. We can write the Euler equation in the form

$$\begin{cases} \frac{Du}{Dt} + 2\Omega w = -\frac{1}{\rho_0} P_x, \\ \frac{Dv}{Dt} + \beta y u = -\frac{1}{\rho_0} P_y, \\ \frac{Dw}{Dt} - 2\Omega u = -\frac{1}{\rho_0} P_z - g, \end{cases}$$

where D/Dt is the material derivative. From a direct differentiation of the system of the coordinates in (9), the velocity of each fluid particle may be expressed as

$$\begin{cases} u = \frac{Dx}{Dt} = ce^{-\xi}\cos\theta - c_0, \\ v = \frac{Dy}{Dt} = 0, \\ w = \frac{Dz}{Dt} = -ce^{-\xi}\sin\theta, \end{cases}$$

and the acceleration is

$$\begin{cases} \frac{Du}{Dt} = kc^2 e^{-\xi}\sin\theta, \\ \frac{Dv}{Dt} = 0, \\ \frac{Dw}{Dt} = kc^2 e^{-\xi}\cos\theta. \end{cases}$$

Due to above statements we can write (2) as

$$\begin{aligned} P_x &= -\rho_0(kc^2 - 2\Omega c)e^{-\xi}\sin\theta, \\ P_y &= -\rho_0\beta y(ce^{-\xi}\cos\theta - c_0), \\ P_z &= -\rho_0(kc^2 e^{-\xi}\cos\theta - 2\Omega c e^{-\xi}\cos\theta + 2\Omega c_0 + g). \end{aligned}$$

Since

$$\begin{pmatrix} P_q \\ P_s \\ P_r \end{pmatrix} = \begin{pmatrix} \frac{\partial x}{\partial q} & \frac{\partial y}{\partial q} & \frac{\partial z}{\partial q} \\ \frac{\partial x}{\partial s} & \frac{\partial y}{\partial s} & \frac{\partial z}{\partial s} \\ \frac{\partial x}{\partial r} & \frac{\partial y}{\partial r} & \frac{\partial z}{\partial r} \end{pmatrix} \cdot \begin{pmatrix} P_x \\ P_y \\ P_z \end{pmatrix},$$

we have

$$\begin{aligned} P_q &= -\rho_0[kc^2 - 2\Omega c + 2\Omega c_0 + g]e^{-\xi}\sin\theta, \\ P_s &= -\rho_0[(kc^2 - 2\Omega c)f_s e^{-2\xi} + (\beta sc + (2\Omega c_0 + g)f_s)e^{-\xi}\cos\theta - c_0\beta s], \\ P_r &= -\rho_0[(kc^2 - 2\Omega c)e^{-2\xi} + (kc^2 - 2\Omega c + 2\Omega c_0 + g)e^{-\xi}\cos\theta + 2\Omega c_0 + g]. \end{aligned} \tag{13}$$

We note that making a natural assumption that the pressure in $\mathcal{M}(t)$ has continuous second partial derivatives, and thus $P_{sr} = P_{rs}$, implies that

$$f_s = \frac{\beta sc}{kc^2 - 2\Omega c},$$

which leads to the expression for $f(s)$ in (11). Now the gradient of the expression

$$\begin{aligned} P(q,r,s,t) =& \rho_0\frac{kc^2 - 2\Omega c + 2\Omega c_0 + g}{k}e^{-\xi}\cos\theta + \rho_0(kc^2 - 2\Omega c)\frac{e^{-2\xi}}{2k} \\ &- \rho_0(2\Omega c_0 + g)r + \rho_0(kc - 2\Omega)c_0 f(s) + \tilde{P}_0, \end{aligned} \tag{14}$$

with respect to the labelling variables is precisely the right-hand side of (13). We showed earlier that the continuity of pressure holds between each layer in the region under the thermocline. Now we want to have the continuity of the pressure across the thermocline. Evaluating the pressure in the layer directly beneath $\mathcal{M}(t)$, given by (8), at the thermocline we obtain

$$\begin{aligned} P =& P_0 + \rho_+(g - 2\Omega(c - c_0))\frac{1}{k}e^{-\xi}\cos\theta - \rho_+(-d_0 + r)(g - 2\Omega(c - c_0)) \\ &- 2\rho_+\Omega(c - c_0)\frac{\beta}{4\Omega}s^2 + \rho_+\Omega(c - c_0)(D + d). \end{aligned} \tag{15}$$

Comparing the respective pressures at the thermocline, (14) and (15), and examining the time-dependent θ terms, it follows that the continuity of the pressure across the thermocline requires

$$\rho_0[kc^2 - 2\Omega c + 2\Omega c_0 + g] = \rho_+[g - 2\Omega(c - c_0)]. \tag{16}$$

Solving the quadratic for c in (16) leads us directly to the dispersion relation (10). We remark further that all realistic wavelengths L lead to decay of oscillations of particles in the meridional direction in (11), because $(\rho_+ - \rho_0)/\rho_0 \approx 4 \times 10^{-3}$ for oceanic equatorial waves. In fact (cf. [13] for details) the dispersion relation (10) ensures that $kc - 2\Omega > 0$ holds if

$$\frac{2\pi}{L} = k > \frac{4\Omega^2}{g}\left(1 + \frac{\rho_0}{\rho_+ - \rho_0}\right) \approx 5 \times 10^{-7} m^{-1}.$$

A consequence of this, bearing in mind (11), is that $f(s) \geq 0$, and it is therefore only with the choice of positive value of wave phase-speed (10) that the system (9) represents a physically plausible model of waves with amplitude which diminish with the distance from the equator. Following (16), a comparison of (14) and (15) with regard to the continuity of pressure across the thermocline leads to the expression

$$\begin{aligned} P_0 + d_0\rho_+ g - \rho_+\Omega(c - c_0)\frac{\beta}{2\Omega}s^2 + \rho_+\Omega(c - c_0)(D + d - 2d_0) = \\ = \rho_0(kc - 2\Omega)c\left(\frac{e^{-2\xi}}{2k} + r\right) + \frac{\rho_0 c_0 \beta}{2}s^2 + \tilde{P}_0, \end{aligned} \tag{17}$$

and thus the thermocline is being determined by setting $r = r_0(s)$, where $r_0(s) > 0$ is the unique solution of (17), for each fixed value $s \in [-s_0, s_0]$. As a result we have

$$\begin{aligned} P_0 - \tilde{P}_0 = \frac{\rho_+(c - c_0) + \rho_0 c_0}{2}\beta s^2 - d_0\rho_+ g - \rho_+\Omega(c - c_0)(D + d - 2d_0) \\ +\rho_0(kc - 2\Omega)c\left(\frac{\exp\left[-2k\left(r_0(s) + \frac{\beta}{2(kc-2\Omega)}s^2\right)\right]}{2k} + r_0(s)\right). \end{aligned} \tag{18}$$

If (18) holds for some $r_0(s)$, then the flow determined by (9) satisfies the governing eqs. (2) to (4). The oscillations of the thermocline described in the absence of an underlying current $c_0 = 0$ propagate eastwards in the shape of trochoid, and each particle in the layer $\mathcal{M}(t)$ describes a counter-clockwise circular vertical closed path of decreasing diameter as we ascend above the thermocline. This situation contrasts with that occurring in irrotational two-dimensional flows beneath Stokes waves where the particle paths are open loops [6, 35, 55].

3.2 Admissible values of the underlying current c_0

To complete our presentation we must consider for which values of the current c_0 the flow is hydrodynamically possible, that is, for which values we can find a unique $r_0(s)$ such that (18) holds. For each fixed $s \in [-s_0, s_0]$ the mapping

$$r \to \frac{e^{-2k\left[r+\frac{\beta}{2(kc-2\Omega)}s^2\right]}}{2k} + r,$$

is a strictly increasing diffeomorphism from $(0,\infty)$ onto $(\frac{1}{2k}e^{-\frac{k\beta}{kc-2\Omega}s^2},\infty)$, so the existence of a unique solution $r_0(s) \geq r^* > 0$ of the equation (18), for fixed $|s| > 0$ is equivalent to setting

$$P_0 - \tilde{P}_0 > \frac{\rho_+(c-c_0)+\rho_0 c_0}{2}\beta s^2 + \frac{\rho_0(kc-2\Omega)c}{2k} - d_0\rho_+ g$$
$$-\rho_+\Omega(c-c_0)(D+d-2d_0).$$

Then it follows that $r_0(s)$ determines the thermocline. The constant $\tilde{P}_0$ is arbitrary, however due to physical considerations we will consider $P_0 - \tilde{P}_0 > 0$. Let us now evaluate the expression (18) at $r = r_0(s)$ and differentiate the outcome with respect to s, giving us

$$r_0'(s) = \frac{-\rho_+(c-c_0)+\rho_0 c e^{-2k[r_0(s)+f(s)]} - \rho_0 c_0}{\rho_0(kc-2\Omega)c(1-e^{-2k[r_0(s)+f(s)]})}\beta s.$$

We impose a restriction on the function $r_0(s)$ by stating that it is strictly decreasing with s, which corresponds to the scenario presented in [13] for the setting $c_0 = 0$. Thus

$$c_0 < \frac{\rho_+ - \rho_0 e^{-2k[r_0(s)+f(s)]}}{\rho_+ - \rho_0} c = (1+\epsilon)c, \tag{19}$$

for $\epsilon > 0$, where $\epsilon = \frac{\rho_0(1-e^{-2k[r_0(s)+f(s)]})}{\rho_+-\rho_0}$. The relation (19) holds for all values $c_0 \leq 0$, and in particular setting $c_0 = 0$ recovers the result of [13]. Interestingly, and specific to our setting, equation (19) provides a bound for positive values of the constant underlying current c_0. By the implicit function theorem, $r_0(s)$ is even and smooth function. Thus we can say that the function $s \mapsto r(s)$ decreases as s increases. We remark that (19) shows that the mean depth of the thermocline $[d_0 - r_0(s)]$ at each latitude s increases slightly with the distance from the equator, while the boundaries of the transitional layer ascends. This implies the fact that at some latitude the two regions will intersect, thus producing a more complex flow.

To complete the solution it remains to specify the boundary delimiting the two layers $\mathcal{M}(t)$ and $L(t)$. This can be obtained by choosing some fixed constant

$$\beta_0 > P_0 - \tilde{P}_0 > \frac{\rho_+(c-c_0)+\rho_0 c_0}{2}\beta s^2 + \frac{\rho_0(kc-2\Omega)c}{2k} - d_0\rho_+ g$$
$$-\rho_+\Omega(c-c_0)(D+d-2d_0),$$

and setting $r = r_+(s)$ at a fixed value $s \in [s_0, -s_0]$, where $r = r_+(s)$ is unique solution of

$$\beta_0 = \frac{\rho_+(c-c_0)+\rho_0 c_0}{2}\beta s^2 + \rho_0(kc-2\Omega)c(\frac{e^{-2\xi}}{2k}+r) - d_0\rho_+ g \\ -\rho_+\Omega(c-c_0)(D+d-2d_0).$$

The previous considerations show that β_0 determines a unique $r_+(s) > r_0(s)$. The function $s \mapsto r_+(s)$ has the same features as the function $s \mapsto r_0(s)$. The function is even, smooth and strictly decreasing for $|s| > 0$. Setting $r^* = r_0(0)$ we ensure condition (12). This completes the proof that (9) is an exact solution of the governing eqs. (2) to (4) for internal water waves propagating in the presence of a constant underlying current.

Mean flow properties for equatorially-trapped internal water wave-current interactions

Adrián Rodríguez-Sanjurjo and Mateusz Kluczek

Applicable Analysis, 96:2333–2345, 2017.

Abstract The aim of this paper is to provide an analysis of the mean flow velocities, and the related mass transport induced by the equatorially-trapped internal water waves with a constant underlying current.

1 Introduction

The present paper is devoted to the analysis of two important and closely-related features regarding the study of water waves, the mean flow velocity and the mass flux. We focus our attention on equatorially-trapped internal waves in the presence of a constant underlying current. In particular, we will examine the exact solution proposed in [78] which incorporates a constant current to the solution initially derived in [12]. It is important to note that equatorially-trapped waves are known to exist [39, 47, 48] and they are regarded as one of the possible factors in the explanation of the El Niño phenomenon. Additionally, the consideration of a thermocline [12, 13, 78], which is an interface separating two vertical ocean layers of different although constant densities, allows to accommodate the stratification, one of the distinctive features of geophysical fluid dynamics. Furthermore, this model has been justified by observations of the equatorial region that reveal the existence of a shallow layer of warm and less dense water overlaying a deeper layer of cold water. In that scenario, a small perturbation may generate an internal wave, which constitutes the three-dimensional analogue of the surface waves. The aim of this paper is to investigate the mean flow velocities and the mass transport induced by the oscillations of the thermocline under the effect of a constant background current. The presence of strong currents in the equatorial Pacific is well-documented and they feature significantly in the geophysical dynamics of the equatorial region [23, 25, 39].

It is noteworthy that, despite of the early works of Stokes in mid-1800 in [131], the precise computation and interpretation of mass-transport velocities in ocean water waves remains a contentious issue. For the case of a gravity irrotational wave of a perfect and inviscid fluid where the Coriolis forces are neglected, Stokes showed that the particles, in addition to its oscillatory motion, are transferred forwards

with a constant velocity decreasing rapidly as the depth increases. It was also stated by Stokes and rigourously proven for exact, nonlinear gravity waver waves in [7, 11, 19, 55, 54] that the individual particles in a progressive and irrotational wave do not describe exactly closed paths, possessing an additional nonlinear mean velocity that is commonly known as the Stokes drift velocity. However, the irrotational wave is not the only type of wave theoretically possible in a perfect fluid, as it was remarkably shown by Gerstner and Rankine in [136] and [124], respectively. In that wave motion, the particles describe circular orbits and the mass-transport velocity vanishes. Furthermore, Dubreil-Jacotin proved in [40] the existence of a family of waves, which includes the waves studied by Stokes and Gerstner as particular cases, having intermediate vorticity distributions and mass transport velocities. Additionally, the vorticity becomes a key factor not only in the boundaries but also in the interior of the fluid when it is transferred by means of a strong velocity gradient in the boundaries. For these reasons, Longuet-Higgins provided a more general definition of the mass-transport velocity (cf. [100]) an approach that was clarified in [101] where it was established that the Stokes drift velocity can be expressed, after some approximations, as a difference of the Lagrangian and the Eulerian mean velocities.

A wide variety of exact and explicit solution have been derived and analysed in [12, 13, 19, 50, 136, 60, 63, 65, 68, 67, 78, 77, 81, 114, 115, 125, 129] including solutions with underlying currents [50, 60, 78, 95]. The Lagrangian description of the Gerstner-like solutions provides a straightforward method for obtaining the first term in the expression of the Stokes drift [19, 50, 75]. Nevertheless, difficulties may arise in determining the Eulerian velocity, specially when the model incorporates an underlying current term as in [78]. In general, the analysis of kinematic properties of the Gerstner-like solutions has been proven to be interesting since they have an explicit representation in terms of Lagrangian variables that allows to present the motion in mathematical terms without any approximation and, regardless of its initial abstract character, it has been proven to provide explanation to several physical models. The understanding of the properties of the water waves treated in this paper, like the mass transport, have been of great interest from both physical and mathematical viewpoints. For instance, a clean analysis of the flow characteristics in the absence of a background current was presented in [12, 19] whereas [75] addresses the more complicated scenario of the incorporation of an underlying current for the equatorially-trapped surface water wave, previously derived in [60]. The manifestation of a constant current in these models could be seen as a simple addition to the Lagrangian representation, however it leads to highly complex modifications in the underlying flow. In this paper we present an analogous analysis for the case of an internal wave motion under the presence of a constant current, a motion which presents quite different flow properties leading to rather different physical implications without major complications of the mathematical analysis derived in [75].

2 Governing equations

One of the distinctive aspects in the study of geophysical flows is the consideration of the effects of rotation in the fluid motion. Accordingly, the governing equations for the geophysical ocean waves are presented in a reference framework rotating with Earth. For the purpose of simplification, the Earth can be taken as a perfect sphere of a radius $R = 6371$ km, rotating with a constant rotational speed of $\Omega = 7.29 \times 10^{-5}$rad s^{-1} around the polar axis toward east. Furthermore, we choose a local Cartesian framework of reference with the x-axis oriented eastward, the y-axis oriented northward, and the z-axis oriented upward with respect to the local vertical (cf. [39]). Let $\mathbf{u} = (u, v, w)$ denote the fluid velocity, if we neglect the viscous effects, the equations of motion take the form of the Euler equations with the acceleration being modified to incorporate the effects of the ambient rotation

$$\begin{cases} u_t + uu_x + vu_y + wu_z + 2\Omega w\cos\phi - 2\Omega v\sin\phi = -\dfrac{1}{\rho}P_x, \\ v_t + uv_x + vv_y + wv_z + 2\Omega u\sin\phi = -\dfrac{1}{\rho}P_y, \\ w_t + uw_x + vw_y + ww_z - 2\Omega u\cos\phi = -\dfrac{1}{\rho}P_z - g, \end{cases} \tag{1}$$

where ϕ represents the latitude, Ω is the Earth's rotational speed, $g = 9.8$m s^{-2} is the gravitational constant, ρ represents the water's density and P is the pressure. The coefficient $f = 2\Omega\sin\phi$ is known as the Coriolis parameter and its multiplication by the velocity provides the so-called Coriolis acceleration. In order to complete the set of the governing equations, the density is taken as a piecewise constant function (which constitutes our equation of state) resulting in the continuity equation

$$\nabla \cdot \mathbf{u} = 0,^{1}$$

easily derived from the mass conservation principle (see [89]) for each different region of constant density. We will consider geophysical waves in the equatorial region, specifically in the region which is within 5° of latitude of the equator. Therefore, we can make use of the approximation $\cos\phi \approx 1$ and use the first-order Taylor expansion of the Coriolis parameter $f = 2\Omega\sin\phi$ around the equator, obtaining the so-called β-plane approximation of the equations (1),

$$\begin{cases} u_t + uu_x + vu_y + wu_z + 2\Omega w - \beta yv = -\dfrac{1}{\rho}P_x, \\ v_t + uv_x + vv_y + wv_z + \beta yu = -\dfrac{1}{\rho}P_y, \\ w_t + uw_x + vw_y + ww_z - 2\Omega u = -\dfrac{1}{\rho}P_z - g, \end{cases}$$

where $\beta = 2\Omega/R = 2.28 \times 10^{-11} m^{-1}s^{-1}$, cf. [39] for a detailed presentation of these equations.

[1] $\nabla \cdot \vec{u}$ expresses the compressibility of the fluid (see [7]).

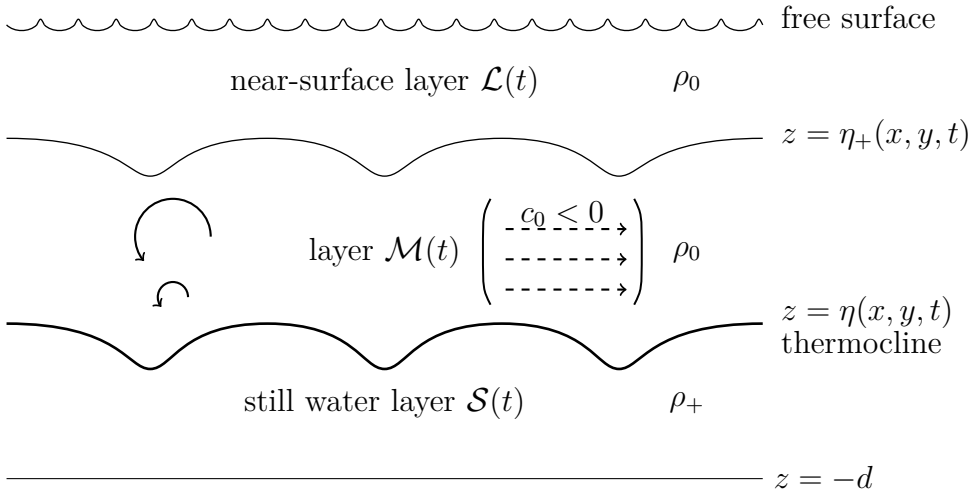


Figure 1: Depiction of the different flow regions for a fixed latitude y for a negative constant value of the underlying current c_0 in the layer $\mathcal{M}(t)$. In the absence of the current, the thermocline is specified by a trochoid propagating eastward at a constant speed. The thermocline separates two layers of different densities $\rho_0 < \rho_+$ in a stable stratification with the denser fluid below.

The model supporting the physical requirements presented in the introduction is depicted in Figure 1 and was originally considered in [12], being subsequently modified in [78] to accommodate a constant underlying current. Following those models, we will distinguish two layers $\mathcal{M}(t)$ and $\mathcal{S}(t)$ separated by a thermocline, with densities ρ_0 and ρ_+ respectively, whereas a third layer $\mathcal{L}(t)$ where the effects of the wind are predominant is not addressed. We assume $\rho_0 < \rho_+$, which corresponds to the state of minimal potential energy provided by the action of the gravitational force, and assure that $\mathbf{u} = \mathbf{0}$ in $\mathcal{S}(t)$. It is worth mentioning that this model has been reformulated in [13] (incorporating an eastward-flowing current beneath the thermocline) to allow a more physically plausible transition from the region above the thermocline to the abyssal region of still water. Furthermore, a constant underlying current may also be incorporated in the region $\mathcal{M}(t)$ as recently was shown in [95]. However, for the purpose of clarity of analysis, we currently restrict our attention to the simple two-layered model derived in [12]. Considering the reasonable case of waves with vanishing meridional velocity ($v = 0$) throughout $\mathcal{M}(t)$, which is necessary for assuring the equatorially-trapped character of the waves, the governing equations are

$$\begin{cases} u_t + uu_x + wu_z + 2\Omega w = -\dfrac{1}{\rho_0} P_x, \\ \beta y u = -\dfrac{1}{\rho_0} P_y, \\ w_t + uw_x + ww_z - 2\Omega u = -\dfrac{1}{\rho_0} P_z - g, \end{cases} \tag{2}$$

for $z \in (\eta_0(x - ct, y), \eta_+(x - ct, y))$, satisfying

$$u_x + w_z = 0 \quad \text{in} \quad \eta_0(x - ct, y) < z < \eta_+(x - ct, y), \tag{3}$$

and coupled with the boundary condition (result of the consideration of a motionless bottom layer)

$$P = P_0 - \rho_+ g z \quad \text{on} \quad z = \eta_0(x - ct, y). \tag{4}$$

We assume that in absence of the wave, the motion of particles will be described by rectilinear uniform motion with constant velocity c_0 in the layer $\mathcal{M}(t)$.

3 Exact solution

We now describe an exact solution for the governing eqs. (2) to (4) as it was derived in [78]. The solution is presented in the Lagrangian framework (for a general discussion of the Lagrangian approach cf. [2]). Thus, for the labelling variables $(q, r, s) \in \mathbb{R} \times [r_0(s), r_+(s)] \times \mathbb{R}$, where the two positive numbers $r_0(s)$ and $r_+(s)$ will be specified later on, the position (x, y, z) of the fluid particles at some time t is explicitly given by

$$\begin{cases} x = q - c_0 t - \dfrac{1}{k} e^{-k[r+f(s)]} \sin[k(q - ct)], \\ y = s, \\ z = r - \dfrac{1}{k} e^{-k[r+f(s)]} \cos[k(q - ct)], \end{cases} \tag{5}$$

where $k = 2\pi/L$ is the wavenumber for a fixed wavelength L. Restricting ourselves to the case of eastward-propagating waves, we obtain the following dispersion relation

$$c = \frac{\Omega + \sqrt{\Omega^2 + k\gamma}}{k},$$

where $\gamma = \tilde{g} - 2\Omega c_0$ and $\tilde{g} = g\left(\rho_+ - \rho_0\right)/\rho_0$. The constant $\tilde{g}$ is usually called the reduced gravity and has the typical value of $6 \times 10^{-3} \mathrm{m} \cdot s^{-2}$ (see [47]). The function f, given by

$$f(s) = \frac{c\beta}{2\gamma} s^2, \tag{6}$$

determines the decay of the particle oscillations in the latitudinal direction away from the equator. We note here that $2\Omega c_0$ is taken less then $\tilde{g}$, which is physically plausible, in order to have $\gamma > 0$. We will adopt the following notation

$$\xi := k[r + f(s)], \quad \theta := k(q - ct),$$

and we assume that

$$r + f(s) \geq r^* > 0. \tag{7}$$

Therefore, the Jacobian matrix of the transformation (5)

$$J = \left(\frac{\partial(x, y, z)}{\partial(q, s, r)}\right) = \begin{pmatrix} 1 - e^{-\xi}\cos\theta & 0 & e^{-\xi}\sin\theta \\ f'(s)e^{-\xi}\sin\theta & 1 & f'(s)e^{-\xi}\cos\theta \\ e^{-\xi}\sin\theta & 0 & 1 + e^{-\xi}\cos\theta \end{pmatrix}$$

has a non-vanishing determinant $1 - e^{-2\xi}$, thus the model is dynamically possible (see [125] for the complete proof). In addition, the determinant is independent of time assuring that (5) is volume preserving (cf. [7]). Consequently, for a region of constant density, the mass is conserved and (3) is clearly satisfied. The velocity field is given by the time derivative of (5),

$$\begin{cases} u = -c_0 + ce^{-\xi}\cos\theta, \\ v = 0, \\ w = -ce^{-\xi}\sin\theta. \end{cases} \tag{8}$$

Once the continuity equation (3) has been satisfied, checking that the explicit solution (5) satisfies the governing eqs. (2) to (4) is equivalent to obtaining a compatible pressure. It follows that a necessary and sufficient condition for the existence of a scalar pressure is that f takes the form (6). In addition, the boundary condition (4) and the consideration of eastward-propagating waves lead to the following dispersion relation

$$c = \frac{\Omega + \sqrt{\Omega^2 + k(\tilde{g} - 2\Omega c_0)}}{k}.$$

On the other hand, the boundary condition (4) allow us to determine the thermocline. Following the method used in [78] the determination of the thermocline is equivalent to finding the unique solution $r = r_0(s) > 0$ for every fixed $s \in [-s_0, s_0]$ of

$$\mathscr{F}(r, s) := r + \frac{c_0}{c}(-2kr - \frac{k\beta c}{\gamma}s^2) + \frac{1}{2k}\exp(-2kr - \frac{k\beta c}{\gamma}s^2) - P_0^* = 0, \tag{9}$$

where P_0^* is an arbitrary constant and $s_0 = \sqrt{\tilde{c}/\beta} \approx 250$ km is the equatorial radius of deformation and the typical value of $\tilde{c}$ for the tropical region is 1.4 m s^{-1} (cf. [12, 39]). It follows from the Intermediate Value theorem and the monotonic character of $\mathscr{F}(r, s)$ that

$$P_0^* > \frac{c_0\beta}{2\gamma}s_0^2 + \frac{1}{2k},$$

is a sufficient condition for the existence and uniqueness of the solution of (9). Summarising, the thermocline $z = \eta_0(x - ct, y)$ will be the surface given by

$$(q, s) \longrightarrow (q - c_0 t - \frac{1}{k} e^{-k[r_0(s)+f(s)]} \sin[k(q-ct)], s, r_0(s) - \frac{1}{k} e^{-k[r_0(s)+f(s)]} \cos[k(q-ct)]),$$

where $r = r_0(s)$ is the unique solution of (9) for each given s. At this point, we take care of the physical implications of this mathematical model. Differentiating (9) with respect to s yields

$$r_0'(s) = \frac{\beta s}{\gamma} \frac{ce^{-2\xi} - c_0}{1 - e^{-2\xi}}.$$

Hence, it is clear that we should restrict the values of the current to

$$c_0 < ce^{-2kr_0(s)}, \tag{10}$$

to assure that $r_0(s)$ is a strictly increasing function for $|s| > 0$ and as a consequence,

$$s \longmapsto \exp\left(-2kr_0(s) - \frac{k\beta c}{\gamma} s^2\right), \tag{11}$$

is strictly decreasing for $|s| > 0$. Otherwise, the amplitude of the waves will grow exponentially with the distance from the equator, constituting an unrealistic model that violates the equatorially-trapped nature of these waves. To complete the solution it remains to specify the boundary delimiting the layers $\mathcal{M}(t)$ and $\mathcal{L}(t)$. This is done by considering the same nonlinear equation (9) with another constant $\mathscr{P}_0 > P_0^*$. The unique solution of that equation for every given latitude $s \in [-s_0, s_0]$ will be denoted by $r_+(s)$ (cf. [78] for the whole discussion).

To conclude this section we specify the crest and the trough levels for both surfaces at a given latitude,

$$z^c(s) = r_0(s) + \frac{1}{k} e^{-k[r_0(s)+f(s)]} \quad \text{and} \quad z^t(s) = r_0(s) - \frac{1}{k} e^{-k[r_0(s)+f(s)]},$$

are respectively the crest and trough levels for the thermocline, whereas

$$z_+^c(s) = r_+(s) + \frac{1}{k} e^{-k[r_+(s)+f(s)]} \quad \text{and} \quad z_+^t(s) = r_+(s) - \frac{1}{k} e^{-k[r_+(s)+f(s)]},$$

correspond in the same manner to the interface $z = \eta_+(x - ct, y)$ delimiting the layers $\mathcal{M}(t)$ and $\mathcal{L}(t)$.

4 Mean velocities and Stokes drift

A commonly misinterpreted fact is that the mass transport passing any fixed point depends exclusively on the mean velocity measured at that point. The confusion emerges from neglecting the difference between the Eulerian and the Lagrangian viewpoint. Thus, the mass-transport velocity should be defined as the Lagrangian mean velocity, i.e, the mean velocity experienced by a marked particle. This difference was noted by Stokes in [131] and is accordingly known as the Stokes drift velocity. Afterwards, Longuet-Higgins established in [101] the following expression

$$U^S = \langle u \rangle_L - \langle u \rangle_E ,$$

relating the Stokes drift U^S with the Lagrangian mean velocity $\langle u \rangle_L$ and Eulerian mean velocity $\langle u \rangle_L$. Therefore, in analysing the Stokes drift we will start by obtaining this two different mean velocities.

4.1 Mean Lagrangian flow velocity

The mean Lagrangian flow velocity provides a measure of the velocity of a marked fluid particle over a wave period. Taking advantage of the Lagrangian description of the exact solution (5), the horizontal mean Lagrangian velocity over a wave period T is readily obtained by

$$\begin{aligned} \langle u \rangle_L &= \frac{1}{T}\int_0^T u(q-ct,s,r)dt = \frac{1}{T}\int_0^T \left(-c_0 + ce^{-\xi}\cos\theta\right) dt = \\ &= \frac{-c_0}{T}\int_0^T dt + \frac{ce^{-\xi}}{T}\int_0^T \cos[k(q-ct)]dt = -c_0, \end{aligned} \tag{12}$$

independently of the initial location of the fluid particle. Thus, it follows that the mean Lagrangian flow velocity is either westwards or eastwards, depending on whether the sign of c_0 is positive or negative respectively, while the special case of $c_0 = 0$ is consistent with previous results shown in [19].

4.2 Mean Eulerian flow velocity

On the contrary, by considering a fixed point in the fluid domain instead of a specific fluid particle, we obtain the mean Eulerian flow velocity. We begin by considering a fixed depth $z \in (z^c(s), z^t_+(s))$, where $z = z^c(s)$ is the vertical position of the wave crest level of the oscillation of the thermocline $z = \eta_0(x-ct, y)$ and $z = z^t_+(s)$ is the vertical position of the wave trough level of the fluctuation of the upper interface $z = \eta_+(x-ct, y)$ for each latitude $y = s$. Now, we have an unique Lagrangian representation of the depth $z(s)$, given by

$$z = R - \frac{1}{k}e^{-\xi(R)}\cos\theta, \tag{13}$$

where for each fixed s, $r = R\,(q - ct; s, z)$ is a function relating q and r by means of the Implicit Function theorem. Considering the mapping

$$\mathscr{G}_s(q - ct, r) := r - \frac{1}{k} e^{-k(r+f(s))} \cos[k(q - ct)],$$

which is a continuously differentiable function such that $\mathscr{G}_s(\tilde{q} - ct, \tilde{r}) = \tilde{z}$ for some $\tilde{z} \in (z^c(s), z^t_+(s))$, $\tilde{r} \geq r^* > 0$, and

$$\frac{\partial \mathscr{G}_s}{\partial r}(\tilde{q} - ct, \tilde{r}) = 1 + e^{-k(\tilde{r}+f(s))} \cos[k(\tilde{q} - ct)] \neq 0,$$

due to the assumption (7) we can state that the relation (13) is well defined. As a consequence of this relation, R is periodic in the q-variable, with period L . Differentiating $\mathscr{G}_s(\tilde{q} - ct, \tilde{r}) = \tilde{z}$ with respect to q it follows that

$$0 = R_q + R_q e^{-\xi(R)} \cos\theta + e^{-\xi(R)} \sin\theta,$$

where R_q is the derivative with respect to q, obtaining

$$R_q = -\frac{e^{-\xi(R)} \sin\theta}{1 + e^{-\xi(R)} \cos\theta},$$

where the denominator is different from zero in some neighbourhood of $\tilde{q}$.

Remark. *The function R is maximised (minimised) with respect to q when* $\sin\theta = 0$. *Therefore, for a fixed depth z, the maximum (minimum) of R is given implicitly by* (13) *with* $\cos\theta = -1$ *(*$\cos\theta = 1$*).*

We are now in position to compute the mean Eulerian flow velocity in the horizontal component for a fixed latitude s and depth $z^c(s) \leq z(s) \leq z^t_+(s)$. Adding the term c will simplify the calculation, thereby

$$c + \langle u \rangle_E (z, s) = \frac{1}{T} \int_0^T [c + u(x - ct, y, z)]\, dt = \frac{1}{L} \int_0^L [c + u(q - ct, s, z)] \frac{\partial x}{\partial q}\, dq,$$

where the periodic character of the wave velocity was considered. Consequently, considering (8) and writing $R \equiv R(q)$ and $R_q := \frac{\partial R}{\partial q}$, it follows that

$$\begin{aligned}
&c + \langle u \rangle_E (s, z) = \\
&= \frac{1}{L} \int_0^L \left(c + ce^{-\xi(R)} \cos\theta - c_0\right) \left(1 + R_q e^{-\xi(R)} \sin\theta - e^{-\xi(R)} \cos\theta\right) dq = \\
&= \frac{c}{L} \int_0^L dq - \frac{c}{L} \int_0^L e^{-2\xi(R)}\, dq - \frac{c_0}{L} \int_0^L \frac{1 - e^{-2\xi(R)}}{1 + e^{-\xi(R)} \cos\theta}\, dq = \\
&= c - \frac{c}{L} \int_0^L e^{-2\xi(R)}\, dq - \frac{c_0}{L} \int_0^L \frac{1 - e^{-2\xi(R)}}{1 + e^{-\xi(R)} \cos\theta}\, dq,
\end{aligned}$$

and the expression for the mean Eulerian flow velocity becomes

$$\langle u\rangle_E(s,z) = -\frac{c}{L}\int_0^L e^{-2\xi(R)}\,dq - \frac{c_0}{L}\int_0^L \frac{1-e^{-2\xi(R)}}{1+e^{-\xi(R)}\cos\theta}\,dq. \tag{14}$$

We clearly see that the mean Eulerian velocity depends on the current c_0 and consequently the mean flow becomes more complex. In order to discern the direction of this velocity, we will make use of the following inequalities

$$\int_0^L \frac{1-e^{-2\xi}}{1+e^{-\xi}}\,dq \le \int_0^L \frac{1-e^{-2\xi}}{1+e^{-\xi}\cos\theta}\,dq \le \int_0^L \frac{1-e^{-2\xi}}{1-e^{-\xi}}\,dq, \tag{15}$$

and we will analyse two different cases in terms of the sign of c_0.

Case I : $c_0 > 0$

Firstly, we examine the mean Eulerian flow in the presence of a positive underlying current c_0, which represents an adverse current. This study differs significantly from the analysis of the flow properties considered in [75] in view of the fact that our internal equatorially-trapped waves have an amplitude that decreases as we move upwards and the motion is restricted to the finite region $\mathcal{M}(t)$. Considering (15) and the sign of c_0, we estimate the mean Eulerian velocity taking advantage of the following inequalities

$$\frac{-c_0}{L}\int_0^L \frac{1-e^{-2\xi}}{1-e^{-\xi}}\,dq \le \frac{-c_0}{L}\int_0^L \frac{1-e^{-2\xi}}{1+e^{-\xi}\cos\theta}\,dq \le \frac{-c_0}{L}\int_0^L \frac{1-e^{-2\xi}}{1+e^{-\xi}}\,dq. \tag{16}$$

In addition, the positive value of the current is bounded by $c_0 < ce^{-2kr_0(s)}$ as it was justified in the previous section as a physical condition for (11) to be decreasing [78]. Consequently $c_0 < c$ for $r_0(s) > 0$, and from the second inequality in (16) we obtain an upper bound for the mean Eulerian velocity for a fixed latitude $s \in [-s_0, s_0]$ and a fixed depth $z^c(s) \le z(s) \le z_+^t(s)$

$$\begin{aligned}
\langle u\rangle_E(s,z) &\le -\frac{c}{L}\int_0^L e^{-2\xi(R)}\,dq - \frac{c_0}{L}\int_0^L \frac{1-e^{-2\xi(R)}}{1+e^{-\xi(R)}}\,dq \\
&\le -\frac{c_0}{L}\int_0^L e^{-2\xi(R)}\,dq - \frac{c_0}{L}\int_0^L \frac{1-e^{-2\xi(R)}}{1+e^{-\xi(R)}}\,dq \\
&= -\frac{c_0}{L}\int_0^L \frac{1+e^{-3\xi(R)}}{1+e^{-\xi(R)}}\,dq < 0.
\end{aligned}$$

where $R \equiv R(q)$. On the other hand, a lower bound is obtained from the first inequality in (16) in the same manner,

$$\begin{aligned}\langle u\rangle_E(s,z) &\geq -\frac{c}{L}\int_0^L e^{-2\xi(R)}\,dq - \frac{c_0}{L}\int_0^L \frac{1-e^{-2\xi(R)}}{1-e^{-\xi(R)}}\,dq \\ &\geq -\frac{c}{L}\int_0^L e^{-2\xi(R)}\,dq - \frac{c}{L}\int_0^L \frac{1-e^{-2\xi(R)}}{1-e^{-\xi(R)}}\,dq = \\ &= -\frac{c}{L}\int_0^L \frac{1-e^{-3\xi(R)}}{1-e^{-\xi(R)}}\,dq < 0.\end{aligned} \tag{17}$$

Therefore, the mean Eulerian velocity will be westward for all admissible values of current c_0 for which $c_0 < ce^{-2kr_0(s)}$ holds. The last integrand in (17) is a continuous function decreasing with respect to $r > 0$, and since $\xi \geq kR > kr^* > 0$, the values of the mean Eulerian velocity will satisfy

$$-c\,\frac{1-e^{-3kr^*}}{1-e^{-kr^*}} < \langle u\rangle_E(s,z) < 0.$$

In the absence of a current, the mean Eulerian flow is westward as in [12]. The westward direction of the mean Eulerian velocity is what we can expect since the current term in (14) only intensifies the effect of the adverse flow.

Case II : $c_0 < 0$

Now we investigate the mean Eulerian velocity under the presence of a negative underlying current $c_0 < 0$, which reflects a following current in the direction of propagation of the internal wave. Generally, it will not be possible to find an analytic expression for the magnitude of the mean Eulerian velocity from the equation (14). Nevertheless, some estimations can be made after restricting the values of the current. Proceeding backwards, we start by considering the case $\langle u\rangle_E(s,z) < 0$, which is equivalent to

$$-\frac{c_0}{L}\int_0^L \frac{1-e^{-2\xi(R)}}{1+e^{-\xi(R)}\cos\theta}dq \leq \frac{c}{L}\int_0^L e^{-2\xi(R)}dq. \tag{18}$$

We claim that a sufficient condition for (18) will be given by the following restriction on the current

$$c_0 > -c\min_{q\in[0,L]}\frac{e^{-2\xi(R)}\left(1-e^{-\xi(R)}\right)}{1-e^{-2\xi(R)}}. \tag{19}$$

Indeed, it follows from this condition that

$$-c_0\max_{q\in[0,L]}\frac{1-e^{-2\xi(R)}}{1-e^{-\xi(R)}} < c\min_{q\in[0,L]}e^{-2\xi(R)},$$

and consequently,

$$-\frac{c_0}{L}\int_0^L \frac{1-e^{-2\xi(R)}}{1+e^{-\xi(R)}\cos\theta}\,dq \le -\frac{c_0}{L}\int_0^L \frac{1-e^{-2\xi(R)}}{1-e^{-\xi(R)}}\,dq \le -c_0 \max_{q\in[0,L]} \frac{1-e^{-2\xi(R)}}{1-e^{\xi(R)}}$$
$$< c \min_{q\in[0,L]} e^{-2\xi(R)} \le \frac{c}{L}\int_0^L e^{-2\xi(R)}\,dq.$$

On the contrary, requiring $\langle u\rangle_E(s,z) > 0$ is equivalent to

$$-\frac{c_0}{L}\int_0^L \frac{1-e^{-2\xi(R)}}{1+e^{-\xi(R)}\cos\theta}\,dq \ge \frac{c}{L}\int_0^L e^{-2\xi(R)}\,dq.$$

In this case, it is sufficient that

$$c_0 < -c \max_{q\in[0,L]} \frac{e^{-2\xi(R)}\left(1+e^{-\xi(R)}\right)}{1-e^{-2\xi(R)}}, \tag{20}$$

in view of the following inequalities

$$-\frac{c_0}{L}\int_0^L \frac{1-e^{-2\xi(R)}}{1+e^{-\xi(R)}\cos\theta}\,dq \ge \frac{c_0}{L}\int_0^L \frac{1-e^{-2\xi(R)}}{1+e^{-\xi(R)}}\,dq \ge -c_0 \min_{q\in[0,L]} \frac{1-e^{-2\xi(R)}}{1+e^{-\xi(R)}}$$
$$> c \min_{q\in[0,L]} e^{-2\xi(R)} \ge \frac{c}{L}\int_0^L e^{-2\xi(R)}\,dq.$$

Finally, in the absence of a current the inequality (19) holds and the mean Eulerian flow is $\langle u\rangle_E \in (-c, 0)$ as it could be seen in [12], being constantly westward.

4.3 Stokes drift

Returning to the expression (4) for the Stokes drift , we can state now that

$$U^S(s,z) = -c_0 + \frac{c}{L}\int_0^L e^{-2\xi(R)}\,dq + \frac{c_0}{L}\int_0^L \frac{1-e^{-2\xi(R)}}{1+e^{-\xi(R)}\cos\theta}\,dq,$$

for fixed latitude $s \in [-s_0, s_0]$ and depth $z^c(s) \le z(s) \le z_+^t(s)$. Furthermore, if $0 \le c_0 < ce^{-2kr_0(s)} < c$ then

$$U^S(s,z) = \frac{1}{L}\int_0^L \left(ce^{-2\xi(R)} - c_0\right)dq + \frac{c_0}{L}\int_0^L \frac{1-e^{-2\xi(R)}}{1-e^{-\xi(R)}\cos\theta}\,dq > 0,$$

proving that the Stokes drift for an adverse current is eastward. For negative underlying currents $c_0 < 0$, it is difficult to estimate the exact magnitude of the Stokes drift. However, we note that for $c_0 < 0$ the mean Stokes drift will be westward under the assumption (20).

5 Mass flux

We now analyse the mass flux through a line $x = x_0$ (for fixed x_0) between the depth $z = \eta_0(x - ct, y)$ and $z = \eta_+(x - ct, y)$ representing the thermocline and the upper boundary of layer $\mathcal{M}(t)$, respectively. For a fixed latitude $s \in [-s_0, s_0]$, the mass flux between the two surfaces depicted in Figure 1 will be determined by

$$m(x_0 - ct, s) = \int_{\eta_0(x_0-ct)}^{\eta_+(x_0-ct)} u(x_0 - ct, y, z)dz.$$

From (5) and (8) we obtain

$$m(x_0 - ct, s) = \int_{r_0(s)}^{r_+(s)} (-c_0 + ce^{-\xi}\cos\theta)\frac{\partial z}{\partial r}dr,$$

in terms of the Lagrangian labelling variables. The exact solution (5) and a straightforward application of the Implicit Function theorem ensures that for a fixed $x = x_0$ the expression

$$x_0 = q - c_0 t - \frac{1}{k}e^{-\xi}\sin\theta, \tag{21}$$

establishes a functional relationship between otherwise independent variables q, r, t. Hence, denoting this relation by $q = \gamma(r, s, t)$ and differentiating (21) with respect to r it follows that

$$0 = \gamma_r + e^{-\xi}\sin\theta - \gamma_r e^{-\xi}\cos\theta,$$

and

$$\gamma_r = -\frac{e^{-\xi}\sin\theta}{1 - e^{-\xi}\cos\theta}. \tag{22}$$

Consequently, (22) allow us to calculate the derivative of z with respect to r

$$\frac{\partial z}{\partial r} = 1 + e^{-\xi}\cos\theta + \gamma_r e^{-\xi}\sin\theta = \frac{1 - e^{-2\xi}}{1 - e^{-\xi}\cos\theta}.$$

Thus, the mass flux is written now in the form

$$m(x_0 - ct, s) = \int_{r_0(s)}^{r_+(s)} (-c_0 + ce^{-\xi}\cos\theta)\frac{1 - e^{-2\xi}}{1 - e^{-\xi}\cos\theta}\, dr. \tag{23}$$

In particular, when the line $x = x_0$ intersects the wave crests or troughs, we have $\cos\theta = \pm 1$. In contrast to the study of the mass flux presented in [75] where the region under the surface wave is infinite, we can take advantage of the fact that the

oscillation we are considering is restricted to the region between the thermocline $z = \eta_0$ and the upper boundary of the region $\mathcal{M}(t)$ $z = \eta_+$. Consequently, if we assume that the magnitude of current c_0 is such that

$$|c_0| \leq ce^{-k(r_+(s)+f(s))}, \tag{24}$$

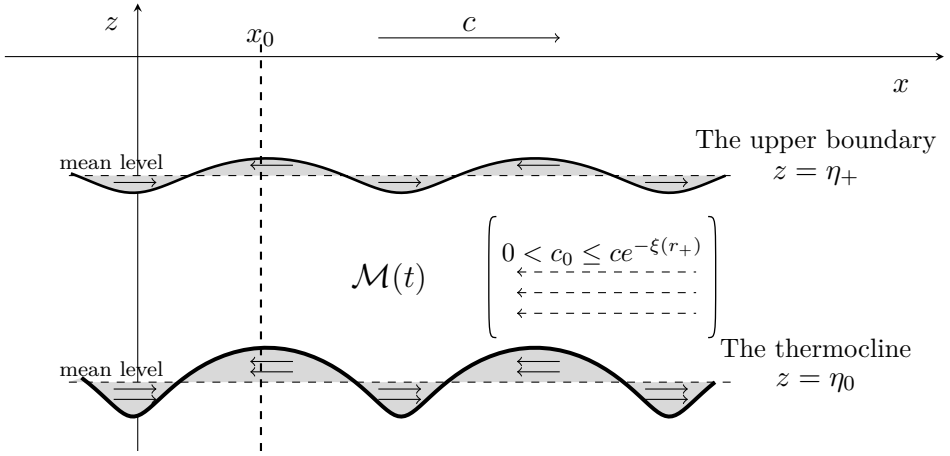


Figure 2: Depiction of the mass flux at any fixed latitude s within a narrow equatorial band in the presence of a current bounded by $|c_0| \leq ce^{k(r_+(s)+f(s))}$. For every wave in the region $\mathcal{M}(t)$ the mass of water is moved forward near the crest and backward near the trough as the wave passes, having a net result depending upon the current.

then the mass flux for waves in layer $\mathcal{M}(t)$ at the crests is backwards while at the troughs is forwards. For currents where (24) holds the properties of the mass flux are similar to the observation in [12] where there is no presence of underlying current. In the model presented in [12] for waves in region between the thermocline and the upper boundary of $\mathcal{M}(t)$ the mass flux at crest is always negative and at the trough is always positive. The opposite situation occurs when

$$c_0 < -ce^{-k(r_+(s)+f(s))},$$

having a mass flux (23) between the thermocline and the upper boundary of layer $\mathcal{M}(t)$ going forward at the crests and troughs of wave. This scenario is rather different from [12]. This is caused entirely by the constant underlying current.

Additionally, we calculate the time average of the mass flux over a wave period T in the case $c_0 = 0$. We deduce from (21) that the function γ is now T-periodic. Moreover, if we differentiate (21) with respect to time t, we obtain

$$\gamma_t = \frac{-ce^{-\xi}\cos\theta}{1 - e^{-\xi}\cos\theta}.$$

Therefore, the mass flux (23) is given by

$$m(x_0 - ct, s) = \int_{r_0(s)}^{r_+(s)} -\gamma_t(1 - e^{-2\xi})dr,$$

and since γ is T-periodic it follows that the average of the mass flux over a period T is zero, what is consistent with study in [12].

Exact Pollard-like internal water waves

Mateusz Kluczek

Journal of Nonlinear Mathematical Physics, 26:1–14, 2019.

Abstract In this paper we construct a new solution which represents Pollard-like three-dimensional nonlinear geophysical internal water waves. The Pollard-like solution includes the effects of the rotation of Earth and describes the internal water wave which exists at all latitudes across Earth and propagates above the thermocline. The solution is provided in Lagrangian coordinates. In the process we derive the appropriate dispersion relation for the internal water waves in a stable stratification and discuss the particles' paths. An analysis of the dispersion relation for the constructed model identifies one mode of the internal water waves.

1 Introduction

The aim of this paper is to present a new exact solution which represents a nonlinear internal water wave. The solution in this study is constructed by adapting the celebrated Pollard solution in order to successfully describe the internal water waves. In 1970, Pollard [121] presented a surface wave solution, where he extended the remarkable Gerstner solution [136] by including the effects of the rotation of Earth.

An extensive analysis of Gerstner's solution was presented in [5, 7, 54]. Recently, there has been a significant research activity deriving Gerstner-like solutions which model various geophysical oceanic waves including equatorially-trapped surface and internal waves [9, 12, 13, 64, 77] or waves in the presence of depth-invariant underlying currents [60, 63, 65, 95, 96, 127]. Furthermore, an instability analysis of Gerstner's solution was presented in [19]. The mathematical importance of the recently derived and analysed Gerstner-like solutions is presented in a form of a review paper in [66, 84, 90].

For rotating flows in the Pollard solution a wave experiences a very slight cross-wave tilt to the wave orbital motion associated with the planetary vorticity. Therefore, the Pollard-like solution is more suitable to describe large-scale global waters rather than Gerstner's solution; since Gerstner's solution describes the motion of a particle in the vertical plane [5, 9, 136, 54], it is more adequate for flows close to the equator where the force alternating the particles paths vanishes and the orbits are indeed vertical. The primary novel feature of this paper is we present an exact solution representing an internal water wave. The Pollard-like internal water wave solution established in

this paper describes still the circular particle orbits but now the orbits lie in a plane slightly tilted to the vertical, therefore the solution is fully three-dimensional and is essentially different to the internal water wave solutions derived for the equatorial region [12, 13]; cf. [3] for a discussion of the oceanographical relevance of these solutions.

The internal water waves in a stably stratified ocean may describe the oscillation of a thermocline [23, 39]. The thermocline is a sharp interface separating two horizontal layers of ocean water with constant but different densities [39, 49, 135]. The thermocline is a phenomenon occurring also at higher latitudes, thus it is important to emphasise the need for a solution which describes the internal water waves applicable beyond the equatorial region, as is the case in this paper. The mechanism of generation of the oscillation of the thermocline is, regrettably, outside of the scope of this paper; cf. [23, 88, 90] for a detailed study of the thermocline and its interaction with the Equatorial Undercurrent.

Subsequently to the work on the Gerstner-like solutions, there has been developments in the analysis of Pollard's solution for surface waves [30, 82, 83]. A Pollard-like solution for the surface waves in the presence of mean currents and rotation was derived in the recent research paper [30], with an instability analysis of the Pollard-like solution presented in [83]. Moreover, the surface wave solution is globally dynamically possible [126]. Our purpose is to modify Pollard's solution to obtain a valid model describing the nonlinear internal water waves. By empirically examining the developed solution, we hope to produce a more complete understanding of the internal oceanic flows [24]. We build on this analysis to identify the dispersion relation for the internal waves, describing the oscillation of the thermocline, which may be expressed as a polynomial of degree four by a suitable non-dimensional transformation. An analysis of the polynomial identifies one mode of the internal water wave that is a standard internal gravity wave modified very slightly by the Earth's rotation.

2 Governing equations

The flow pattern we investigate is described in a rotating frame with the origin at a point on the Earth's surface. Therefore, the (x, y, z) Cartesian coordinates represent the directions of the longitude, latitude and local vertical, respectively. The governing equations for the geophysical ocean waves are given by the Euler equations [39, 135]

$$\begin{cases} u_t + uu_x + vu_y + wu_z + 2\Omega w\cos\phi - 2\Omega v\sin\phi = -\dfrac{1}{\rho}P_x, \\ v_t + uv_x + vv_y + wv_z + 2\Omega u\sin\phi = -\dfrac{1}{\rho}P_y, \\ w_t + uw_x + vw_y + ww_z - 2\Omega u\cos\phi = -\dfrac{1}{\rho}P_z - g, \end{cases}$$

coupled with the equation of mass conservation

$$\rho_t + (u \cdot \nabla)\rho + \rho(\nabla \cdot u) = 0,$$

together with the resulting equation for incompressibility

$$u_x + v_y + w_z = 0. \tag{1}$$

Here t is time, ϕ represents the latitude, $g = 9.81\mathrm{m}s^{-2}$ is the constant gravitational acceleration at the Earth's surface, ρ is the water's density, and P is the pressure, while u, v and w are the respective fluid velocity components. The Earth is taken to be a sphere of a radius $R = 6371$ km, rotating with a constant rotational speed $\Omega = 7.29 \times 10^{-5}\mathrm{rad}{\cdot}s^{-1}$ round the polar axis towards the east.

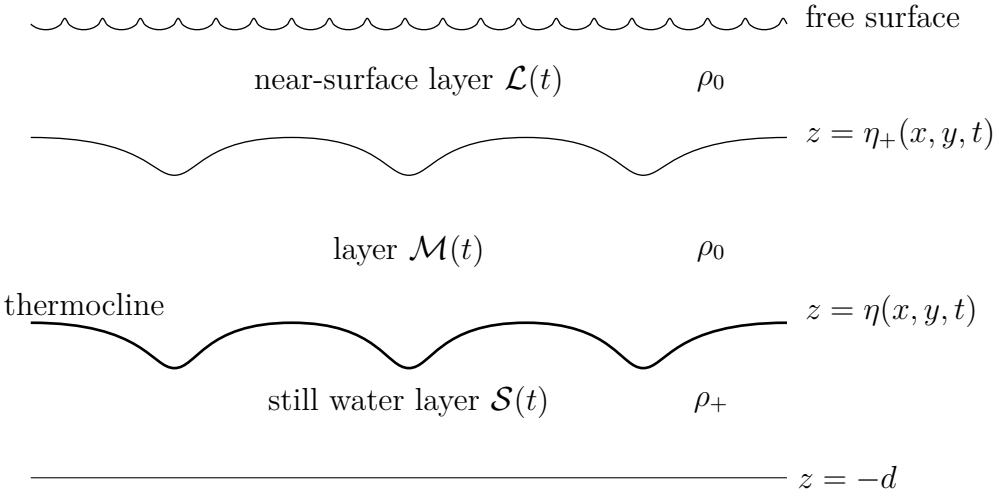


Figure 1: The depiction of the main flow regions at a fixed latitude y. The thermocline is described by a trochoid propagating at a speed c. The thermocline separates two layers of water of constant however different densities $\rho_0 < \rho_+$ in a stable stratification. In the solution that we present the amplitude of the internal waves decays exponentially above the thermocline and is reduced to less then 4% of its thermocline value at the hight of half a wavelength above the thermocline.

The solution that we construct models the internal water waves describing the oscillation of a thermocline and the hydrostatic model is presented as follow. The thermocline separates layers of ocean water of different densities [39]. The layer of less dense water $\mathcal{M}(t)$ with density ρ_0 overlays the layer of more dense water $\mathcal{S}(t)$ with density $\rho_+ > \rho_0$. The wave motion in $\mathcal{M}(t)$ is describing the oscillations of the thermocline. The layer $\mathcal{M}(t)$ is bounded by the thermocline $z = \eta(x, y, t)$ and by the upper boundary $z = \eta_+(x, y, t)$. In the solution which we present below the amplitude of the internal waves decays exponentially with the hight above the thermocline. The amplitude of the internal waves is reduced to less then 4% of its thermocline value at the hight of half a wavelength above the thermocline, since $e^{-\pi} \approx 0.04$ (cf. [9]), therefore for the purposes of this model, it is justifiable to consider that the layer $\mathcal{M}(t)$ is finite and bounded. The motion in the near surface layer $\mathcal{L}(t)$ is neglected as it is a small perturbation of the free surface caused primarily by the wind and the geophysical effect has little bearing there. The layer $\mathcal{S}(t)$ of

water under the thermocline describes a motionless abyssal deep-water region. The idea is to approximate the thermal structure of the ocean in the simplest form. We investigate the internal water waves in a relatively narrow ocean strip less than a few degrees of latitude wide, and so we regard the Coriolis parameters

$$f = 2\Omega \sin\phi, \qquad \hat{f} = 2\Omega \cos\phi,$$

as constants, where f is called the Coriolis parameter and $\hat{f}$ has no traditional name but usually is called the reciprocal Coriolis parameter [39]. The typical values of the Coriolis parameters at 45° on the Northern Hemisphere are $f = \hat{f} = 10^{-4}s^{-1}$ [53]. On a rotating sphere, such as Earth, the Coriolis term varies with the sine of latitude, however in the β-plane approximation the Coriolis parameter is set to vary linearly in space. Furthermore, this variation can be ignored and a value of the Coriolis parameter appropriate for a particular latitude can be used in the whole domain [39]. Thus, the Euler equations reduce in the f-plane approximation to

$$\begin{cases} u_t + uu_x + vu_y + wu_z + \hat{f}w - fv = -\dfrac{1}{\rho}P_x, \\ v_t + uv_x + vv_y + wv_z + fu = -\dfrac{1}{\rho}P_y, \\ w_t + uw_x + vw_y + ww_z - \hat{f}u = -\dfrac{1}{\rho}P_z - g. \end{cases}$$

Water is still under the thermocline which indicates that the velocity field is in the form

$$(u, v, w) = (0, 0, 0) \text{ for } z < \eta(x, y, t).$$

Since there is no motion in the layer $\mathcal{S}(t)$ the governing equations imply the hydrostatic pressure

$$P = P_0 - \rho_+ gz \qquad z < \eta(x, y, t).$$

The governing equations for the internal water waves in the layer $\mathcal{M}(t)$ are

$$\begin{cases} u_t + uu_x + vu_y + wu_z + \hat{f}w - fv = -\dfrac{1}{\rho_0}P_x, \\ v_t + uv_x + vv_y + wv_z + fu = -\dfrac{1}{\rho_0}P_y, \\ w_t + uw_x + vw_y + ww_z - \hat{f}u = -\dfrac{1}{\rho_0}P_z - g. \end{cases} \tag{2}$$

The appropriate boundary conditions for the internal water waves are the dynamic and kinematic conditions,

$$P = P_0 - \rho_+ gz \text{ on the thermocline } z = \eta(x, y, t)$$

$$w = \eta_t + u\eta_x + v\eta_y \text{ on the thermocline } z = \eta(x, y, t),$$

respectively. The kinematic condition prevents mixing of particles between the abyssal water region and the layer $\mathcal{M}(t)$. The particle initially on the boundary stays on the boundary at all times.

3 Discussion of the model

3.1 Exact and explicit solution

In this section we present an exact solution to the governing equations for the internal water waves in the layer $\mathcal{M}(t)$. The Pollard-like solution represents a periodic travelling wave in the longitudinal direction at a speed of propagation c. For the explicit description of this flow it is convenient to use the Lagrangian framework [2]. The Lagrangian positions (x, y, z) of a fluid particle are given as functions of the labelling variables (q, r, s), time t and real parameters a, b, c, d, k, m. We show that the explicit solution to the governing equations (2) satisfying the incompressibility condition is given by

$$\begin{cases} x = q - be^{-ms}\sin[k(q-ct)], \\ y = r - de^{-ms}\cos[k(q-ct)], \\ z = s - ae^{-ms}\cos[k(q-ct)]. \end{cases} \tag{3}$$

The constant $k = 2\pi/L$ is the wavenumber corresponding to the wavelength L. The parameter q covers the real line, while $r \in [-r_0, r_0]$, for some r_0, because the solution is set up around a fixed latitude ϕ. For every fixed value of $r \in [-r_0, r_0]$, we require $s \in [s_0, s_+]$, where the choice $s = s_0 \geq s^* > 0$ represents the thermocline $z = \eta(x, y, t)$ at the latitude ϕ, while $s = s_+ > s_0$ prescribes the interface $z = \eta_+(x, y, t)$ separating $\mathcal{L}(t)$ and $\mathcal{M}(t)$ at the same latitude. We set the parameter of the amplitude $a > 0$, wavenumber $k > 0$ and for waves with amplitude decreasing above the thermocline we require $m > 0$. The parameter d varies from $d > 0$ in the Southern Hemisphere, $d < 0$ in the Northern Hemisphere to $d = 0$ on the equator since it is related to the Coriolis parameter f, which we show later on. Moreover, the parameters b, c, d must be suitably chosen in terms of k, m, a.

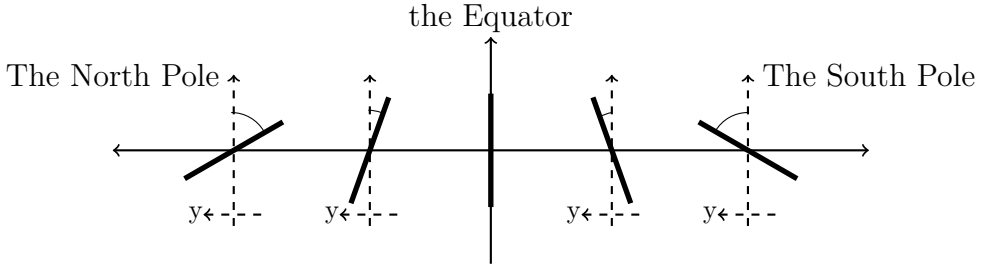


Figure 2: The figure presents the inclination of the particles orbits when the latitude increases. At the equator the orbit becomes vertical.

Before we proceed to proving the validity of the explicit solution (3) we want to provide a brief discussion about the particle trajectory. For the setting of a surface wave (cf. [30]), it is shown that the solution (3) with parameters for the surface waves describes circles, which also applies to the internal waves. A feature of the Pollard-like solution is that the path of a particle is a slightly tilted circle [30, 121] where the Gerstner-like solution describes circles in the vertical plane [54]. In the Pollard-like solution for the internal waves the top of the circle made by the particle is closer to the equator and the bottom of the circle deviates to the pole at an angle of inclination $\arctan(-d/a)$ to the local vertical, which is a reversed state to the one of the surface waves [30]. The angle of the inclination is increasing with the distance from the equator (Figure 2). The orbits of the water particles in three-dimensions are presented in Figure 3. The internal waves are in this setting in the shape of a trochoid (cf. [7]), whereas the surface wave is an inverted trochoid. The internal wave has narrow troughs and wide crests. The shape of the internal wave is depicted in Figure 4 taking into account the three-dimensional character. For a better explanation of the shape of the internal wave the intersection of the wave and the vertical plane is presented in Figure 5. Moreover, our setting of the internal wave evaluated on the equator particularises to the Gerstner-like equatorial internal wave solution [77]. Note that in Gerstner's and Pollard's surface waves [5, 30, 54, 121] the amplitude of wave oscillations decreases as we descend into fluid, which is a reverse of the present setting, whereby the amplitude of the internal waves decreases exponentially as we ascend above the thermocline [12, 13]. Let us now verify that (3) is indeed the exact solution of (2) representing the internal water waves. For notational convenience we set

$$\theta = k(q - ct).$$

We require

$$s \geq s^* > 0,$$

so that $e^{-ms} < 1$ throughout the layer $\mathcal{M}(t)$, since $ms \geq ks^* > 0$. The Jacobian of the map relating the particle positions to the Lagrangian labelling variables is given by

$$\begin{pmatrix} \frac{\partial x}{\partial q} & \frac{\partial y}{\partial q} & \frac{\partial z}{\partial q} \\ \frac{\partial x}{\partial r} & \frac{\partial y}{\partial r} & \frac{\partial z}{\partial r} \\ \frac{\partial x}{\partial s} & \frac{\partial y}{\partial s} & \frac{\partial z}{\partial s} \end{pmatrix} = \begin{pmatrix} 1 - kbe^{-ms}\cos\theta & kde^{-ms}\sin\theta & kae^{-ms}\sin\theta \\ 0 & 1 & 0 \\ mbe^{-ms}\sin\theta & mde^{-ms}\cos\theta & 1 + mae^{-ms}\cos\theta \end{pmatrix} \tag{4}$$

The flow is volume preserving and the condition of incompressibility (1) holds in the layer $\mathcal{M}(t)$ if and only if the determinant of the Jacobian is time independent and different than zero. The Jacobian determinant of (3) is precisely

$$J = 1 + (ma - kb)e^{-ms}\cos\theta - kmabe^{-2ms}.$$

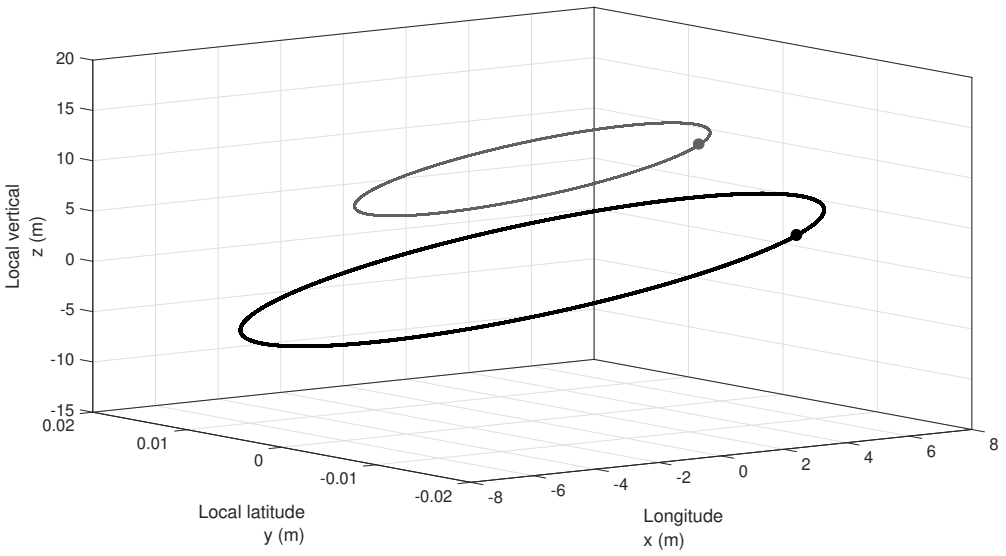


Figure 3: The path of the fluid particles when the wave propagates through water. The trajectory of the particle is a circle slightly tilted towards the equator. The parameters of the wave-induced motion at the thermocline are $a = 10$ m, $k = 6.28 \times 10^{-2} m^{-1}$, $\phi = 45°$N and $\Delta\rho/\rho_0 = 4 \times 10^{-3}$. We present the motion at two depths in the ocean. The mean difference of the depths is 10 m.

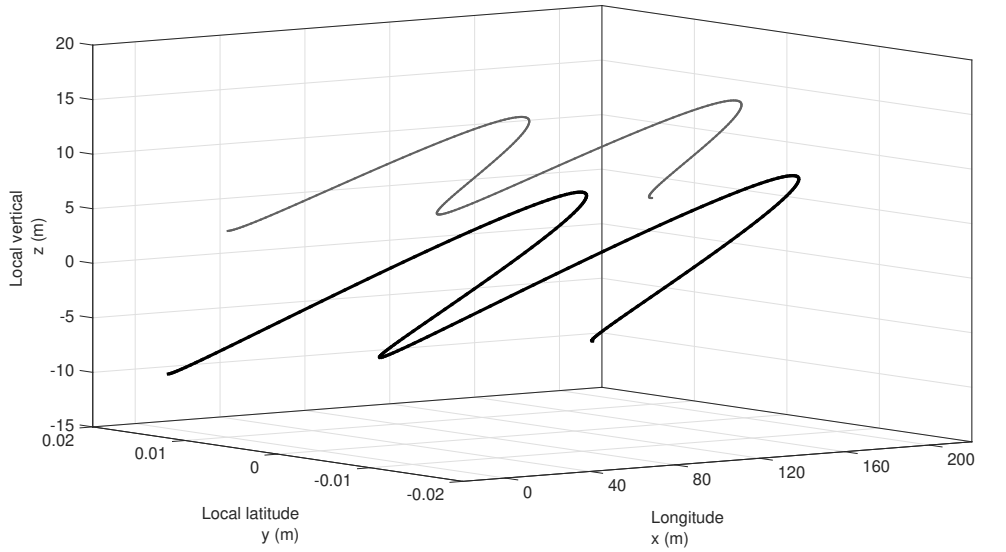


Figure 4: The trochoidal wave profile in three-dimensions representing the oscillation of the thermocline. The wave is evaluated at two depths in an ocean (the mean difference of the depths is 10 m) for $a = 10$ m, $k = 6.28 \times 10^{-2} m^{-1}$, $\phi = 45°$N and $\Delta\rho/\rho_0 = 4 \times 10^{-3}$ at the thermocline. The wave profile is slightly tilted toward the equator.

We need the condition

$$ma - kb = 0, \tag{5}$$

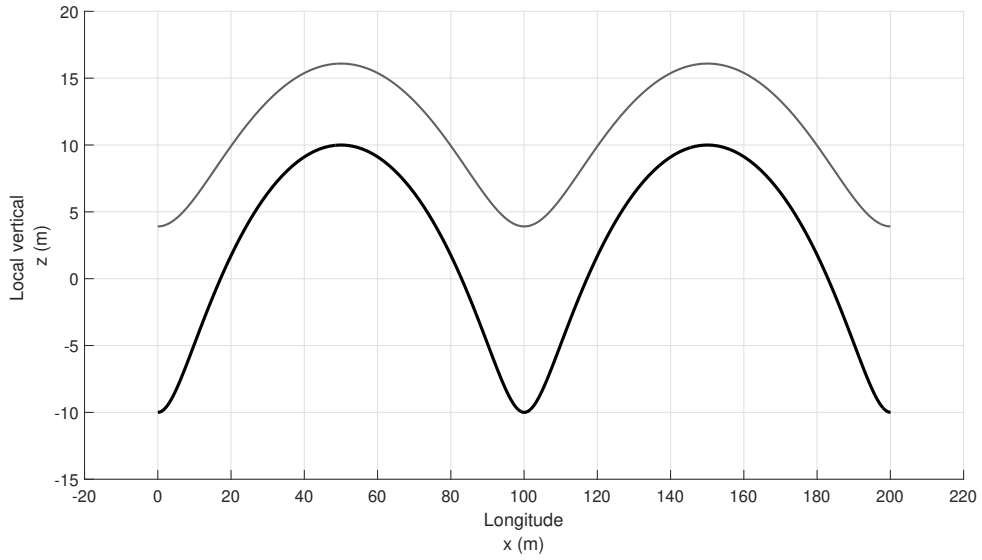


Figure 5: The projection on the vertical plane of the wave representing the oscillation of the thermocline for two different depths (the mean difference of the depths is 10 m) at the latitude $\phi = 45°$ on the Northern Hemisphere. The parameters of the wave at the thermocline are $a = 10$ m, $k = 6.28 \times 10^{-2} m^{-1}$, $\Delta\rho/\rho_0 = 4 \times 10^{-3}$. The amplitude of the internal wave decreases as we ascend above the thermocline. The internal water wave is in the shape of a trochoid with narrow troughs and wide crests.

to ensure that the determinant of the Jacobian is time independent. It follows that

$$mkabe^{-2ms} \neq 1,$$

throughout the flow in order to ensure a valid local diffeomorphism of (3) by means of the inverse function theorem. Due to the condition (5) and $s \geq s^* > 0$ the above statement implies

$$m^2 a^2 e^{-2ms^*} < 1. \tag{6}$$

From the explicit solution (3) we can deduce that the upper bound for the amplitude of internal waves is $1/m$. The Euler equations can be rewritten in the form

$$\begin{cases} \frac{Du}{Dt} + \hat{f}w - fv = -\frac{1}{\rho_0} P_x, \\ \frac{Dv}{Dt} + fu = -\frac{1}{\rho_0} P_y, \\ \frac{Dw}{Dt} - \hat{f}u = -\frac{1}{\rho_0} P_z - g, \end{cases} \tag{7}$$

where D/Dt is the material derivative. From the direct differentiation of the system of coordinates in (3), the velocity of each fluid particle may be expressed as

$$\begin{cases} u = \frac{Dx}{Dt} = kcbe^{-ms}\cos\theta, \\ v = \frac{Dy}{Dt} = -kcde^{-ms}\sin\theta, \\ w = \frac{Dz}{Dt} = -kcae^{-ms}\sin\theta, \end{cases} \tag{8}$$

and the acceleration is

$$\begin{cases} \frac{Du}{Dt} = k^2c^2be^{-ms}\sin\theta, \\ \frac{Dv}{Dt} = k^2c^2de^{-ms}\cos\theta, \\ \frac{Dw}{Dt} = k^2c^2ae^{-ms}\cos\theta. \end{cases}$$

Due to the velocity and acceleration in the Lagrangian setting we can write (7) as

$$\begin{aligned} P_x &= -\rho_0(k^2c^2b - kca\hat{f} + kcdf)e^{-ms}\sin\theta, \\ P_y &= -\rho_0 kc(kcd + bf)e^{-ms}\cos\theta, \\ P_z &= -\rho_0(k^2c^2ae^{-ms}\cos\theta - \hat{f}kcbe^{-ms}\cos\theta + g). \end{aligned} \tag{9}$$

Since

$$\begin{pmatrix} P_q \\ P_r \\ P_s \end{pmatrix} = \begin{pmatrix} \frac{\partial x}{\partial q} & \frac{\partial y}{\partial q} & \frac{\partial z}{\partial q} \\ \frac{\partial x}{\partial r} & \frac{\partial y}{\partial r} & \frac{\partial z}{\partial r} \\ \frac{\partial x}{\partial s} & \frac{\partial y}{\partial s} & \frac{\partial z}{\partial s} \end{pmatrix} \cdot \begin{pmatrix} P_x \\ P_y \\ P_z \end{pmatrix}$$

we have

$$\begin{aligned} P_q &= -\rho_0\Big[k^3c^2(a^2+d^2-b^2)e^{-ms}\cos\theta - \hat{f}kca + fkcd + k^2c^2b + kag\Big]e^{-ms}\sin\theta, \\ P_r &= -\rho_0 kc[kcd + bf]e^{-ms}cos\theta, \\ P_s &= -\rho_0\Big[k^2c^2m(a^2+d^2-b^2)e^{-2ms}\cos^2\theta - \hat{f}kcmabe^{-2ms} + fkcmbde^{-2ms} \\ &+k^2c^2b^2me^{-2ms} + (k^2c^2a - kcb\hat{f} + mag)e^{-ms}\cos\theta + g\Big]. \end{aligned} \tag{10}$$

Making a natural assumption that the pressure in $\mathcal{M}(t)$ has continuous second order mixed partial derivatives we obtain the following conditions

$$kcd + bf = 0, \tag{11}$$

$$mkc^2b + mcdf = k^2c^2a. \tag{12}$$

We note that the equation (11) implies by means of (9) that the pressure is independent of the variable y throughout the layer $\mathcal{M}(t)$. Moreover, the gradient of the following pressure distribution is precisely the right-hand side of (10)

$$P = -\rho_0\Big[-\frac{1}{2}k^2c^2(a^2+d^2-b^2)e^{-2ms}\cos^2\theta - \frac{1}{2}k^2c^2b^2e^{-2ms} + \frac{1}{2}\hat{f}kcabe^{-2ms}$$
$$-\frac{1}{2}fkcbde^{-2ms} + (ca\hat{f} - cdf - kc^2b - ag)e^{-ms}\cos\theta + gs\Big] + \tilde{P}_0.$$

For the Pollard-like internal water waves we define that

$$\begin{aligned} P_0 - \tilde{P}_0 = -\rho_0\Big[&-\frac{1}{2}k^2c^2(a^2+d^2-b^2)e^{-ms_0}\cos^2\theta - \frac{1}{2}k^2c^2b^2e^{-2ms_0} \\ &+\frac{1}{2}\hat{f}kcabe^{-2ms_0} - \frac{1}{2}fkcbde^{-2ms_0} + gs_0\Big] + \rho_+ gs_0, \end{aligned} \tag{13}$$

to satisfy the dynamic condition. The solution s_0 to the equation (13) represents the thermocline. The right-hand side of (13) is a strictly increasing diffeomorphism if

$$k > 4\Omega^2/\tilde{g} \approx 5\times 10^{-8}\mathrm{m}^{-1}, \tag{14}$$

where $\tilde{g} = g(\rho_0 - \rho_+)/\rho_0$ is called a coefficient of reduced gravity and $\Delta\rho/\rho_0 = 4\times 10^{-3}$ is a typical value for the equatorial region [93]. Therefore, taking $\beta_0 > P_0 - \tilde{P}_0$ we can determine the solution s_+ representing the interface $z = \eta_+$ between the layer $\mathcal{M}(t)$ and $\mathcal{L}(t)$. Additionally, we require the continuity of pressure across the thermocline, which yields

$$\rho_+ ga = \rho_0(kc^2b + cdf - ca\hat{f} + ag), \tag{15}$$

and pressure must be time independent hence

$$b^2 = a^2 + d^2.$$

From the equations (5) and (11) we get

$$b = \frac{ma}{k},$$

$$d = -\frac{fma}{k^2c}.$$

Therefore, the equation of continuity of the pressure (15) becomes

$$\rho_0^2 m^2(c^2k^2 - f^2)^2 = k^4(\rho_0 c\hat{f} + g(\rho_+ - \rho_0))^2, \tag{16}$$

Moreover, the condition (12) yields

$$m^2 = \frac{k^4 c^2}{k^2 c^2 - f^2},$$

where $m > 0$, otherwise if $m < 0$ the amplitude of the wave is increasing when we ascend above the thermocline. Furthermore, $m^2 > 0$ is ensured by (14) and $m = k$ at the equator. Summarizing the aforementioned facts we obtain the dispersion relation for the internal water waves describing the oscillation of the thermocline

$$\rho_0^2 c^2 (c^2 k^2 - f^2) = (\rho_0 c \hat{f} + g(\rho_+ - \rho_0))^2.$$

The dispersion relation can be simplified by including the coefficient of reduced gravity $\tilde{g} = g(\rho_0 - \rho_+)/\rho_0$. Consequently, we get

$$c^2 (c^2 k^2 - f^2) = (c\hat{f} + \tilde{g})^2. \tag{17}$$

Choosing suitable non-dimensional variables

$$X = c\sqrt{\frac{k}{\tilde{g}}} \qquad \epsilon = \frac{f}{\sqrt{\tilde{g}k}} \qquad F = \frac{\hat{f}}{f}, \tag{18}$$

the dispersion relation (17) can be rewritten as a polynomial equation of degree four $P(X) = 0$ where

$$P(X) = X^4 - \epsilon^2 (1 + F^2) X^2 - 2F\epsilon X - 1. \tag{19}$$

The roots of the polynomial $P(X)$ allows us to identify the wave speed by means of the non-dimensional variables. Moreover, we can prove that for fixed parameters there exist more than one phase speed and we can estimate the intervals containing the roots of (19) (see section (4)). The exact value of the roots can be found by Ferrari's method. However, we focus our attention only on the existence of the real roots of the polynomial $P(X)$. The relation $c = \sqrt{\tilde{g}/k}$ refers to a standard dispersion relation for the internal waves where the Coriolis parameters are neglected [133], which is analogous to the deep-water wave dispersion relation for surface waves [5, 7, 30, 54].

3.2 Equatorial region

Let us now consider the special case of a solution close to the equator in order to substantiate the validity of the Pollard-like solution. For the equatorial waves we take the Coriolis parameters

$$f = 0, \qquad \hat{f} = 2\Omega,$$

and as a result, the dispersion relation (17) reduces to

$$kc^2 - 2\Omega c - \tilde{g} = 0. \tag{20}$$

The solution to the quadratic equation (20) is

$$c = \frac{\Omega \pm \sqrt{\Omega^2 + k\tilde{g}}}{k},$$

which readily agrees with the result for the internal equatorial water waves in the f-plane obtained in [77].

3.3 Vorticity

The vorticity plays important part on the trajectory of fluid particles. For an irrotational gravity-driven flow the lack of vorticity ensures that the particle paths are open loops [6, 55]. For Gerstner-like rotational flows the particle path is a closed circle [5, 7, 54]. We prove that the Pollard-like solution we have constructed in (3) is indeed rotational which explains somewhat the fact that the particle paths are closed circles. The vorticity is obtained by considering the product

$$\left(\frac{\partial(q,r,s)}{\partial(x,y,z)}\right)\left(\frac{\partial(u,v,w)}{\partial(q,r,s)}\right) = \left(\frac{\partial(u,v,w)}{\partial(x,y,z)}\right), \tag{21}$$

where we exploit the inverse of (4) and the velocity field (8). Moreover, the matrix (21) yields that the velocity field of fluid in $\mathcal{M}(t)$ is independent of the variable y. We are now in position to calculate the vorticity in the layer $\mathcal{M}(t)$

$$\omega = (w_y - v_z, u_z - w_x, v_x - u_y) = \frac{1}{1 - m^2a^2e^{-2ms}} \times \begin{pmatrix} \dfrac{m^2af}{k} e^{-ms}\sin\theta \\ -c(m^2-k^2)ae^{-ms}\cos\theta + cma^2(m^2+k^2)e^{-2ms} \\ fma(\cos\theta - mae^{-ms})e^{-ms} \end{pmatrix}^T. \tag{22}$$

We can validate our result by considering the vorticity in the equatorial region. Taking the Coriolis parameters for the equatorial waves $f = 0$, $\hat{f} = 2\Omega$, the vorticity (22) takes the form

$$\omega = \frac{1}{1 - m^2a^2e^{-2ms}}(0, 2kcm^2a^2e^{-2ms}, 0),$$

where taking the critical value of the amplitude of waves $a = 1/m$ and $m = k$ we recover the vorticity for the internal equatorial water waves in the f-plane approximation [77]

$$\omega = \left(0, \frac{2kce^{-2ks}}{1 - e^{-2ks}}, 0\right),$$

and it also coincides with the vorticity in the β-plane approximation [12].

4 Solution of the dispersion relation

This section presents an analytic approach towards identifying the location of roots of the polynomial (19). If we can find the roots of the polynomial (19), we can discern a wave phase speed by means of the non-dimensional change of variables (18). Moreover, we show that the polynomial $P(X)$, which is of degree four, has only two real roots and both are of order $O(1)$ indicating two wave speeds. It is readily seen that the constants of (19) are positive on both hemispheres of Earth and we can perform an analysis of the polynomial (19) on both hemispheres simultaneously nonetheless, we exclude the equator since F is not defined there. We recall Cauchy's theorem [123].

Theorem. *Let $f(x) = x^n - b_1 x^{n-1} - ... - b_n$ where all b_i are non-negative and at least one of them is non-zero. The polynomial f has a unique (simple) positive root p and the absolute values of the other roots do not exceed p.*

According to Cauchy's theorem the polynomial $P(X)$ has a unique positive root $X_0^+ > 0$. However, the polynomial (19) still can have three negative roots. We can easily compute the first derivative of the polynomial $P(X)$

$$P'(X) = 4X^3 - 2\epsilon^2(1 + F^2)X - 2F\epsilon$$

and its discriminant

$$\Delta P'(X) = 128\epsilon^6(1 + F^2)^3 - 1728F^2\epsilon^2.$$

Making an assumption that we are outside the tropical zone, at latitudes exceeding $23°26'16"$, we have that $|F| < 2.4$. Since the water temperature in the subpolar regions of Earth is constant the thermocline does not have favorable conditions to exist there and to produce the internal wave motion [49]. Moreover, for the latitudes at most $15°$ away from the poles we have $|F| \geq 2 - \sqrt{3}$ and therefore, we infer that the polynomial $P'(X)$ for the mid-latitudes $(23°26'16" - 75°)$ has exactly one real root as

$$\Delta P'(X) < 0,$$

which means that the polynomial $P(X)$ has one critical point. Together with $P(0) = -1$, it proves that there exist one unique positive root $X_0^+ > 0$ and one unique negative root $X_0^- < 0$. For the polynomial $P(X)$ we can estimate

$$\begin{aligned} &P(\pm 1) = \mp 2\epsilon F + O(\epsilon^2) \\ &P(1 + \epsilon F) = 2\epsilon F + O(\epsilon^2) > 0 \\ &P(-1 + \epsilon F) = -2\epsilon F + O(\epsilon^2) < 0 \end{aligned} \tag{23}$$

since $F = O(1)$ and $\epsilon = O(10^{-2})$ for internal waves with the wavelength 150-250m. Hence, the estimates (23) yield that

$$X_0^+ - 1 \in (0, \epsilon F) \qquad X_0^- + 1 \in (0, \epsilon F).$$

for both hemispheres (see the result for the surface water waves in [30]). We have proved therefore the existence of two real roots of the polynomial (19). The exact wave speed for the internal water waves describing the oscillation of the thermocline can be found by the non-dimensional change of variables (18) indicating two phase speeds in dimensional terms close to

$$c \approx \pm\sqrt{\frac{\tilde{g}}{k}}.$$

Therefore, the analysis identifies one mode of the internal wave that is a standard internal wave $c = \sqrt{\tilde{g}/k}$ [133] very slightly modified by the Earth's rotation.

Physical flow properties for Pollard-like internal water waves

Mateusz Kluczek

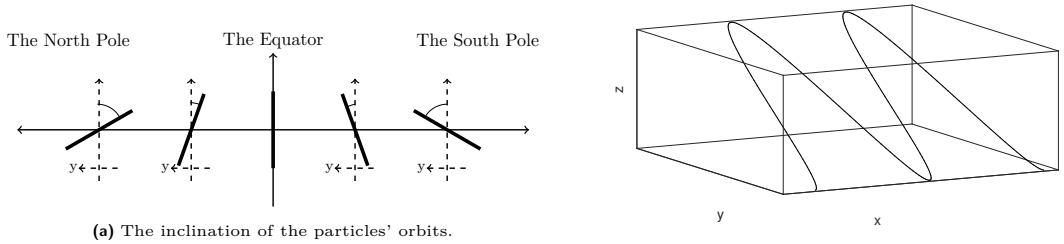
Journal of Mathematical Physics, 59:1–12, 2018.

Abstract We present study of the physical flow properties for a recently derived three-dimensional nonlinear geophysical internal wave solution. The Pollard-like internal wave solution is explicit in terms of Lagrangian labelling variables, enabling us to examine the mean flow velocities and mass flux in the three-dimensional setting. We show that the Pollard-like internal water wave does not have a net wave transport.

1 Introduction

This paper is devoted to an analysis of the mean flow properties for a recently derived [97] nonlinear geophysical internal water wave solution. In [97], the derived exact and explicit solution for internal water waves is a significant modification of the solution given by Pollard for surface waves [121]. The Pollard-like internal wave solution is explicit in terms of Lagrangian labelling variables, enabling us to examine the mean flow properties and mass transport, which in the case of the Pollard-like solution are three-dimensional vectors. Since particles paths in the internal water wave solution are circles tilted toward the equator (cf. Figure 1) we must distinguish the flow properties in the zonal, meridional and vertical direction.

The Gerstner-like solution represents a two-dimensional periodic travelling water



(a) The inclination of the particles' orbits.

(b) The schematic 3D profile of the internal water wave outside the equatorial region.

Figure 1: The figure of the inclination of the particles' orbits with an angle of inclination $\arctan(-d/a)$ increasing with latitude 1a, resulting in the three-dimensional profile 1b of the internal water wave [97].

wave with the particles' paths in the vertical plane [5, 136, 54, 64], whereas in the Pollard-like solution waves experience a slight cross-wave tilt [30, 97, 121]. Various Gerstner-like solutions of the geophysical fluid dynamic equations in the equatorial region were derived in particular to describe nonlinear internal water waves [12, 13] and wave-current interactions [60, 63, 95, 96, 127]. An analysis of the mean physical flow properties for those equatorially-trapped waves is presented in [75, 128]. A survey of this extensive research activity concerning the generalised Gerstner-like solutions is summarised in [66, 84, 90], and a discussion on the oceanographical relevance of those solutions can be found in [3].

The aim of this paper is to present an analysis of the physical flow properties for internal water waves. The internal water waves may describe the oscillation of a thermocline [23, 39, 135], which is an interface separating two layers of ocean water of different but constant densities in a stable stratification [39, 49, 135]; we remark that the mechanism of generation of the oscillation of the thermocline is out of the scope of this paper. The waves propagate over the thermocline with the amplitude decreasing with the height above the thermocline. The study of the thermocline and its interaction with surface waves and the Equatorial Undercurrent can be found in [23, 88].

The Pollard-like solution is an extension of the remarkable Gerstner solution by including the effects of the rotation of Earth [121]. In the paper [30], a Pollard-like solution was constructed to describe the wave-current interactions for surface waves. Moreover, the surface wave solution was subjected to the stability analysis [81, 83, 84] and it was proved by degree-theoretic methods to be globally dynamically possible [126]. Subsequently, in recent work by the author a new Pollard-like solution was constructed to model the internal water waves [97]. We use the newly developed Pollard-like solution for internal water waves to examine the mean physical flow properties, which serves as an opportunity to develop an understanding of the nature of oceanic flows on Earth [24].

2 Internal water waves – Pollard-like solution

2.1 Governing equations

We consider geophysical internal water waves, where we assume that Earth is a perfect sphere. The frame of reference is rotating with Earth whose origin is fixed at a point on Earth. In this case, the (x, y, z) Cartesian coordinates represent the directions of the longitude, latitude and local vertical, respectively. The governing equations for the geophysical water waves are given by [39]

$$\begin{cases} u_t + uu_x + vu_y + wu_z + 2\Omega w\cos\phi - 2\Omega v\sin\phi = -\dfrac{1}{\rho}P_x, \\ v_t + uv_x + vv_y + wv_z + 2\Omega u\sin\phi = -\dfrac{1}{\rho}P_y, \\ w_t + uw_x + vw_y + ww_z - 2\Omega u\cos\phi = -\dfrac{1}{\rho}P_z - g, \end{cases}$$

together with the equation of mass conservation

$$\rho_t + (u \cdot \nabla)\rho + \rho(\nabla \cdot u) = 0,$$

and the resulting equation for incompressibility

$$u_x + v_y + w_z = 0. \tag{1}$$

In those equations t stands for time, ϕ represents the latitude, (u, v, w) is the fluid velocity, $g = 9.81\text{m } s^{-2}$ is the gravitational acceleration on the Earth's surface, ρ is the water's density, and P is the pressure. The radius of Earth is assumed to be $R = 6371$ km and $\Omega = 7.29 \times 10^{-5}\text{rad } s^{-1}$ is a constant rotational speed of Earth. Since we investigate the flow in a relatively narrow strip less then few degrees [39], the Coriolis parameters

$$f = 2\Omega \sin\phi, \qquad \hat{f} = 2\Omega \cos\phi, \tag{2}$$

can be taken as constants. The typical values of the Coriolis parameters at the latitude of 45°N are $f = \hat{f} = 10^{-4}s^{-1}$ [53].

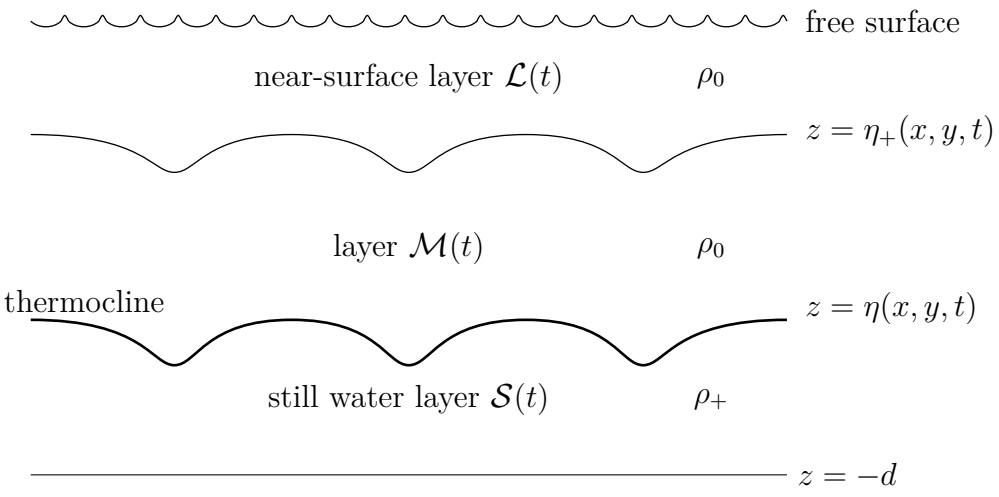


Figure 2: The figure presents the main regions of the flow at a fixed latitude y. The thermocline separates two layers of different densities $\rho_0 < \rho_+$ in a stable stratification. The internal wave is described by a trochoid propagating with a speed c. The amplitude of the internal water wave decreases exponentially. At the depth of half a wavelength above the thermocline the amplitude is reaching 4% of its initial value at the thermocline.

The solution to the governing equations constructed in [97] describes internal waves representing the oscillation of a thermocline. The thermocline is defined as an interface separating layers of ocean water of two constant but different densities [39, 49]. The layer $\mathcal{M}(t)$ of less dense, warmer ocean water of density ρ_0 overlays the layer $\mathcal{S}(t)$ of colder, more dense water with density $\rho_+ > \rho_0$. The thermocline

is denoted by $z = \eta(x, y, t)$, where there is a dramatic jump in the density of water. The oscillation of the thermocline propagates in the layer $\mathcal{M}(t)$. The layer $\mathcal{M}(t)$ is finite and is bounded by the interface $z = \eta_+(x, y, t)$, above which we have the near-surface layer $\mathcal{L}(t)$. We can consider the layer $\mathcal{M}(t)$ as finite since the amplitude of internal waves decreases exponentially as we ascend above the thermocline and at the height of half a wavelength the amplitude is 4% of its value at the thermocline (cf. [9]). The geophysical internal wave motion, for the purpose of this model, can be neglected in the near-surface layer, since the wave motion there is only a small perturbation of the surface generated primarily by the wind. The schematic is presented in Figure 2. The assumption of still water under the thermocline is expressed as

$$(u, v, w) = (0, 0, 0) \text{ for } z < \eta(x, y, t),$$

it implies the hydrostatic pressure in the layer $\mathcal{S}(t)$

$$P = P_0 - \rho_+ g z \text{ for } z < \eta(x, y, t).$$

We have to emphasise that close to the thermocline there is a region of high shear and strong stratification. Therefore, the velocity field is continuous in the normal direction at the thermocline, on the other hand it can be or even is discontinuous in the tangential direction. The assumption of a hydrostatic still water layer $\mathcal{S}(t)$ is a rather strong assumption in this context, however it still represents a complex (if quite simplified) model whereby a nonlinear exact internal geophysical wave solution can be constructed at mid latitudes. It is hoped that future work may result in an exact solution for a more physically realistic nonhydrostatic layered model (as exists for internal equatorial waves in [13]), yet this situation promises to be vastly more complex and technical mathematically due to the fact that flows are not considered to be purely equatorial. Nevertheless, it appears that the simplified model that we include in this paper manages to capture the salient geophysical features of flows.

In the f-plane approximation the governing equations of the internal water waves in the layer $\mathcal{M}(t)$ are

$$\begin{cases} u_t + uu_x + vu_y + wu_z + \hat{f}w - fv = -\dfrac{1}{\rho_0} P_x, \\ v_t + uv_x + vv_y + wv_z + fu = -\dfrac{1}{\rho_0} P_y, \\ w_t + uw_x + vw_y + ww_z - \hat{f}u = -\dfrac{1}{\rho_0} P_z - g. \end{cases} \tag{3}$$

which are coupled with the boundary conditions

$$P = P_0 - \rho_+ g z \text{ on the thermocline } z = \eta(x, y, t), \tag{4}$$

$$w = \eta_t + u\eta_x + v\eta_y \text{ on the thermocline } z = \eta(x, y, t). \tag{5}$$

The first equation is the dynamic condition and the second is the kinematic condition. The kinematic condition prevents mixing of particles between layers.

2.2 Exact and explicit solution

In this section we briefly describe a recently constructed exact and explicit solution for internal water waves [97], which is described in terms of Lagrangian labelling variables [2]. It represents a periodic internal wave propagating zonally with a wave speed c. The Lagrangian positions (x, y, z) of a fluid particle are given as functions of the labelling variables (q, r, s), time t and real parameters a, b, c, d, k, m. However, the parameters b, c, d must be suitably chosen in terms of k, m, a. The explicit solution to the governing equation (3) satisfying the incompressibility condition is given by [97]

$$\begin{cases} x = q - be^{-ms}\sin[k(q-ct)], \\ y = r - de^{-ms}\cos[k(q-ct)], \\ z = s - ae^{-ms}\cos[k(q-ct)]. \end{cases} \tag{6}$$

The constant $k = 2\pi/L$ is the wavenumber corresponding to the wavelength L, with the parameter q covering the real line. The solution is set up around a fixed latitude ϕ and therefore $r \in [-r_0, r_0]$, for some r_0. For every fixed value of $r \in [-r_0, r_0]$, we require $s \in [s_0, s_+]$, where the choice $s = s_0 \geq s^* > 0$ represents the thermocline $z = \eta(x, y, t)$ at the fixed latitude, while $s = s_+ > s_0$ prescribes the upper boundary $z = \eta_+(x, y, t)$ at the same latitude. The remaining parameters are defined to be positive: $a > 0$, $k > 0$ and $m > 0$ for waves with a decreasing amplitude as we ascend above the thermocline. For notational convenience we set

$$\theta = k(q - ct).$$

The Jacobian of the map (6) is given by

$$\left(\frac{\partial(x,y,z)}{\partial(q,r,s)}\right) = \begin{pmatrix} 1 - kbe^{-ms}\cos\theta & kde^{-ms}\sin\theta & kae^{-ms}\sin\theta \\ 0 & 1 & 0 \\ mbe^{-ms}\sin\theta & mde^{-ms}\cos\theta & 1 + mae^{-ms}\cos\theta \end{pmatrix} \tag{7}$$

The Jacobian determinant is precisely $J = 1 + (ma - kb)e^{-ms}\cos\theta - m^2a^2e^{-2ms}$ and is time-independent if

$$b = \frac{ma}{k}. \tag{8}$$

Thus, the flow is volume preserving and the condition of incompressibility holds. Moreover, the amplitude of waves decreases when we ascend above the thermocline, which implies

$$m^2 a^2 e^{-2ms^*} < 1, \tag{9}$$

and it also ensures, by means of the inverse function theorem, a local diffeomorphic character of (6). In this solution the maximum amplitude of internal waves is $1/m$. The velocity and acceleration of each fluid particle is obtained by taking the derivative of (6)

$$\begin{cases} u = \frac{Dx}{Dt} = kcbe^{-ms}\cos\theta, \\ v = \frac{Dy}{Dt} = -kcde^{-ms}\sin\theta, \\ w = \frac{Dz}{Dt} = -kcae^{-ms}\sin\theta, \end{cases} \tag{10}$$

where D/Dt is the material derivative. Checking that the velocity field (10) satisfies the governing equations (3) is equivalent to obtaining a suitable pressure (cf. [97]). Moreover, we get following conditions, which define the relation between the parameters of the Pollard-like solution

$$d = -\frac{maf}{k^2 c}, \quad mkc^2 b + mcdf = k^2 c^2 a, \quad a^2 + d^2 = b^2.$$

Finally, the dynamic boundary condition (4) leads to the dispersion relation for the internal water waves

$$c^2(c^2k^2 - f^2) = (c\hat{f} + \tilde{g})^2, \tag{11}$$

where $\tilde{g} = g(\rho_+ - \rho_0)/\rho_0$ is a coefficient of reduced gravity. Choosing suitable non-dimensional variables

$$X = c\sqrt{\frac{k}{\tilde{g}}}, \qquad \epsilon = \frac{f}{\sqrt{\tilde{g}k}}, \qquad F = \frac{\hat{f}}{f},$$

the dispersion relation (11) can be rewritten as a polynomial equation of degree four

$$P(X) = X^4 - \epsilon^2(1 + F^2)X^2 - 2F\epsilon X - 1 = 0, \tag{12}$$

with two roots, one positive and one negative

$$X_0^+ - 1 \in (0, \epsilon F) \qquad X_0^- + 1 \in (0, \epsilon F),$$

for mid-latitudes $\phi \in (23°26'16", 75°)$ on both hemispheres of Earth (cf. [97]). Although, we solved the polynomial equation in the mid-latitudes, we note that the exact solution (6) and the dispersion relation (11) can be reduced since f vanishes in the equatorial region. In this case both, the solution and dispersion relation, particularise directly to a recently derived Gerstner-like solution and its dispersion relation in the f-plane [77].

3 Mean flow properties

In this section we examine and describe the physical properties of the flow in the presence of the wave motion. We examine the mean velocities, the Stokes drift and the mass flux for the internal water waves. An advantage of the transition from the Eulerian to the Lagrangian description of the flow is that we can relatively easily calculate the mean Eulerian and Lagrangian velocity. The mean Eulerian velocity is considered as the mean velocity of the flow at a fixed point, whereas the mean Lagrangian velocity is the mean velocity of a marked water particle. Moreover, the mass transport velocity arises from the mean Lagrangian velocity rather than the mean Eulerian velocity, which was noted by Stokes [131]. As a consequence we can present the Stokes drift $\mathbf{U}^S$, which is the difference between the mean Lagrangian $\langle \mathbf{u} \rangle_L$ and the mean Eulerian $\langle \mathbf{u} \rangle_E$ velocity [100, 101]

$$\mathbf{U}^S = \langle \mathbf{u} \rangle_L - \langle \mathbf{u} \rangle_E \,, \tag{13}$$

where $\mathbf{u} = (u, v, w)$ is a vector with the components of the velocity in the longitudinal, latitudinal and vertical direction, respectively. The mean flow properties are considered as three-dimensional since the particles' paths are circles slightly tilted toward the equator and the particles' motion is purely three-dimensional.

3.1 Lagrangian mean velocity

From the exact solution (6) we calculated the flow velocity in the Lagrangian setting. The explicit velocity in terms of the Lagrangian labelling variables is used to find the mean Lagrangian flow. Taking the average of the velocity over the period $T = \frac{L}{c}$ we obtain the zonal mean Lagrangian velocity

$$\langle u \rangle_L = \frac{1}{T} \int_0^T u(q - ct, r, s)\, dt = \frac{1}{T} \int_0^T kcbe^{-ms} \cos\theta dt = 0,$$

next, we get the meridional mean velocity

$$\langle v \rangle_L = \frac{1}{T} \int_0^T v(q - ct, r, s)\, dt = -\frac{1}{T} \int_0^T kcde^{-ms} \sin\theta dt = 0,$$

and finally, the vertical mean velocity

$$\langle w \rangle_L = \frac{1}{T} \int_0^T w(q - ct, r, s)\, dt = -\frac{1}{T} \int_0^T kcae^{-ms} \sin\theta dt = 0.$$

As the integral of the trigonometric functions over the wave period is equal to zero, all of the components of the mean Lagrangian velocity are zero.

3.2 Eulerian mean velocity

The mean Eulerian velocity is computed by taking the average of the velocity over the wave period at any fixed depth. First we fix a depth z_0 over the crest of the

thermocline and under the trough of the upper boundary $z^c < z_0 < z_+^t$, where z^c represents the level of crest of the thermocline $z = \eta(x, y, t)$ and z_+^t represents the level of trough of the boundary $z = \eta_+(x, y, t)$. The crests and troughs of the thermocline are given by

$$z^c = s_0 + ae^{-ms_0}, \qquad z^t = s_0 - ae^{-ms_0},$$

and the crests and troughs of the interface $z = \eta_+(x, y, t)$ between the layers $\mathcal{M}(t)$ and $\mathcal{L}(t)$ are

$$z_+^c = s_+ + ae^{-ms_+}, \qquad z_+^t = s_+ - ae^{-ms_+},$$

respectively. The fixed depth z_0 is characterised by

$$z_0 = s - ae^{-ms}\cos\theta, \tag{14}$$

where $s = S(z_0, q, t)$. Taking the derivative with respect to the variable q of the equation (14) we get

$$S_q = -\frac{kae^{-ms}\sin\theta}{1 + mae^{-ms}\cos\theta}.$$

We introduce following equation in order to obtain the zonal mean Eulerian velocity

$$\begin{aligned} c + \langle u\rangle_E(z_0) &= \frac{1}{T}\int_0^T [c + u(x - ct, y, z_0)]\, dt = \frac{1}{L}\int_0^L [c + u(x - ct, y, z_0)]\, dx = \\ &= \frac{1}{L}\int_0^L [c + u(q - ct, z_0)]\frac{\partial x}{\partial q}\, dq = \\ &= \frac{1}{L}\int_0^L (c + kcbe^{-ms}\cos\theta)\frac{1 - a^2m^2e^{-2ms}}{1 + mae^{-ms}\cos\theta}\, dq = \\ &= c - \frac{m^2a^2c}{L}\int_0^L e^{-2mS}\, dq. \end{aligned}$$

It implies that the zonal mean Eulerian velocity is

$$\langle u\rangle_E(z_0) = -\frac{m^2a^2c}{L}\int_0^L e^{-2mS} dq,$$

indicating a nonuniform wave-induced current, whereas $\langle u\rangle_E(z_0) \in (-m^2a^2c, 0)$ for $c > 0$ and $\langle u\rangle_E(z_0) \in (0, m^2a^2c)$ for $c < 0$. The Pollard-like solution in the equatorial region particularises to the Gerstner-like solution since f vanishes in the equatorial region. Therefore, substituting the parameters for the equatorial region and the critical value of the amplitude parameter $a = 1/m$ into the zonal Eulerian velocity, the zonal mean Eulerian velocity recalls the mean velocity for the equatorial waves in the f-plane [77].

Subsequently, we can compute the meridional mean Eulerian velocity

$$\begin{aligned}\langle v\rangle_E(z_0) &= \frac{1}{T}\int_0^T v(x-ct,y,z_0)\,dt = \\ &= \frac{1}{L}\int_0^L v(x-ct,y,z_0)\,dx = \frac{1}{L}\int_0^L v(q-ct,z_0)\frac{\partial x}{\partial q}\,dq = \\ &= \frac{1}{L}\int_0^L -kcde^{-mS}\sin\theta\frac{1-m^2a^2e^{-2mS}}{1+mae^{-mS}\cos\theta}\,dq = \\ &= \frac{fma}{kL}\int_0^L e^{-mS}\sin\theta\frac{1-m^2a^2e^{-2mS}}{1+mae^{-mS}\cos\theta}\,dq.\end{aligned}$$

We can estimate the meridional mean Eulerian velocity as

$$|\langle v\rangle_E(z_0)| < \frac{fma}{kL}\int_0^L e^{-mS}(1+mae^{-mS})\,dq,$$

keeping in mind that f changes sign across the equator. Moreover, for the equatorial internal water waves the Coriolis parameter is equal to zero ($f=0$) and the meridional mean Eulerian velocity vanishes. As we know, at the equator the orbits of particles are vertical and the particles do not move in the meridional direction [12, 77], which confirms the absence of the meridional mean velocity. Following the steps above we can find the vertical mean Eulerian velocity

$$\begin{aligned}\langle w\rangle_E(z_0) &= \frac{1}{T}\int_0^T w(x-ct,y,z_0)\,dt = \\ &= \frac{1}{L}\int_0^L w(x-ct,y,z_0)\,dx = \frac{1}{L}\int_0^L w(q-ct,z_0)\frac{\partial x}{\partial q}\,dq = \\ &= \frac{1}{L}\int_0^L -kcae^{-mS}\sin\theta\frac{1-m^2a^2e^{-2mS}}{1+mae^{-mS}\cos\theta}\,dq = \\ &= -\frac{kca}{L}\int_0^L e^{-mS}\sin\theta\frac{1-m^2a^2e^{-2mS}}{1+mae^{-mS}\cos\theta}\,dq,\end{aligned}$$

where it is estimated to be

$$|\langle w\rangle_E(z_0)| < \frac{kca}{L}\int_0^L e^{-mS}(1+mae^{-mS})\,dq.$$

However, we have to be aware that the phase speed c can be negative or positive in the case of Pollard-like solutions in the f-plane approximation.

3.3 Stokes drift

Finally, we can compute the Stokes drift in the longitudinal, meridional and vertical direction. From the definition (13) we obtain the zonal Stokes drift

$$U^S(z_0) = \frac{m^2a^2c}{L}\int_0^L e^{-2mS}dq,$$

the meridional Stokes drift

$$V^S(z_0) = -\frac{fma}{kL}\int_0^L e^{-mS}\sin\theta\frac{1-m^2a^2e^{-2mS}}{1+mae^{-mS}\cos\theta}dq,$$

and the vertical Stokes drift

$$W^S(z_0) = \frac{kca}{L}\int_0^L e^{-mS}\sin\theta\frac{1-m^2a^2e^{-2mS}}{1+mae^{-mS}\cos\theta}dq.$$

The meridional Stokes drift is zero for the equatorially-trapped internal water waves since $f = 0$ at the equator. The zonal Stokes drift in the case of the Pollard-like solution is a generalised formula of the Stokes drift obtained in [77]. Considering the critical value of the amplitude parameter a at the equator, which is $a = 1/m$, the zonal Stokes drift reduces to the Stokes drift for the equatorial internal water waves in the f-plane [77].

3.4 Mass flux

To conclude the paper we calculate the mass flux in the layer $\mathcal{M}(t)$. An advantage of this model is that we consider the mass flux in the restricted layer $\mathcal{M}(t)$ which indicate that the mass flux is finite. As the motion of water particles is three-dimensional we consider the flux through three planes. The mass flux through any plane S is defined as [122]

$$m = \int\limits_S \rho\mathbf{u}\cdot\mathbf{n}dS, \tag{15}$$

where $\mathbf{n}$ is the normal vector to the surface S.

Zonal mass flux

We begin with the mass flux in the longitudinal direction m^{zonal}. We fix at the point $x = x_0$ the plane $S = [\eta, \eta_+]\times[y_1, y_2]$, where $y_1 < y_2$. The zonal mass flux is given by

$$m^{zonal} = \iint\limits_{[\eta,\eta_+]\times[y_1,y_2]} u(x_0-ct,y,z)dydz = \int\limits_{s_0}^{s_+}\int\limits_{-r_0}^{r_0} u\begin{vmatrix}\frac{\partial y}{\partial r} & \frac{\partial y}{\partial s}\\ \frac{\partial z}{\partial r} & \frac{\partial z}{\partial s}\end{vmatrix}drds, \tag{16}$$

after changing to the Lagrangian labelling variables. The fixed point $x = x_0$ implies a functional relationship $q = \gamma(x_0, s, t)$. Taking the derivative of

$$x_0 = q - be^{-ms}\sin\theta,$$

with respect to the variable s we obtain

$$\gamma_s = -\frac{bme^{-ms}\sin\theta}{1 - mae^{-ms}\cos\theta}. \tag{17}$$

From (6) we have $\frac{\partial y}{\partial r} = 1$ and $\frac{\partial z}{\partial r} = 0$, which implies that the determinant of the Jacobian in (16) is exactly $J = \frac{\partial z}{\partial s}$. Using (17) we can easily find

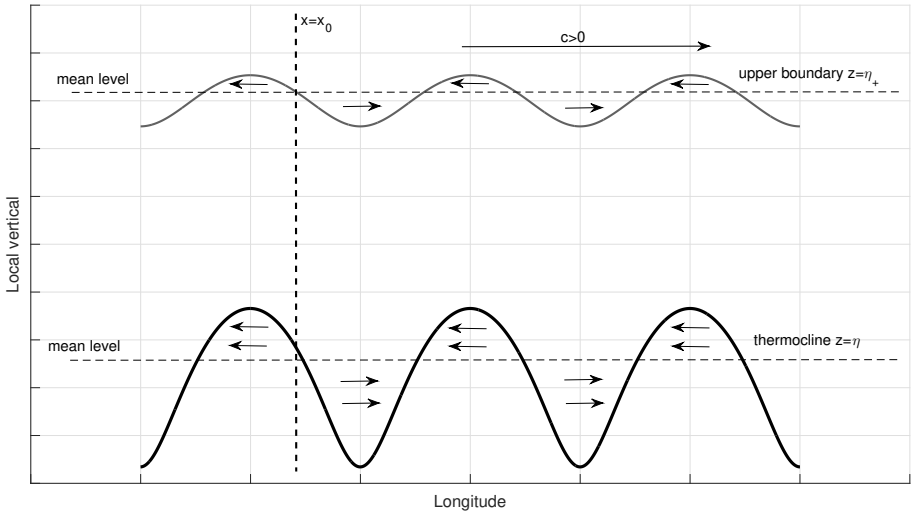


Figure 3: The instantaneous zonal mass flux for the eastward-propagating wave $c > 0$. The direction of the mass flux in this case is negative for the crest and positive for the trough of wave, since $\cos\theta = \mp 1$, respectively. It is independent of the Earth's hemisphere, however the direction of mass flux is reversed if we consider $c < 0$.

$$\frac{\partial z}{\partial s} = \frac{1 - m^2a^2e^{-2ms}}{1 - mae^{-ms}\cos\theta}.$$

Therefore, the zonal mass flux per unit of width is precisely

$$\begin{aligned} m^{zonal} &= \int_{s_0}^{s_+} kcbe^{-ms}\cos\theta\frac{1 - m^2a^2e^{-2ms}}{1 - mae^{-ms}\cos\theta}ds = \\ &= cma\int_{s_0}^{s_+} e^{-ms}\cos\theta\frac{1 - m^2a^2e^{-2ms}}{1 - mae^{-ms}\cos\theta}ds, \end{aligned} \tag{18}$$

The example of an instantaneous zonal mass flux is presented in Figure 3. From the explicit form of the mass flux we can conclude that the zonal mass flux stays unchanged in terms of the Northern or Southern Hemisphere, since it is independent of the Coriolis parameter f, but depends on the wave phase speed c. If we consider the parameter of amplitude $a = 1/m$ at the equator the zonal mass flux (18) reassembles the expression of the mass flux obtained in [77] for the equatorial internal waves in the f-plane. Moreover, we can show that the average mass flux over a wave period is equal to zero. From the fixed point $x = x_0$ we get

$$\gamma_t = -\frac{mace^{-ms}\cos\theta}{1 - ame^{-ms}\cos\theta},$$

for a T-periodic function $t \mapsto \gamma(x_0, s, t)$. Therefore, the time average of the mass flux over a wave period T is zero, which is expected since the mean Lagrangian velocity is zero $\langle u \rangle_L = 0$.

Meridional mass flux

In the next step we compute the meridional mass flux by fixing at a point $y = y_0$ a plane $S = [\eta, \eta_+] \times [0, L]$. From (15) we have

$$m^{meridional} = \iint\limits_{[\eta,\eta_+]\times[0,L]} v(x - ct, y_0, z)dxdz = \int\limits_{s_0}^{s_+}\int\limits_{0}^{L} v \begin{vmatrix} \frac{\partial x}{\partial q} & \frac{\partial x}{\partial s} \\ \frac{\partial z}{\partial q} & \frac{\partial z}{\partial s} \end{vmatrix} dqds,$$

in terms of the Lagrangian labelling variables. The variables x, z of (6) are independent of r, therefore without making any assumption of any functional relationship in $y = y_0$ we obtain

$$\begin{vmatrix} \frac{\partial x}{\partial q} & \frac{\partial x}{\partial s} \\ \frac{\partial z}{\partial q} & \frac{\partial z}{\partial s} \end{vmatrix} = \begin{vmatrix} 1 - mae^{-ms}\cos\theta & mbe^{-ms}\sin\theta \\ kae^{-ms}\sin\theta & 1 + mae^{-ms}\cos\theta \end{vmatrix} = 1 - m^2a^2e^{-2ms}.$$

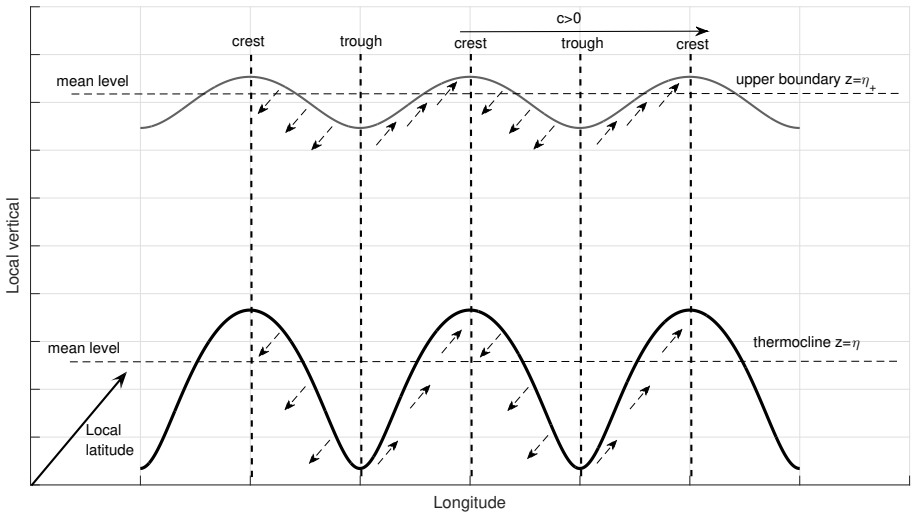


Figure 4: The schematic of the instantaneous meridional mass flux for the eastward-propagating wave $c > 0$ on the Northern Hemisphere. For the crest and troughs of the wave the meridional mass flux vanishes since $\sin\theta = 0$ at those points. If we consider this scenario on the Southern Hemisphere, the direction of the instantaneous mass flux is reversed. However, the meridional mass flux stays unchanged if we take the westward-propagating wave $c < 0$.

Thus the meridional mass flux per unit length is

$$m^{meridional} = \frac{1}{L}\int_{s_0}^{s_+}\int_0^L -kcde^{-ms}\sin\theta(1-m^2a^2e^{-2ms})dqds = \\ = \frac{fma}{kL}\int_{s_0}^{s_+}\int_0^L e^{-ms}\sin\theta(1-m^2a^2e^{-2ms})dqds. \tag{19}$$

The average of the meridional mass flux over the wave period T is equal to zero. The integrand in (19) depends on the sine function and $\int_0^T \sin\theta dt = 0$. The vanishing meridional mass flux over the wave period is a natural result since the meridional mean velocity is zero $\langle v\rangle_L = 0$. The meridional mass flux is independent of the direction of wave propagation c, however it depends on the hemisphere of Earth. An instantaneous meridional mass flux is depicted in Figure 4. Furthermore, for the equatorial internal water wave $f = 0$ and the meridional mass flux is zero all times. This is reasonable, because for the equatorial internal waves the particles' orbits are vertical and there is no motion in the meridional direction indicating any meridional mean Lagrangian velocity.

Vertical mass flux

Finally, we can present the vertical mass flux. We fix a point $z^c < z_0 < z_+^t$ between the crest of the thermocline z^c and the trough z_+^t of the interface between $\mathcal{M}(t)$ and $\mathcal{L}(t)$

$$z_0 = s - ae^{-ms}\cos\theta, \text{ where } s = \beta(z_0, q, t). \tag{20}$$

At the point $z = z_0$ we fix the plane $S = [0, L] \times [y_1, y_2]$ and the vertical mass flux in the Lagrangian labelling variable is

$$m^{vertical} = \iint\limits_{[0,L]\times[y_1,y_2]} w(x-ct, y, z_0)dxdy = \int\limits_0^L\int\limits_{-r_0}^{-r_0 1} w\begin{vmatrix}\frac{\partial x}{\partial q} & \frac{\partial x}{\partial r}\\ \frac{\partial y}{\partial q} & \frac{\partial y}{\partial r}\end{vmatrix} dqdr.$$

Since $\frac{\partial x}{\partial r} = 0$ and $\frac{\partial y}{\partial r} = 1$, we have that the Jacobian determinant of the transformation is precisely $J = \frac{\partial x}{\partial q}$. Taking the derivative of (20) with respect to q we get

$$\beta_q = -\frac{kae^{-m\beta}\sin\theta}{1 + mae^{-m\beta}\cos\theta},$$

which yields

$$\frac{\partial x}{\partial q} = \frac{1 - m^2a^2e^{-2m\beta}}{1 + mae^{-m\beta}\cos\theta}.$$

Following the above, we obtain the vertical mass flux per unit width

$$m^{vertical} = -kca \int_0^L e^{-m\beta} \sin\theta \frac{1 - m^2 a^2 e^{-2m\beta}}{1 + mae^{-m\beta} \cos\theta} dq. \tag{21}$$

The Figure 5 presents the schematic of the instantaneous vertical mass flux. The direction of the vertical mass flux depends on the direction of the wave propagation, but is independent of the Earth's hemisphere.

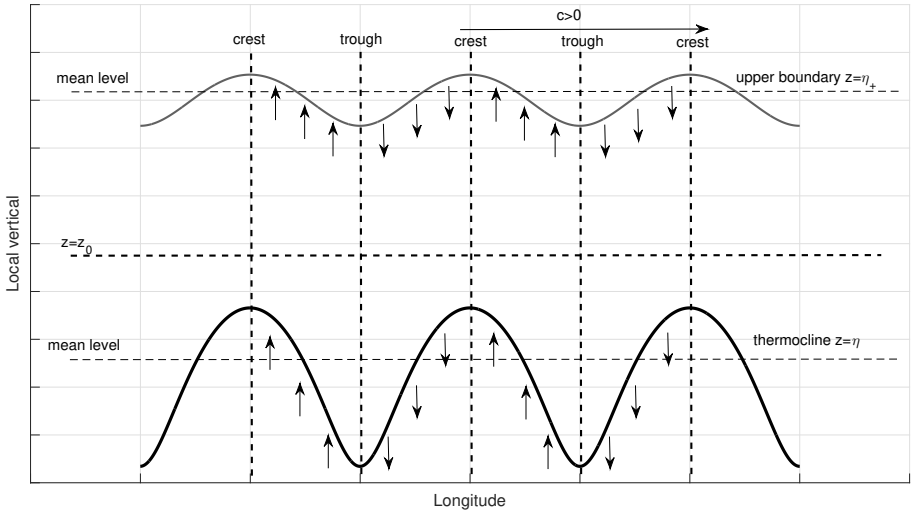


Figure 5: The instantaneous vertical mass flux for the eastward-propagating wave $c > 0$. For the westward-propagating wave the state is reversed, although it is unaltered after change of the Earth's hemisphere. The instantaneous mass flux is zero for the crests and troughs of the wave, since $\sin\theta = 0$ at those points.

Furthermore, we obtain

$$\beta_t = \frac{kcae^{-m\beta} \sin\theta}{1 + mae^{-m\beta} \cos\theta},$$

for a T-periodic function $t \mapsto \beta(q, t, z_0)$. If we consider β_t we can see that the time average of the vertical mass flux over a wave period is zero. We proved that the vertical mean Lagrangian velocity is zero $\langle w \rangle_L = 0$. Therefore, it is reasonable that the total vertical mass flux over a wave period vanishes. In conclusion, we have proved that the Pollard-like internal wave solution has no net wave transport over the wave period.

Discussion

In this paper we considered a new Pollard-like internal water wave solution which is a remarkable extension of Pollard's solution [121] to describe nonlinear internal water waves, whereas Pollard's solution is a modification of Gerstner's solution [136] to vertically stratified fluid in a rotating system. The wave in the Pollard-like solution experiences a cross-wave tilt and particles move in planes slightly tilted

to the vertical [30, 121], where in the Gerstner-like solutions [5, 136, 77] the path of particles is contained in parallel vertical planes. We analysed the mean flow velocities of the flow which are three-dimensional vectors, since the Pollard-like solution represents a fully three-dimensional periodic zonally travelling wave, in contrast to the mean velocities derived for the equatorially-trapped waves [75, 128]. In papers [12, 75, 77, 128] the mean velocities and mass flux are presented only in the zonal direction. Although, in [12, 75, 128] the three-dimensional effect is captured by considering the decay of the amplitude of waves in the meridional direction, the solution represents a two-dimensional wave, therefore the physical properties are considered only in the zonal direction. However, two-dimensional mean velocities and mass transport were presented for the equatorial flows in the f-plane in the case of solutions including a transverse variable current [96, 127]. Recent studies considered Gerstner-like solutions in a region close to the equator [12, 13, 77, 96, 127], whereas a study here considers a Pollard-like solution which is not only three-dimensional without underlying currents but also valid for mid-latitudes, which is a significant improvement and extension of exact and explicit solutions for nonlinear geophysical flows.

Summarising the results, we proved that the mean Lagrangian mean velocities over a wave period are equal to zero. We calculated the Stokes drift and, although there exists a hallmark of Stokes drift, it is balanced by the mean Eulerian velocity. According to [101] the mean Lagrangian velocity is being called sometimes mass-transport velocity, and it represents somewhat the mass transport in oceans. Arguing along this line we showed that the mass flux vanishes over a wave period resulting in a zero net wave transport, which is expected since the mean Lagrangian velocities are zero.

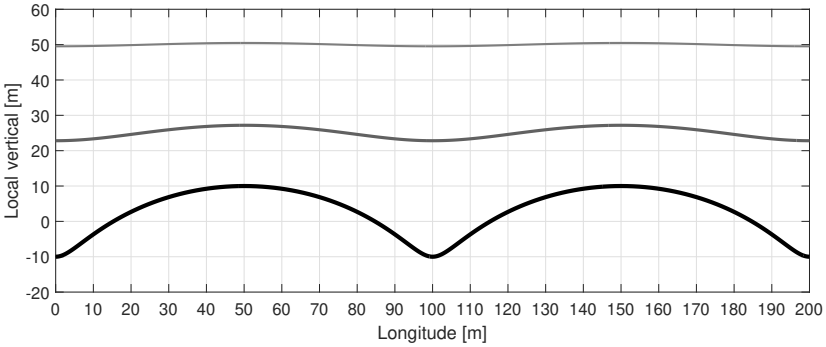


Figure 6: This figure presents the internal wave amplitude. The wave propagating at the thermocline is set to have the wavelength $L = 100$m and $k = 6.28 \times 10^{-2} m^{-1}$. The wave propagates at a latitude $\phi = 45°N$ with $\Delta\rho/\rho = 6 \times 10^{-3}$. Taking the amplitude of the oscillation of the thermocline 10m, the amplitude of wave at the hight 25m and 50m above the thermocline is 2.11m and 0.4m, respectively.

A quantitative discussion can be done as follow. Let us consider the latitude $\phi = 45°N$ and the difference in the density $\Delta\rho/\rho = 6\times10^{-3}$. The wave of the wavelength $L = 100$m is associated with the wavenumber $k \approx 0.0628 m^{-1}$ and yields the phase speed in the considered model $c \approx -0.9671$m s^{-1} or $c \approx 0.9687$m s^{-1}, whereas the

phase speed of a standard Gerstner deep-water wave is $c \approx 0.9679\text{m } s^{-1}$. The period of the considered wave is $T \approx 103.09\text{s}$. Given the phase speed and wavenumber we can calculate $m \approx 0.0622m^{-1}$, which gives the maximal amplitude of the wave about 16.0772m. Setting the amplitude of the wave at the thermocline 10m and the average $s_+ - s_0 = 50\text{m}$ we get that the oscillation of the upper boundary of layer $\mathcal{M}(t)$ is $ae^{-m(s_0+50)} \approx 0.4\text{m}$, whereas at 100m above the thermocline the oscillation is about 0.02m. Considering the wave motion extends undisturbed to the ocean's surface the oscillation of the free surface caused by the internal water waves are indistinguishable from the ocean's surface perturbation caused by the wind, because of the exponential decrease of the amplitude of the internal waves.

Nonhydrostatic Pollard-like internal geophysical waves

Mateusz Kluczek

Discrete & Continuous Dynamical Systems, accepted

Abstract We present a new exact and explicit Pollard-like solution describing internal water waves representing the oscillation of the thermocline in a nonhydrostatic model. The derived solution is a significant modification of Pollard's surface wave solution in order to describe internal water waves at general latitudes. The novelty of this model consists in the embodiment of transitional layers beneath the thermocline. We present a Lagrangian analysis of the nonlinear internal water waves and we show the existence of two modes of the wave motion.

1 Introduction

The aim of this paper is to construct a new exact solution of the geophysical fluid dynamics governing equations at a fixed latitude which prescribes an internal wave motion induced by the thermocline. The important aspect of this solution is that it includes the effects of the Earth's rotation. The author presented an exact internal water wave solution in [97] for a model assuming that the water is still beneath the thermocline. Consequently, we develop a more realistic scenario, which requires the imposition of transitional layers. In this new model the transition from the oscillation of the thermocline to the still deep water is realised by means of a current flowing beneath the thermocline. Therefore, the flow characteristics are quite different to those presented in [97] and result in a new additional second slow wave mode being a nonlinear phenomenon.

Quite recently the classical Gerstner solution [136] is of great interest to the mathematical society. It results in number of papers deriving solutions for various geophysical waves, e.g. equatorially-trapped waves [10, 12, 13, 64, 77, 80], waves in the presence of underlying depth-invariant currents [23, 27, 60, 63, 65, 95, 96, 127], and a solution for trapped waves at an arbitrary latitude [46] with an instability analysis of Gerstner-like solutions in [19, 84]. The mathematical importance of those solutions is presented in [66, 84, 90]; cf. [3] for a discussion of the oceanographical relevance of those solutions. Moreover, new exact and explicit three-dimensional solutions of the nonlinear governing equations capturing strong depth variations of the flow are given in [25, 26, 27, 85, 90].

Although, it is remarkable that Gerstner's solution can describe such unique and complex flows, the solution is more suitable for flows close to the equator. Pollard modified Gerstner's solution and derived a new extended solution applicable at higher latitudes to rotating flows [121]. In this new solution the planetary vorticity affects the waves and causes a slight cross-wave tilt to the wave orbital motion [30, 97, 121]. The particles paths are still described as closed circles in the fixed reference framework [30, 121]. However, the circles are now in the plane slightly tilted from the local vertical, whereas in Gerstner's solution the plane is genuinely vertical [5]. Consequently, the wave-current interactions in Pollard's solution for surface waves are described in [30] by including in the exact solution an underlying depth-invariant current interpreted as the mean flow velocity. Moreover, an instability of this solution is available in [82, 83] and the solution has been proven to be globally dynamically possible [126].

Following Pollard's work on the surface wave solution we construct a new internal water wave solution of the nonlinear governing equations in the nonhydrostatic model. We derive a dispersion relation for the nonhydrostatic model and by a suitable non-dimensional change of variables we transform it to a polynomial equation of degree six. The degree of the resulting polynomial is dependent on the complexity of the model, therefore introducing additional layers beneath the thermocline we increase the degree of the polynomial — the polynomial derived for a model with one layer beneath the thermocline is of order four, which is the case presented in [97]. An analysis of the polynomial identifies four roots, which are equivalent to two modes of the internal water wave in the dimensional terms; one is a standard internal gravity wave modified slightly by the rotation of Earth and one is a slow mode describing almost inertial circles made by a particle of water. We hope that our study serves as a window to a genuine understanding of complex geophysical flows across Earth [24].

2 Governing equations

Geophysical fluid dynamics refers to natural flows, which have appropriate physical scaling such that the effects of Earth's rotation play an appreciable role [39]. The rotation of the fluid due to the planetary rotation and the stratification are two significant physical features of the geophysical flows [48]. In order to accommodate Earth's rotation, the flow pattern we investigate is described in a rotating frame with the origin at a point on the Earth's surface. The stratification of the fluid is represented by a consideration of a thermocline, which is explained in more detail in section 3. The Earth is taken to be a sphere of the radius $R = 6371$ km, rotating with the constant rotational speed $\Omega = 7.29 \times 10^{-5}$rad s^{-1} round the polar axis towards the east. The Cartesian coordinates (x, y, z) represent the directions of the longitude, latitude and local vertical, where (u, v, w) is the velocity field. The governing equations for the geophysical ocean waves, where the viscous effects are neglected, are given by the Euler equations [39, 120]

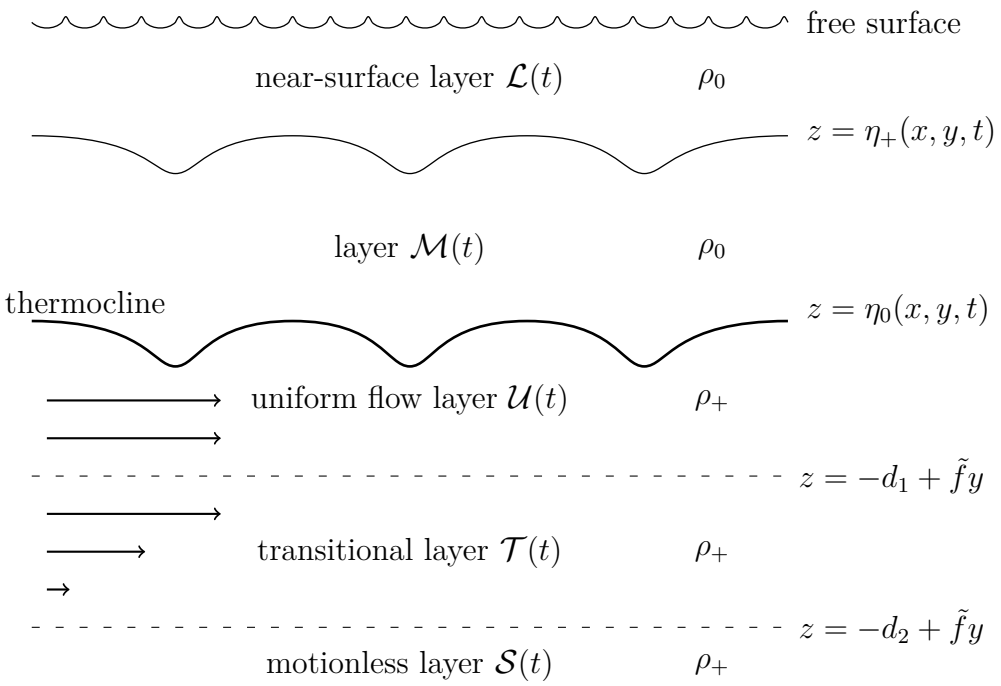


Figure 1: The nonhydrostatic model and its flow regions for fixed y and ϕ. The thermocline separates two layers of ocean water with different but constant densities $\rho_+ > \rho_0$ in a stable stratification [39, 49, 135]. The thermocline is described by a trochoid propagating with a phasespeed c. The transitional layer $\mathcal{T}(t)$ provide a transition from the wave motion region to the motionless abyssal deep-water region of the ocean. The schematic is presented for fixed $\tilde{f} = f/\hat{f} = \tan\phi$.

$$\begin{cases} u_t + uu_x + vu_y + wu_z + 2\Omega w\cos\phi - 2\Omega v\sin\phi = -\frac{1}{\rho}P_x, \\ v_t + uv_x + vv_y + wv_z + 2\Omega u\sin\phi = -\frac{1}{\rho}P_y, \\ w_t + uw_x + vw_y + ww_z - 2\Omega u\cos\phi = -\frac{1}{\rho}P_z - g. \end{cases}$$

In the aforementioned equations t is time, ϕ represents the latitude, $g = 9.81$ m s^{-2} is the constant gravitational acceleration at the Earth's surface, P is the pressure and ρ is the density of water. In order to complete the governing equations the density is taken as a piecewise constant function resulting in the continuity equation

$$u_x + v_y + w_z = 0, \tag{1}$$

for each region of constant density. We investigate the internal water waves in a relatively narrow ocean strip less then a few degrees of latitude wide. Therefore, the f-plane approximation of the governing equation is used [39, 53, 135]. The Euler equations in the f-plane are expressed by taking the Coriolis parameters

$$f = 2\Omega\sin\phi, \qquad \hat{f} = 2\Omega\cos\phi,$$

as constants [39] at a fixed latitude. Thus, the equations reduce to

$$\begin{cases} u_t + uu_x + vu_y + wu_z + \hat{f}w - fv = -\frac{1}{\rho}P_x, \\ v_t + uv_x + vv_y + wv_z + fu = -\frac{1}{\rho}P_y, \\ w_t + uw_x + vw_y + ww_z - \hat{f}u = -\frac{1}{\rho}P_z - g. \end{cases} \tag{2}$$

For further description of the model we introduce the quotient $\tilde{f} = f/\hat{f} = \tan\phi$, which is a constant at a fixed latitude.

3 Description of the nonhydrostatic model

In this section we give a short description of the layered model used in the study of an exact and explicit solution derived here. We extend the hydrostatic model described in [97] by way of a series of transitional layers which represents a transition from the region where the internal water waves propagate to the motionless abyssal deep-water region (cf. Figure 1).

In a stable stratification two horizontal layers of oceanic water of constant but different densities $\rho_+ > \rho_0$ are separated by a thermocline [39, 49, 135]. The oscillating thermocline is in the shape of a trochoid propagating with the phasespeed c, which is quite different to the setting of surface waves, which are described by an inverted trochoid [5, 7, 30]. The geophysical internal water waves represents the oscillation of the thermocline and propagate above the thermocline. The thermocline is a phenomenon occurring predominantly at latitudes in the range $\phi \sim 75°$N–$75°$S. In the subpolar regions of Earth ($\phi > 75°$ N or S) the temperature of water is constant [49] and therefore, the conditions prevailing there do not support the existence of the thermocline. In the flow discussed here the amplitude of the internal water waves decreases with the height above the thermocline in the exponential rate and at the hight of half a wavelength it is less than 4% of its value at the thermocline. We present the internal water waves in the nonhydrostatic model. The model is described as follows (cf. Figure 1). The thermocline oscillates and induces the fluid motion above the thermocline in the layer $\mathcal{M}(t)$. Below the thermocline we introduce the uniform flow layer $\mathcal{U}(t)$ accommodating a uniform horizontal current in the direction of the wave propagation. Beneath $\mathcal{U}(t)$ there is the transitional layer $\mathcal{T}(t)$ where the horizontal velocity of the fluid decreases linearly with the depth. Finally, we have the motionless abyssal deep-water layer $\mathcal{S}(t)$ where the water is still. We distinguish two regions in the fresh and less dense oceanic water above the thermocline, because the flow induced by the oscillating thermocline dies out exponentially fast as one ascends in the fluid. We separate the layer $\mathcal{M}(t)$, where the geophysical internal water wave propagates, and the near-surface layer $\mathcal{L}(t)$ where the geophysical effect is neglected. The motion in the layer $\mathcal{L}(t)$ is a small perturbation of the free surface caused primarily by the wind. The nonhydrostatic model was used previously in [13, 95] to describe internal water waves represented by solutions symmetric about the equator in the β-plane approximation. The aim of this paper is to generalise [13] for an arbitrary latitude in the f-plane.

4 Main results

The solution for the nonlinear internal water waves is constructed by building up from the motionless layer and it has to be developed for each layer of the fluid separately. It is a delicate matter since the normal components of the velocity and pressure have to be continuous across each interface. We seek for a solution to (2) keeping in mind that when we work above the thermocline we denote the density of less dense water as ρ_0 and when we work below the thermocline the density of more dense and colder water is referred as ρ_+. To complete the governing equations we introduce the kinematic condition at each interface in the nonhydrostatic model

$$w = \frac{\partial \eta_i}{\partial t} + u\frac{\partial \eta_i}{\partial x} + v\frac{\partial \eta_i}{\partial y} \text{ on } z = \eta_i(x, y, t) \text{ for } i = 0, 1, 2. \tag{3}$$

preventing mixing particles of water between layers. The solution is designed as follows. First, we find a suitable velocity field satisfying the appropriate kinematic conditions in each layer and next, a pressure continuous at the interfaces satisfying the governing equations.

The motionless layer $\mathcal{S}(t)$

For the motionless layer we define the upper boundary of the layer

$$z = \eta_2(x, y, t) = -d_2 + \tilde{f}y,$$

for some fixed depth $d_2 > 0$ and $\tilde{f} = f/\hat{f} = \tan\phi$, where the assumption of the infinite depth of water is taken into consideration. The velocity field of the still water is

$$u = v = w = 0 \qquad z \leq -d_2 + \tilde{f}y.$$

It implies the hydrostatic pressure

$$P(x, y, z, t) = P_0 - \rho_+ gz \qquad z \leq -d_2 + \tilde{f}y,$$

where P_0 is an arbitrary constant.

The transitional layer $\mathcal{T}(t)$

Above the interface $\eta_2(x, y, t) = -d_2 + \tilde{f}y$ we distinguish the transitional layer with the upper boundary

$$z = \eta_1(x, y, t) = -d_1 + \tilde{f}y,$$

where $d_2 > d_1 > 0$. The horizontal velocity of water's particles increases linearly in this layer. Taking into account appropriate boundary conditions

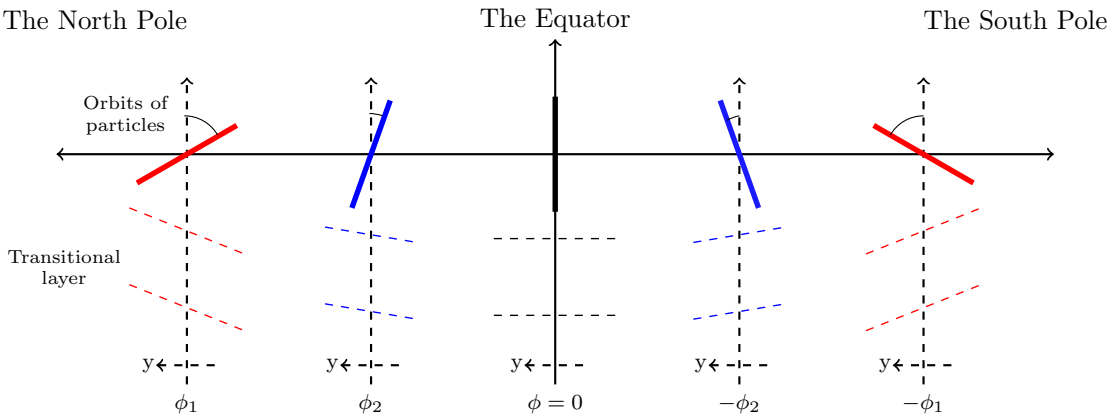


Figure 2: The angle of the inclination of particles' orbits is $\arctan(-d/a)$ [30, 97] and is increasing with latitude resulting in the three-dimensional profile of the internal water wave [97] (see Figure 3). The upper and lower interface of the transitional layer becomes also inclined at the angle ϕ with respect to the local meridional axis. The inclination of the orbits and the interfaces is the result of Earth's constant rotation.

$$u = 0 \text{ on } z = -d_2 + \tilde{f}y,$$
$$u = c \text{ on } z = -d_1 + \tilde{f}y,$$

where c is the wave speed of the oscillating thermocline, we obtain the horizontal component of the velocity field

$$u(y,z) = \frac{c}{d_2 - d_1}(z + d_2 - \tilde{f}y).$$

with the meridional and vertical velocities

$$v = w = 0.$$

Substituting the above into the governing equations we get the pressure function for the transitional layer

$$P(x,y,z,t) = \frac{1}{2}\frac{c}{d_2 - d_1}\rho_+ \hat{f}\left(z + d_2 - \tilde{f}y\right)^2 - \rho_+ gz + P_0.$$

We note that the upper and lower interface of the transitional layer are tilted at an angle ϕ to the local meridional axis. It is a manifestation of the effects of Earth's rotation at higher latitudes.

The uniform flow layer $\mathcal{U}(t)$

In the layer precisely beneath the thermocline particles experience a uniform rectilinear motion expressed physically as a uniform current. The magnitude and direction of the current is equivalent to the wave phasespeed c, therefore the velocity field in the uniform flow layer is defined as

$$u = c, \qquad v = w = 0.$$

Following that, the pressure takes the form

$$P(x,y,z,t) = \rho_+ \hat{f} c \left(z - \tilde{f} y\right) + \frac{1}{2} c \rho_+ \hat{f} \left(d_2 + d_1\right) - \rho_+ g z + P_0.$$

The continuity of all velocity fields and pressures derived above holds across each interface. Moreover, the continuity condition (1) and the kinematic condition (3) are trivially satisfied.

The layer $\mathcal{M}(t)$ above the thermocline

In the layer $\mathcal{M}(t)$ the wave motion is induced by the oscillation of the thermocline. An explicit Pollard-like solution represents a periodic zonally travelling wave with a wave speed c and is described in Lagrangian labelling variables [2]. The Lagrangian positions (x,y,z) of fluid particles are functions of labelling variables (q,r,s), where $q \in \mathbb{R}$, $r \in (-r_0, r_0)$ and $s \in (s_0(r), s_+(r))$. We set up the solution at a fixed latitude ϕ, therefore we take that $r \in (-r_0, r_0)$. Moreover, $s_0(r), s_+(r)$ represent the thermocline and upper boundary of the layer $\mathcal{M}(t)$ for a fixed latitude ϕ, where $s(r) \geq s^* > 0$. We construct the explicit solution for the internal water waves

$$\begin{cases} x = q - be^{-ms}\sin[k(q-ct)], \\ y = r - de^{-ms}\cos[k(q-ct)], \\ z = -d_0 + s - ae^{-ms}\cos[k(q-ct)], \end{cases} \tag{4}$$

where $d_0 > 0$ such that $d_0 < d_1 < d_2$ is introduced to adjust the depth of the thermocline. The solution describes closed circles [30, 97] in a plane slightly tilted to the local vertical (cf. Figure 2), which is caused by the constant rotation of Earth and results in the three-dimensional profile of the wave (cf. Figure 3). For the internal water waves we set the parameter of the amplitude $a > 0$, wavenumber $k > 0$, whereas the remaining parameters b, d, c, m must be suitably chosen in terms of a, k and the Coriolis parameters $f, \hat{f}$. The wavenumber $k = 2\pi/L$ corresponds to the wavelength L. Additionally, the upper bound of the amplitude of the internal wave is $1/m$ (see condition (8)) and we propose to call the parameter m as a modified wavenumber (16) — this parameter is also a decay factor of the amplitude of the internal water wave (4). For notational convenience we set

$$\theta = k(q - ct).$$

For the explicit solution in terms of the Lagrangian labelling variables (4) we can easily calculate the velocity and acceleration of the particles

$$\begin{cases} u = \frac{Dx}{Dt} = kcbe^{-ms}\cos\theta, \\ v = \frac{Dy}{Dt} = -kcde^{-ms}\sin\theta, \\ w = \frac{Dz}{Dt} = -kcae^{-ms}\sin\theta, \end{cases} \quad \begin{cases} \frac{Du}{Dt} = k^2c^2be^{-ms}\sin\theta, \\ \frac{Dv}{Dt} = k^2c^2de^{-ms}\cos\theta, \\ \frac{Dw}{Dt} = k^2c^2ae^{-ms}\cos\theta, \end{cases}$$

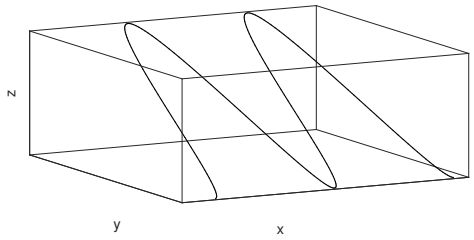


Figure 3: The schematic three-dimensional profile of the internal water waves. The cross-wave tilt is the result of the Earth's rotation [30, 97, 121]. At the equator the wave profile is in the vertical plane [5].

where D/Dt defines the material derivative. The governing equations of the fluid motion above the thermocline are

$$\begin{cases} \frac{Du}{Dt} + \hat{f}w - fv = -\frac{1}{\rho_0}P_x, \\ \frac{Dv}{Dt} + fu = -\frac{1}{\rho_0}P_y, \\ \frac{Dw}{Dt} - \hat{f}u = -\frac{1}{\rho_0}P_z - g. \end{cases} \tag{5}$$

Therefore, checking that (4) is the solution of the governing equations (5) is equivalent to obtaining a compatible pressure. In order to proceed further and to find the pressure we rewrite the governing equations in the Lagrangian labelling variables by using the Jacobian of the mapping (4)

$$\begin{pmatrix} \frac{\partial x}{\partial q} & \frac{\partial y}{\partial q} & \frac{\partial z}{\partial q} \\ \frac{\partial x}{\partial r} & \frac{\partial y}{\partial r} & \frac{\partial z}{\partial r} \\ \frac{\partial x}{\partial s} & \frac{\partial y}{\partial s} & \frac{\partial z}{\partial s} \end{pmatrix} = \begin{pmatrix} 1 - kbe^{-ms}\cos\theta & kde^{-ms}\sin\theta & kae^{-ms}\sin\theta \\ 0 & 1 & 0 \\ mbe^{-ms}\sin\theta & mde^{-ms}\cos\theta & 1 + mae^{-ms}\cos\theta \end{pmatrix}, \tag{6}$$

where the Jacobian determinant is

$$D = 1 + (ma - kb)e^{-ms}\cos\theta - kmabe^{-2ms}.$$

Given the determinant of the Jacobian, the incompressibility condition is satisfied if the determinant is time-independent, thus we take

$$ma - kb = 0. \tag{7}$$

The local diffeomorphic character of the constructed solution is ensured by the inverse function theorem when

$$m^2a^2e^{-2ms^*} < 1, \tag{8}$$

where $s(r) \geq s^* > 0$. From the governing equations (5) we get

$$\begin{aligned} P_x =& -\rho_0 kc[kcb - a\hat{f} + df]e^{-ms}\sin\theta, \\ P_y =& -\rho_0 kc[kcd + bf]e^{-ms}\cos\theta, \\ P_z =& -\rho_0[kc(kca - \hat{f}b)e^{-ms}\cos\theta + g]. \end{aligned}$$

Making use of the Jacobian (6)

$$\begin{pmatrix} P_q \\ P_s \\ P_r \end{pmatrix} = \begin{pmatrix} \frac{\partial x}{\partial q} & \frac{\partial y}{\partial q} & \frac{\partial z}{\partial q} \\ \frac{\partial x}{\partial r} & \frac{\partial y}{\partial r} & \frac{\partial z}{\partial r} \\ \frac{\partial x}{\partial s} & \frac{\partial y}{\partial s} & \frac{\partial z}{\partial s} \end{pmatrix} \cdot \begin{pmatrix} P_x \\ P_y \\ P_z \end{pmatrix},$$

we obtain derivatives with respect to the labelling variables (q, s, r)

$$\begin{aligned} P_q =& -\rho_0\Big[k^3c^2(a^2 + d^2 - b^2)e^{-ms}\cos\theta + kc(kcb - a\hat{f} + df) + kag\Big]e^{-ms}\sin\theta, \\ P_r =& -\rho_0 kc[kcd + bf]e^{-ms}cos\theta, \\ P_s =& -\rho_0\Big[k^2c^2m(a^2 + d^2 - b^2)e^{-2ms}\cos^2\theta - \hat{f}kcmabe^{-2ms} + fkcmbde^{-2ms} \\ & + k^2c^2b^2me^{-2ms} + (k^2c^2a - kcb\hat{f} + mag)e^{-ms}\cos\theta + g\Big]. \end{aligned} \tag{9}$$

Taking into consideration mixed second order derivatives of (9) and the relation (7) we get supplementary relationships between the parameters of the Pollard-like solution

$$kcd + bf = 0, \tag{10}$$

$$mkc^2b + mcdf = k^2c^2a. \tag{11}$$

In the view of the obtained constraints (10), (11) and an arbitrary constant $\tilde{P}_0$ the gradient of the function

$$\begin{aligned} P(q,r,s,t) =& -\rho_0\Big[-\frac{1}{2}k^2c^2\left(a^2 + d^2 - b^2\right)e^{-2ms}\cos^2\theta \\ & - \frac{1}{2}k^2c^2b^2e^{-2ms} + \frac{1}{2}\hat{f}kcabe^{-2ms} - \frac{1}{2}fkcbde^{-2ms} \\ & + \left(ca\hat{f} - cdf - kc^2b - ag\right)e^{-ms}\cos\theta + gs\Big] + \tilde{P}_0, \end{aligned} \tag{12}$$

is exactly the right-hand side of (9), therefore (12) is the pressure in the layer $\mathcal{M}(t)$ satisfying (5). We require the pressure to be continuous across each interface. Thus evaluating the pressure on the thermocline we define

$$P_0 - \tilde{P}_0 = \frac{1}{2}\rho_0 kcb(kcb - a\hat{f} + df)e^{-2ms_0} - \left(\rho_+ \hat{f}c - (\rho_+ - \rho_0)g\right) s_0 + \rho_+ fcr - \frac{1}{2}c\rho_+ \hat{f}(d_2 - d_1) + d_0\rho_+(\hat{f}c - g). \tag{13}$$

which is the product of the continuity of the pressure across the thermocline. The solution $s_0(r)$ to the equation (13) represents the thermocline. The upper boundary of the layer $\mathcal{M}(t)$ is specified by setting $s = s_+(r)$ at a fixed value of $r \in (-r_0, r_0)$ with $s_+(r) > s_0(r)$ in (13) so that it also represents an interface. Moreover, the continuity condition of pressure across the thermocline yields

$$\frac{\rho_+ - \rho_0}{\rho_0}(fcd + ag - ca\hat{f}) = kc^2 b. \tag{14}$$

and additionally, the pressure must be time-independent hence

$$b^2 = a^2 + d^2. \tag{15}$$

The continuity of the pressure across the thermocline is possible if and only if the conditions (14), (15) and (13) hold for $s = s_0(r)$. From the relations (7), (10) and (11) we get

$$b = \frac{ma}{k}, \qquad d = -\frac{fma}{k^2 c}, \qquad m^2 = \frac{k^4 c^2}{k^2 c^2 - f^2}, \tag{16}$$

respectively. The third equation indicates that $|c| > f/k$. We substitute the above parameters into the equation of continuity of the pressure across the thermocline (14); consequently, we derive the dispersion relation for the nonhydrostatic internal water waves induced by the oscillation of the thermocline

$$\left(\frac{\rho_+ - \rho_0}{\rho_0}\right)^2 \left(k^2 c^2 - f^2\right)\left(g - c\hat{f}\right)^2 = c^2 \left(k^2 c^2 + f^2 \frac{\rho_+ - \rho_0}{\rho_0}\right)^2. \tag{17}$$

It is readily seen by comparing the above dispersion relation to the one obtained in [97] that the embodiment of the transitional layer increases the complexity of the dispersion relation. To check the validity of our result we can consider the internal water waves in the equatorial region. For the solution evaluated at the equator the Coriolis parameters are equal to $f = 0$, $\hat{f} = 2\Omega$. Then the dispersion relation (17) becomes

$$\rho_0(kc^2 - 2\Omega c + g) = \rho_+(g - 2\Omega c),$$

which agrees with the dispersion relation obtained in [127] in the absence of currents.

5 Solution for the dispersion relation

The dispersion relation gives the exact value of the wave phasespeed for fixed parameters. In our case it is convenient to express the dispersion relation in terms of the non-dimensional variables

$$X = c\sqrt{\frac{k}{\tilde{g}}} \qquad \epsilon = \frac{f}{\sqrt{\tilde{g}k}} \qquad F = \frac{\hat{f}}{f},$$

where $\tilde{g} = g(\rho_+ - \rho_0)/\rho_0 \approx 4 \times 10^{-3}$ is a typical value of the reduced gravity in the equatorial region [93]. The dispersion relation becomes a polynomial equation of degree six $P(X) = 0$, where

$$\begin{aligned} P(X) =& X^6 + \left(2\epsilon^2 \frac{\rho_+ - \rho_0}{\rho_0} - F^2\epsilon^2 \left(\frac{\rho_+ - \rho_0}{\rho_0}\right)^2\right) X^4 + 2\frac{\rho_+ - \rho_0}{\rho_0} F\epsilon X^3 \\ &+ \left(\epsilon^4 \left(\frac{\rho_+ - \rho_0}{\rho_0}\right)^2 + F^2\epsilon^4 \left(\frac{\rho_+ - \rho_0}{\rho_0}\right)^2 - 1\right) X^2 \\ &- 2\frac{\rho_+ - \rho_0}{\rho_0} F\epsilon^3 X + \epsilon^2. \end{aligned} \tag{18}$$

We note that the polynomial obtained in the paper [97] is of degree four. Therefore, the consideration of the series of transitional layers beneath the thermocline increase the degree of the polynomial by two orders.

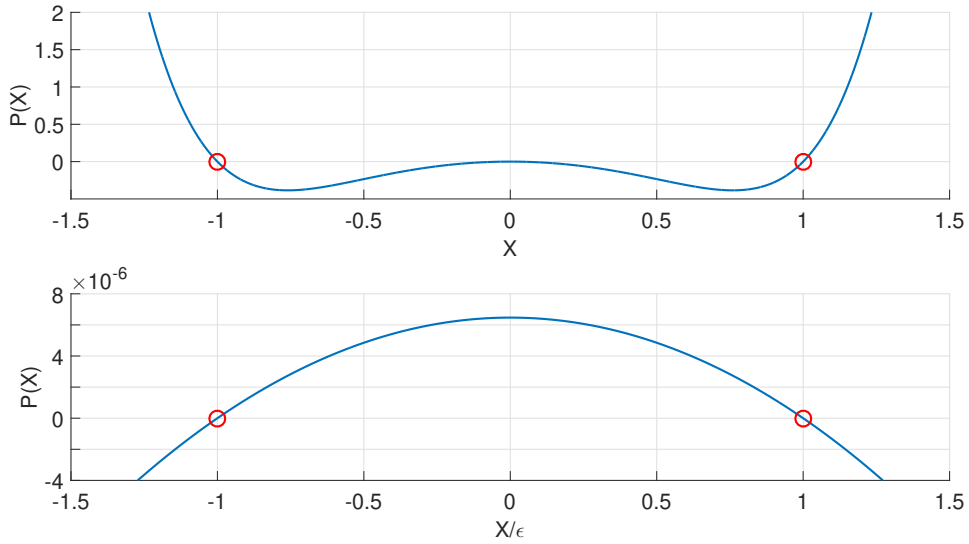


Figure 4: The plot of the polynomial P(X) evaluated at 45°N for $(\rho_+ - \rho_0)/\rho_0 = 4 \times 10^{-3}$, $k = 6.28 \times 10^{-2}\ m^{-1}$. The upper plot shows two roots of order $O(1)$, whereas the lower plot presents two roots of order $O(\epsilon)$.

We seek real roots of (18). Given the real roots of (18), the phase speed of the internal water waves can be found by using the relations introduced in the non-dimensional change of variables. We can readily see that the coefficients of polynomial (18) for a fixed latitude ϕ are the same independently of the hemisphere of Earth. Therefore, we analyse the polynomial for both hemispheres simultaneously. We only exclude the equator from analysis as F is not defined there and the solution particularises there to the Gerstner-like solution for equatorial waves. It is highly complex and complicated to analytically find the exact value of the roots of (18), therefore we focus our attention on estimating the value of the real roots. We consider the internal waves to range from 150 to 250 m [118]. For those wavelengths we obtain $O(F) = 1$, $O(\epsilon) = 10^{-2}$ and we assume $O(\frac{\rho_+ - \rho_0}{\rho_0}) = 10^{-3}$ [93]. Following that, we can estimate the sign of coefficients of the polynomial (18). Hence

$$a_6 = 1, \qquad a_5 = 0, \qquad a_4 > 0, \qquad a_3 > 0, \qquad a_2 < 0, \qquad a_1 < 0, \qquad a_0 > 0,$$

where a_n is the respective coefficient of the term $a_n X^n$ in (18). The polynomial (18) is of degree six, and therefore there are six possible real roots. In order to determine precisely the number of the real roots we use the de Gua corollary to the Fourier-Budan theorem [123].

Corollary. *(de Gua) If in the polynomial $2m + 1$ consecutive terms are missing, then if they are between terms of different signs, the polynomial has no less than $2m$ imaginary roots, whereas if the missing terms are between terms of the same sign the polynomial has no less than $2m + 2$ imaginary roots.*

As a consequence, the polynomial (18) has at most four real roots. Moreover, evaluating the polynomial for the internal waves at 45°N, $(\rho_+ - \rho_0)/\rho_0 = 4 \times 10^{-3}$ and $k = 6.28 \times 10^{-2}\ m^{-1}$ we can see that indeed the polynomial has four real roots and we can expect two roots of order $O(1)$ and two of order $O(\epsilon)$ (cf. Figure 4). For the polynomial $P(X)$ we infer the estimates

$$\begin{aligned}
&P(\pm 1) = \pm 2\epsilon F \frac{\rho_+ - \rho_0}{\rho_0} + O(\epsilon^2),\\
&P(\pm\epsilon) = \epsilon^6 \left(1 + 2\frac{\rho_+ - \rho_0}{\rho_0} + \left(\frac{\rho_+ - \rho_0}{\rho_0}\right)^2\right) > 0,\\
&P(1 - \epsilon F) = 2\epsilon F \left(\frac{\rho_+ - \rho_0}{\rho_0} - 2\right) + O(\epsilon^2) < 0,\\
&P(-1 - \epsilon F) = 2\epsilon F \left(2 - \frac{\rho_+ - \rho_0}{\rho_0}\right) + O(\epsilon^2) > 0,\\
&P(\epsilon + \epsilon^2) = -2\epsilon^4 + O(\epsilon^6) < 0,\\
&P(-\epsilon - \epsilon^2) = -2\epsilon^4 + O(\epsilon^6) < 0.
\end{aligned}$$

Following these estimations we can state that there are two roots of order $O(1)$, which belong to the intervals

$$X_1^+ \in (1-\epsilon F, 1) \qquad X_1^- \in (-1-\epsilon F, -1), \tag{19}$$

and two roots of order $O(\epsilon)$ in the intervals

$$X_2^+ \in (\epsilon, \epsilon+\epsilon^2) \qquad X_2^- \in (-\epsilon-\epsilon^2, -\epsilon). \tag{20}$$

The non-dimensional change of variables indicates four roots in the dimensional terms. The roots (19) yield a solution close to

$$c \approx \pm\sqrt{\tilde{g}/k},$$

which is a standard internal wave [133] very slightly modified by the rotation of Earth. On the other hand, the roots (20) imply in the dimensional terms second solution approximately

$$c \approx \pm f/k.$$

As a result we can distinguish two modes of waves; one fast mode expressing a standard internal wave altered by the rotation of Earth and second slow with the period close to the inertial period $T_i = 2\pi/f$. It is proposed by Constantin & Monismith [30] to call the slow mode as an inertial Gerstner wave. The slow mode results in waves with a relatively small vertical decay scale — for waves of wavelengths 150 m and 10^4 km the wave speed of the inertial internal Gerstner wave is $c = 2.46 \times 10^{-3}$ m s^{-1} and $c = 16.408$ m s^{-1} with the maximal amplitude $a < 4.212 \times 10^{-7}$ m and $a < 1.9856 \times 10^{-3}$ m, respectively. Nevertheless, the inertial Gerstner waves occurs when the transitional layers are introduced, which is in contrast to the results obtained in [97]. In the study of the hydrostatic model [97] there is only one solution of the respective polynomial (only the fast mode equivalent to a standard internal Gerstner wave slightly modified by the rotation of Earth), this is due to the lower order of the polynomial which pertains to the dispersion relation. The inertial Gerstner wave is a nonlinear phenomenon, which in not captured by the linear analysis [30]. Moreover, the study here and in [30] indicate that the slow mode wave is a peculiar marvel that develop in presence of an underlying zonal current.

Dispersion relations for fixed mean-depth flows with two discontinuities in vorticity

Mateusz Kluczek and Calin-Iulian Martin

Journal of Nonlinear Analysis, 181:62–86, 2019.

Abstract We derive the dispersion relation for small-amplitude steady two-dimensional periodic water waves that propagate over a flat bed with a specified and fixed mean-depth. The water flow has a discontinuous vorticity distribution reflecting an isolated rotational layer of fluid. We then use the dispersion relation to obtain necessary and sufficient conditions for local bifurcation to occur. Moreover, a stability analysis of the laminar flows is presented.

1 Introduction

We perform here an analysis of wave-current interactions for small-amplitude, two-dimensional, steady, periodic gravity water waves. The water waves we consider represent the free surface of a water flow bounded below by a flat bed, with a fixed mean-depth and in the presence of a discontinuous vorticity. The discontinuity in vorticity is as follows: the fluid domain presents an isolated rotational layer, of constant non-zero vorticity, surrounded by two layers of irrotational flow adjacent to the surface and the bed, respectively (cf. Figure 1 for the case of a flow with a flat surface). On the physical level, this scenario can be illustrated through a strong undercurrent that does not extend either to the surface or to the bed of ocean. A well known example of this situation is the Equatorial Undercurrent in the Pacific Ocean, which extends nearly across the whole length of the ocean basin and is typically about 300 km in width and symmetric about the equator [10].

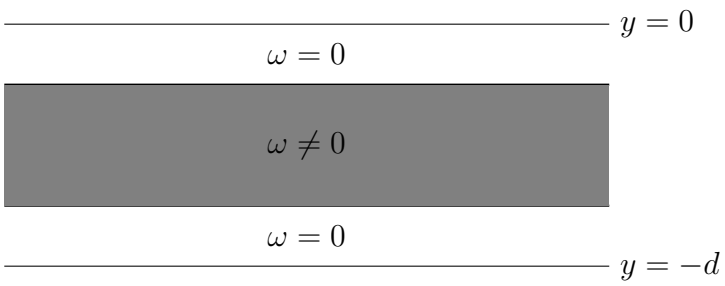


Figure 1: The fluid domain with an isolated layer of constant vorticity $\omega \neq 0$

.

The presence of vorticity highly complicates the mathematical description of the flow. However, this setting is more interesting and intriguing from a physical point of view then the irrotational flow since it describes the wave-current interactions, cf. [7, 91, 134]. The existence of small and large amplitude steady periodic gravity water waves with a fixed mass-flux and exhibiting a general regular vorticity distribution was rigorously proven by Constantin and Strauss, cf. [33]. Targeted and specialized aspects concerning the mathematical analysis of water waves exhibiting vorticity were considered thereafter in regard to features like symmetry [15, 16, 17, 71, 116], stability [34], regularity [18, 37, 42, 56, 58, 44] (continuous) stratification [43, 72, 73, 70, 74, 138, 139], or the presence of stagnation points and critical layers [37, 32, 41, 43, 112, 119, 137].

The more desirable (from the physical point of view) circumstance of having the depth fixed was addressed by Henry [62, 61]; employing a novel reformulation of the governing equations local and global bifurcation tools were used to prove the existence of small and large-amplitude steady periodic water waves, which propagate over a flat bed with a specified mean-depth $d > 0$, and which have a general (continuous) vorticity distribution.

Undoubtedly, the occurrence of a discontinuous vorticity is a realistic scenario — as illustrated in the beginning of this section. The rigorous existence proof of water waves over flows presenting a discontinuous distribution of vorticity was carried out by Constantin and Strauss [36] in the fixed mass-flux case, and by Henry and Sastre-Gómez [76] and Henry, Martin and Sastre-Gómez [69] in the situation of the fixed mean-depth.

Working in the frame of the fixed mean-depth setting and considering a special discontinuous vorticity (of piecewise constant type) we analyze here the existence of small-amplitude water waves that are perturbations of the laminar flow solutions — flows with a flat surface and parallel streamlines. More precisely, the problem of existence of the before mentioned water waves is equivalent to the existence of a unique positive solution of a certain algebraic equation. The formula for the unique positive solution of the former algebraic equation is called the *dispersion relation* and indicates how the relative speed of the wave at the free surface varies with respect to parameters like the wavelength, the fixed mean-depth, the vorticity distribution and the location of the jump in the vorticity distribution.

Apart from capturing connections between the various physical parameters of the water flow, dispersion relations are vital for studying the resonance problem [29, 107].

More precisely, we are concerned here with the dispersion relation for water waves in the newly developed setting, where the mean-depth of the fluid is fixed [62, 61, 76], setting of increased physical relevance, if compared with the fixed mass flux approach [36]. Dispersion relations in the fixed mean-depth setting were derived previously by Henry for the case of a vorticity layer adjacent to the free surface [59] and of a layer adjacent to the bed [57] by applying the local bifurcation theory from [76]. Dispersion relations for flows with piecewise constant vorticity in fixed mass-flux flows were obtained recently and relatively recently [8, 36, 103, 104, 105, 111]; see also

the more demanding situation of the presence of stagnation points in flows exhibiting two rotational layers of constant vorticity [112] or the admission of geophysical effects, cf. [109].

In this paper we consider the case of an isolated layer of vorticity as in [104], but, instead of fixing the mass flux, we derive the dispersion relation for the fixed mean-depth setting.

Furthermore, we show that the dispersion relation we derive, coincides with the corresponding one from [104], valid also for the case of a configuration with two jumps in the vorticity distribution, but in the fixed mass-flux setting. This aspect suggests that the differences in the two approaches are more susceptible to occur for large-amplitude waves. Moreover, the dispersion relations found in [57, 59] can be obtained as limit cases from ours, cf. Section 3.1. That is, letting $d_2 := 0$ in one case, and setting $d_1 := d$ in another one, (cf. Figure 3), we obtain the dispersion relations from [58, 62], valid for two-layered fluid domains. We would also like to mention that the fixed mean-depth setting is also studied further in the case of two adjacent rotational layers [113]. We note that dispersion relations for several types of continuous non-constant vorticity were investigated by Karageorgis [92]. Recently, the dispersion relation is analyzed in [98] for certain parallel shear flows.

We conclude our presentation with a stability analysis of the laminar flow solutions which is based on a variational formulation devised from the one presented in [31]. We would like to mention that variational formulations (of Hamiltonian type) were recently and relatively recently employed in the study of rotational water waves allowing for a constant or piecewise constant vorticity, cf. [20, 21, 22, 86]. Unlike the latter formulations, which rewrite the water wave problem only in terms of the wave variables (represented by the free surface and the traces of the velocity potential on the surface), we need both the horizontal and the vertical variables in our analysis.

Piecewise constant vorticity, a particular type of which we consider here, is highly relevant to the modeling of wave-current interactions. A thorough understanding of the wave-current interactions — aspect that we analyze here from the point of view of dispersion relations — can potentially impact the present knowledge on oceanic flows by facilitating more accurate analyses of water flows on Earth, according to the recent papers by Constantin and Johnson [24, 28] or [110].

2 Governing equations

We consider two-dimensional, steady, periodic water waves propagating, with a constant speed $c > 0$, in the horizontal direction over a rotational, inviscid and incompressible fluid. The waves propagate with a constant, in time, speed $c > 0$. The assumption of steadiness means that the velocity field, denoted (u, v), the pressure, denoted by P, and the surface wave, exhibit a dependence in the horizontal variable x of the kind $x - ct$, where t stands for time. Let by $D_\eta := \{(x, y) \in \mathbb{R}^2 : -d < y < \eta(x)\}$ denote the fluid domain, where $y = -d$ represents the flat bed and $y = \eta(x)$ is the equation of the free surface, which, in the setting of small-amplitude water waves, is

small perturbation of the flat surface $y = 0$. Moreover, we retain the same average free surface level, that is η satisfies

$$\int \eta(x)dx = 0.$$

We also make the physically reasonable assumption that the water flow is homogeneous, cf. [99]. For simplicity we consider the case of a unit density. The governing equations of the water flow acted upon by gravity are [7]

$$\begin{aligned}(u-c)u_x + vu_y &= -P_x \text{ in } \overline{D_\eta},\\ (u-c)v_x + vv_y &= -P_y - g \text{ in } \overline{D_\eta},\end{aligned}$$

together with the incompressibility condition

$$u_x + v_y = 0 \text{ in } \overline{D_\eta},$$

where g is the constant gravitational acceleration. The equations of motion are supplemented by the kinematic boundary conditions

$$\begin{aligned}v = (u-c)\eta_x \text{ on } y = \eta(x),\\ v = 0 \text{ on } y = -d,\end{aligned}$$

and the dynamic boundary condition

$$P = P_{atm} \text{ on } y = \eta(x). \tag{1}$$

The dynamic boundary condition (1) decouples the motion of the air above from the motion of the water. The kinematic boundary conditions state the impermeability of the two boundaries of the fluid domain.

We will assume throughout the paper that there are no stagnation points, that is

$$u(x,y) < c, \quad \text{for all} \quad (x,y) \in \overline{D}_\eta, \tag{2}$$

holds.

The modelling of wave-current interactions is realized through the utilization of the vorticity function, denoted here ω, and defined as

$$\omega(x,y) = u_y - v_x.$$

We will work with periodic water waves and we choose the period to be 2π, without loss of generality. To reduce the number of the unknowns we introduce the stream function $\psi(x,y)$, which is given (up to constant) by

$$\begin{aligned} \psi_x &= -v, \\ \psi_y &= u - c. \end{aligned} \tag{3}$$

The kinematic boundary conditions imply that the stream function ψ is constant on both boundaries. Therefore, we can set $\psi = 0$ on $y = \eta(x)$. By integrating (3) we see that $\psi = -p_0$ on $y = -d$, where

$$p_0 = \int_{-d}^{\eta(x)} (u(x,y) - c)dy < 0,$$

is a negative constant which, is called the relative mass flux. We note that the vorticity can be rewritten by means of (3) as

$$\omega = \psi_{yy} + \psi_{xx} = \Delta\psi.$$

The previous discussion allows the reformulation of the equations of motion and of their boundary conditions as the free boundary value problem

$$\begin{aligned} \Delta\psi &= \omega \text{ in } \overline{D}_\eta, \\ |\nabla\psi|^2 + 2g(y+d) &= Q \text{ on } y = \eta(x), \\ \psi &= 0 \text{ on } y = \eta(x), \\ \psi &= -p_0 \text{ on } y = -d. \end{aligned} \tag{4}$$

Here, the constant Q is called the total head, cf. [7, 36].

We introduce now the semi-Lagrangian hodograph transformation given by

$$\begin{cases} q = x, \\ p = \dfrac{\psi(x,y)}{p_0}, \end{cases} \tag{5}$$

which has the advantage that transforms the free boundary problem (4) with the domain $\overline{D_\eta} = \{(x,y) \in \mathbb{R}^2 : -\pi \leq x \leq \pi, -d \leq y \leq \eta(x)\}$ into a problem with the fixed rectangular domain $R = [-\pi, \pi] \times [-1, 0]$, cf. Figure 2.

The condition of non-stagnation (2) ensures that the change of variables (5) is an isomorphism. Moreover, it can be easily shown that $\omega_q = 0$, which leads to

$$\omega = \gamma(p),$$

where γ is a function dependent on p only and is referred to as the vorticity function. Now we can reformulate the problem (4) by means of the modified-height function

$$h(q,p) = \frac{y}{d} - p. \tag{6}$$

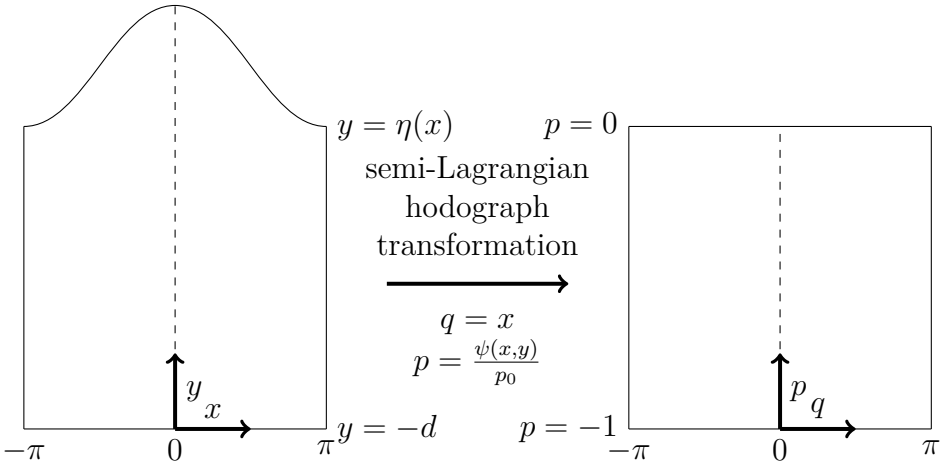


Figure 2: The semi-Lagrangian hodograph transformation for steady water waves with period 2π.

More precisely, we get

$$\begin{aligned}\left(\frac{1}{d^2}+h_q^2\right)h_{pp}-2h_qh_{pq}(h_p+1)+h_{qq}(h_p+1)^2+&\frac{\gamma(p)}{p_0}(h_p+1)^3=0\\ &\text{in } -1<p<0,\\ h_q^2+\frac{1}{d^2}+[2gd(h+1)-Q]&\frac{(h_p+1)^2}{p_0^2}=0 \text{ on } p=0,\\ &h=0 \text{ on } p=-1,\end{aligned}\tag{7}$$

with the no stagnation condition (2) equivalent to

$$h_p+1>0.$$

Remark. *We reiterate that we work in the setting of the fixed mean-depth, as developed by Henry [62, 61] in the case of a continuous vorticity, and extended to discontinuous vorticity by Henry and Sastre-Gómez [76], and Henry, Martin and Sastre-Gómez [69]. The choice* (6)*, for the (modified) height function, keeps the parameter d in the water wave problem. Thus, it fixes the depth. This represents a significant difference from the approach in [33, 36], where the mass-flux is fixed.*

A solution $h(q,p)$ of (7) is even and 2π-periodic in q cf. [76]. The derivatives of the modified-height function in terms of the variables q, p are given by

$$\begin{aligned}h_q&=\frac{v}{d(u-c)},\\ h_p&=\frac{p_0}{d(u-c)}-1.\end{aligned}$$

Since we model an isolated region of vorticity surrounded by irrotational flow we allow the vorticity function to be discontinuous. To work in the above setting we will use the reformulation of (7) in the weak form, [62, 76]

$$\begin{aligned}\left[\frac{d^2h_q^2+1}{2d^2(h_p+1)^2}-\frac{\Gamma(p)}{2d^2}\right]_p-\left[\frac{h_q}{h_p+1}\right]_q&=0 \text{ in } -1<p<0,\\ \frac{1+d^2h_q^2}{d^2(h_p+1)^2}+\frac{2gd(h+1)-Q}{p_0^2}&=0 \text{ on } p=0,\\ h&=0 \text{ on } p=-1,\end{aligned}\tag{8}$$

where

$$\Gamma(p)=\int_0^p\frac{2d^2\gamma(s)}{p_0}ds$$

and $h\in W^{2,r}_{per}(R)\subset C^{1,\alpha}_{per}(R)$ with $r>2/(1-\alpha)$ for $\alpha\in(1/3,1)$. The subscript "*per*" indicates evenness and 2π-periodicity in the q-variable.

Remark. *It was established by Henry and Sastre-Gómez [76] that, for sufficiently small $\epsilon>0$ there exists a C^1-curve $\mathscr{C}_{loc}=\{(\lambda^s,h^s)\in\mathbb{R}\times C^{1,\alpha}_{per}(\overline{R}):|s|<\epsilon\}$ of solutions to the water wave problem* (8)*, subject to $h_p+1>0$. Moreover, it was proved in [130] that the height function formulation in the weak form* (8) *is equivalent with the stream function formulation.*

A laminar solution $H(p)$ of the system (8) represents a water flow whose streamlines are horizontal, that is, it describes a parallel shear flow with a flat surface. A routine computation shows that, the laminar solutions are

$$H(p)=\int_0^p\frac{ds}{\sqrt{\lambda+\Gamma(s)}}+\frac{1}{2gd}\left(Q-\frac{p_0^2}{d^2}\lambda\right)-(p+1) \text{ in } -1<p<0,\tag{9}$$

where, the parameter λ is related to the fluid velocity at the flat surface by the relation

$$\sqrt{\lambda}=\left.\frac{1}{H_p+1}\right|_{p=0}=\left.\frac{d(u-c)}{p_0}\right|_{y=0},\tag{10}$$

and it is implicitly related to Q by the formula

$$Q=2gd\int_{-1}^0\frac{ds}{\sqrt{\lambda+\Gamma(s)}}+\frac{p_0^2}{d^2}\lambda>0.$$

We assume that the small-amplitude waves are perturbations of the laminar flow solutions $p\to H(p)$. Therefore, we search for $h(q,p)$ in the form

$$h(q,p)=H(p)+\varepsilon\tilde{m}(q,p).\tag{11}$$

According to [76], the previous Ansatz allows us to reformulate the system (8) in the form

$$\begin{cases} (a^3\tilde{m}_p)_p = -d^2 a\tilde{m}_{qq} & \text{in } R, \\ a^3\tilde{m}_p = \dfrac{gd^3}{p_0^2}\tilde{m} & \text{on } p = 0, \\ \tilde{m} = 0 & \text{on } p = -1, \end{cases}$$

where $a(\lambda, p) = \sqrt{\lambda + \Gamma(p)} \in C^\alpha([-1, 0])$.

As it follows from [76], the necessary and sufficient condition for the existence of waves of small-amplitude that are perturbations of the laminar flow solutions (9) is equivalent to the existence of a nontrivial solution $m(p) \in C^{1,\alpha}(-1, 0)$ of the Sturm-Liouville problem

$$\begin{cases} (a^3 m_p)_p = d^2 am & \text{in } -1 < p < 0, \\ a^3 m_p = \dfrac{gd^3}{p_0^2} m & \text{on } p = 0, \\ m = 0 & \text{on } p = -1. \end{cases} \tag{12}$$

After we solve for the general solution m that satisfies the first equation in (12) and the boundary condition on $p = -1$, we require m to satisfy the second equation in (12). This delivers a polynomial equation for the parameter λ. The existence of a unique positive solution, say λ^*, of the latter polynomial equation is equivalent to the existence of waves of small-amplitude which are perturbations (of the type (11)) of the laminar flow whose speed at the free surface is related to λ^* in the fashion

$$(u^* - c)\Big|_{\text{at the flat surface}} = \frac{p_0\sqrt{\lambda^*}}{d}. \tag{13}$$

The formula for λ^* obtained by solving the above mentioned polynomial equation is called the *dispersion relation* and will be dealt with in the next section.

3 Dispersion relation

In this section we derive the dispersion relation for water waves, propagating over a water flow of fixed mean-depth and exhibiting a discontinuous vorticity. The approach by Constantin [8] and by Constantin and Strauss [36] can be modified to bear relevance to our setting that differs from the one in [8, 36]. Indeed, we reiterate that we use the non-standard Dubreil-Jacotin transformation (5) and we allow for two jumps in the vorticity distribution.

We need to establish first some notation. Let $p_1, p_2 \in [-1, 0]$ with $p_1 < p_2$, be the values of the variable p corresponding to the depths d_1, d_2, respectively. We recall that the depths $d_1 > d_2$ are the levels where the discontinuities of the vorticity

function occur. We consider a layer of constant vorticity $\gamma \neq 0$ in the middle layer corresponding to $[p_1, p_2]$ squeezed in by irrotational layers adjacent to the bottom $p = -1$ and to the surface $p = 0$, respectively, cf. Figure 3. Throughout the section we will make the distinction between the non-dimensional quantities p, p_1, p_2 that are elements of the interval $[-1, 0]$ and the physical quantity, p_0, representing the mass flux. We then have

$$\Gamma(p) = \begin{cases} 0, & p \in [p_2, 0], \\ \dfrac{2d^2\gamma}{p_0}(p - p_2), & p \in [p_1, p_2], \\ \dfrac{2d^2\gamma}{p_0}(p_1 - p_2), & p \in [-1, p_1], \end{cases}$$

and therefore,

$$a(\lambda, p) = \sqrt{\lambda + \Gamma(p)} = \begin{cases} \sqrt{\lambda}, & p \in [p_2, 0], \\ \sqrt{\lambda + \dfrac{2d^2\gamma}{p_0}(p - p_2)}, & p \in [p_1, p_2], \\ \sqrt{\lambda + \dfrac{2d^2\gamma}{p_0}(p_1 - p_2)}, & p \in [-1, p_1]. \end{cases}$$

We search for the function $m \in C^{1,\alpha}(-1, 0)$ subject to (12), whose restrictions to $[-1, p_1]$, $[p_1, p_2]$, $[p_2, 0]$ are denoted with u, v, w, respectively, as in Figure 3.

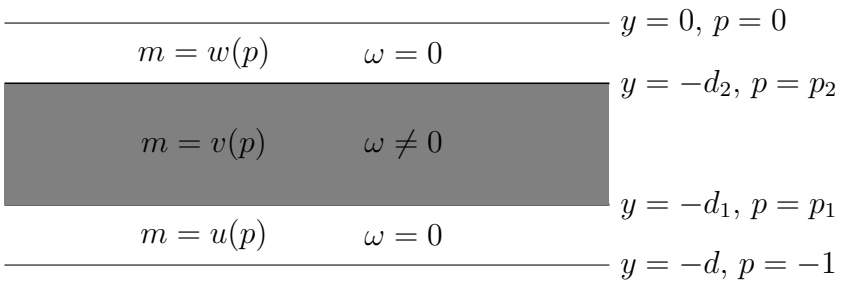


Figure 3: The fluid domain with an isolated layer of vorticity $\omega \neq 0$ and the functions satisfying the Sturm-Liouville problem in each layer.

It follows easily that the functions u, v, w, satisfy the equations

$$(a^3 w_p)_p = d^2 a w, \qquad p \in [p_2, 0], \tag{14}$$

$$(a^3 v_p)_p = d^2 a v, \qquad p \in [p_1, p_2], \tag{15}$$

$$(a^3 u_p)_p = d^2 a u, \qquad p \in [-1, p_1], \tag{16}$$

respectively, with the matching conditions at the interfaces $p = p_1$ and $p = p_2$ being given by

$$u(p_1) = v(p_1), \qquad u'(p_1) = v'(p_1), \tag{17}$$

$$v(p_2) = w(p_2), \qquad v'(p_2) = w'(p_2). \tag{18}$$

Moreover, the two boundary conditions in the Sturm-Liouville problem (12) take the form

$$a^3 w_p = \frac{gd^3}{p_0^2} w \qquad \text{on } p = 0, \tag{19}$$

$$u = 0 \qquad \text{on } p = -1, \tag{20}$$

The compatibility conditions (17) and (18) ensure that $m \in C^1([-1, 0])$. Applying a Schauder-type estimate, cf. [52], as in [36] and [69], leads to a gain of a better regularity, namely, we obtain that, in fact, $m \in C^{1,\alpha}([-1, 0])$.

We determine now the function m. First we consider the layer of zero vorticity adjacent to the bottom. In this layer the solution to the equation (16) is

$$u(p) = c \sinh\left(\frac{d(p+1)}{\sqrt{\lambda + \frac{2d^2\gamma}{p_0}(p_1 - p_2)}}\right),$$

which is obtained by the boundary condition (20). In the second step we look for the solution to equation (15) in the rotational layer. We consider the substitution

$$v(p) = \frac{1}{a(p)} \tilde{v}\left(\frac{p_0 a(p)}{d\gamma}\right).$$

Therefore, the equation (15) reduces to

$$\tilde{v}'' = \tilde{v}.$$

The solution in the rotational layer is

$$v(p) = \frac{1}{a(p)}\left(c_1 \cosh\left(\frac{p_0 a(p)}{d\gamma}\right) + c_2 \sinh\left(\frac{p_0 a(p)}{d\gamma}\right)\right),$$

where $a(p) = \sqrt{\lambda + \frac{2d^2\gamma}{p_0}(p - p_2)}$ for $p \in [p_2, p_1]$. In the final step we have to solve the equation (14) in the irrotational layer adjacent to the surface. We see immediately that

$$w(p) = \alpha_1 \cosh\left(\frac{dp}{\sqrt{\lambda}}\right) + \alpha_2 \sinh\left(\frac{dp}{\sqrt{\lambda}}\right). \tag{21}$$

We now rewrite the matching conditions (17), (18) in terms of solutions which were found for each layer. The matching condition (18) corresponding to the line $p = p_2$ can be reexpressed as

$$\begin{cases} \alpha_1 \cosh\left(\dfrac{dp_2}{\sqrt{\lambda}}\right) + \alpha_2 \sinh\left(\dfrac{dp_2}{\sqrt{\lambda}}\right) = \dfrac{1}{\sqrt{\lambda}}\left(c_1 \cosh\left(\dfrac{p_0\sqrt{\lambda}}{d\gamma}\right) + c_2 \sinh\left(\dfrac{p_0\sqrt{\lambda}}{d\gamma}\right)\right) \\ \dfrac{d}{\sqrt{\lambda}}\left(\alpha_1 \sinh\left(\dfrac{dp_2}{\sqrt{\lambda}}\right) + \alpha_2 \cosh\left(\dfrac{dp_2}{\sqrt{\lambda}}\right)\right) = \\ -\dfrac{d^2\gamma}{p_0\lambda\sqrt{\lambda}}\left(c_1 \cosh\left(\dfrac{p_0\sqrt{\lambda}}{d\gamma}\right) + c_2 \sinh\left(\dfrac{p_0\sqrt{\lambda}}{d\gamma}\right)\right) \\ +\dfrac{d}{\lambda}\left(c_1 \sinh\left(\dfrac{p_0\sqrt{\lambda}}{d\gamma}\right) + c_2 \cosh\left(\dfrac{p_0\sqrt{\lambda}}{d\gamma}\right)\right). \end{cases} \tag{22}$$

Similarly, the compatibility condition between the irrotational layer adjacent to the bottom and the rotational layer (17) on $p = p_1$ takes form

$$\begin{cases} c \sinh\left(\dfrac{d(p_1+1)}{a(p_1)}\right) = \dfrac{1}{a(p_1)}\left(c_1 \cosh\left(\dfrac{p_0 a(p_1)}{d\gamma}\right) + c_2 \sinh\left(\dfrac{p_0 a(p_1)}{d\gamma}\right)\right) \\ \dfrac{d}{a(p_1)} c \cosh\left(\dfrac{d(p_1+1)}{a(p_1)}\right) = \\ -\dfrac{d^2\gamma}{p_0 a^3(p_1)}\left(c_1 \cosh\left(\dfrac{p_0 a(p_1)}{d\gamma}\right) + c_2 \sinh\left(\dfrac{p_0 a(p_1)}{d\gamma}\right)\right) \\ +\dfrac{d}{a^2(p_1)}\left(c_1 \sinh\left(\dfrac{p_0 a(p_1)}{d\gamma}\right) + c_2 \cosh\left(\dfrac{p_0 a(p_1)}{d\gamma}\right)\right). \end{cases} \tag{23}$$

For simplicity we introduce here the notation

$$\theta := \frac{p_0 a(p_1)}{d\gamma}, \qquad \rho := \frac{d(p_1+1)}{a(p_1)}.$$

Therefore, the compatibility condition (23) becomes

$$\begin{cases} c \sinh(\rho) = \dfrac{1}{a(p_1)}\left(c_1 \cosh(\theta) + c_2 \sinh(\theta)\right), \\ \dfrac{d}{a(p_1)} c \cosh(\rho) = -\dfrac{d^2\gamma}{p_0 a^3(p_1)}\left(c_1 \cosh(\theta) + c_2 \sinh(\theta)\right) \\ \qquad\qquad +\dfrac{d}{a^2(p_1)}\left(c_1 \sinh(\theta) + c_2 \cosh(\theta)\right). \end{cases} \tag{24}$$

Solving the system of equations (24) for c_1 and c_2 we get

$$c_1 = \frac{d\gamma}{p_0} c\left[-\sinh(\rho)\sinh(\theta) + \theta \sinh(\rho - \theta)\right],$$

$$c_2 = \frac{d\gamma}{p_0} c \left[\cosh(\theta) \sinh(\rho) + \theta \cosh(\rho - \theta) \right].$$

We focus now our attention on finding the value of parameters θ, ρ, which leads to re-expressing the compatibility conditions in a neater form. Recall that, while the depths $-d_1, -d_2$ are associated with the discontinuities in vorticity occurring in the physical domain, p_1, p_2 represent the jumps in vorticity in the transformed domain.

Since the velocity field is independent of the horizontal variable in the case of laminar flows, we have that the vorticity is given (in the latter case) as $\omega = u_y$. Therefore, by means of (10),

$$(c-u)(y) = \begin{cases} -\dfrac{p_0\sqrt{\lambda}}{d}, & y \in [-d_2, 0], \\ -\dfrac{p_0\sqrt{\lambda}}{d} - \gamma(y + d_2), & y \in [-d_1, -d_2], \\ -\dfrac{p_0\sqrt{\lambda}}{d} + \gamma(-d_2 + d_1), & y \in [-d, -d_1]. \end{cases} \tag{25}$$

We evaluate in the following p_1 and p_2 by means of the other physical quantities of the flow. Using (25) and $\psi_y = c - u$ we have first

$$\psi(-d_2) = \int_{-d_2}^{0} (c-u)(y)dy = \int_{-d_2}^{0} -\frac{p_0\sqrt{\lambda}}{d} dy = -\frac{p_0\sqrt{\lambda}}{d} d_2,$$

which yields

$$p_2 = -\frac{\sqrt{\lambda}}{d} d_2, \tag{26}$$

by the mapping (5). Likewise,

$$\begin{aligned} \psi(-d_1) = \int_{-d_1}^{0} (c-u)(y)dy = \int_{-d_1}^{-d_2} \left(-\frac{p_0\sqrt{\lambda}}{d} - \gamma(y + d_2) \right) dy \\ + \int_{-d_2}^{0} -\frac{p_0\sqrt{\lambda}}{d} dy = -\frac{p_0\sqrt{\lambda}}{d} d_1 + \frac{\gamma}{2}(-d_1 + d_2)^2, \end{aligned}$$

which implies

$$p_1 = -\frac{\sqrt{\lambda}}{d} d_1 + \frac{\gamma}{2p_0} d_2^2 - \frac{\gamma}{p_0} d_1 d_2 + \frac{\gamma}{2p_0} d_1^2. \tag{27}$$

We reformulate now (27) as the quadratic equation in d_1

$$\frac{\gamma}{2p_0}d_1^2 - \left(\frac{\sqrt{\lambda}}{d} + \frac{\gamma}{p_0}d_2\right)d_1 + \frac{\gamma}{2p_0}d_2^2 - p_1 = 0,$$

whose solutions are given by

$$d_1 = \frac{\frac{\sqrt{\lambda}}{d} + \frac{\gamma}{p_0}d_2 \pm \sqrt{\frac{\lambda}{d^2} + \frac{2\gamma}{p_0}(p_1 - p_2)}}{\frac{\gamma}{p_0}},$$

The above equation yields

$$d_1 - d_2 = \frac{p_0}{d\gamma}\left(\sqrt{\lambda} \pm \sqrt{\lambda + \frac{2\gamma d^2}{p_0}(p_1 - p_2)}\right). \tag{28}$$

To decide upon the sign in (28) we take into account that $d_1 - d_2 > 0$, $p_1 - p_2 < 0$ and $p_0 < 0$. It is straightforward to see that if $\gamma > 0$ one has to choose the minus sign in (28). To decide the sign in (28) for the case $\gamma < 0$ we consider the value of $c - u$ for $y \in [-d, -d_1]$, where we have

$$(c-u)(y) = -\frac{p_0\sqrt{\lambda}}{d} + \gamma(-d_2 + d_1) > 0, \qquad y \in [-d, -d_1]. \tag{29}$$

Substituting (28) into (29) we see that only the minus sign is possible in (28). Therefore,

$$d_1 - d_2 = \frac{p_0}{d\gamma}\left(\sqrt{\lambda} - \sqrt{\lambda + \frac{2\gamma d^2}{p_0}(p_1 - p_2)}\right) = \frac{p_0}{d\gamma}(a(p_2) - a(p_1)). \tag{30}$$

Using the definition of the stream function ψ and that of the mass flux p_0 we compute

$$\begin{aligned}\psi(-d_1) + p_0 &= -\int_{-d}^{-d_1}(c-u)(s)ds = \frac{p_0\sqrt{\lambda}}{d}(d - d_1) - \gamma(d_1 - d_2)(d - d_1) \\ &= \frac{d - d_1}{d}(p_0\sqrt{\lambda} - d\gamma(d_1 - d_2)).\end{aligned}$$

Dividing above by the total mass flux and substituting in (30) we obtain the equation

$$p_1 + 1 = \frac{d - d_1}{d}(\sqrt{\lambda} - \frac{d\gamma}{p_0}(d_1 - d_2)) = \frac{d - d_1}{d}a(p_1),$$

which yields

$$\rho = \frac{d(p_1+1)}{a(p_1)} = d - d_1.$$

The matching condition (22) can now be detailed by means of (26) as

$$\begin{cases} \alpha_1 \cosh(d_2) - \alpha_2 \sinh(d_2) = \dfrac{1}{\sqrt{\lambda}} \left(c_1 \cosh\left(\dfrac{p_0\sqrt{\lambda}}{d\gamma}\right) + c_2 \sinh\left(\dfrac{p_0\sqrt{\lambda}}{d\gamma}\right)\right), \\ -\alpha_1 \sinh(d_2) + \alpha_2 \cosh(d_2) = -\dfrac{d\gamma}{p_0\lambda} \left(c_1 \cosh\left(\dfrac{p_0\sqrt{\lambda}}{d\gamma}\right) + c_2 \sinh\left(\dfrac{p_0\sqrt{\lambda}}{d\gamma}\right)\right) \\ \qquad\qquad + \dfrac{1}{\sqrt{\lambda}} \left(c_1 \sinh\left(\dfrac{p_0\sqrt{\lambda}}{d\gamma}\right) + c_2 \cosh\left(\dfrac{p_0\sqrt{\lambda}}{d\gamma}\right)\right). \end{cases}$$

Therefore, we easily find that α_1, α_2 are given by

$$\begin{aligned} \alpha_1 =& \frac{1}{\sqrt{\lambda}} \left(c_1 \cosh\left(\frac{p_0\sqrt{\lambda}}{d\gamma} + d_2\right) + c_2 \sinh\left(\frac{p_0\sqrt{\lambda}}{d\gamma} + d_2\right)\right) \\ & - \frac{d\gamma}{p_0\lambda} \left(c_1 \cosh\left(\frac{p_0\sqrt{\lambda}}{d\gamma}\right) + c_2 \sinh\left(\frac{p_0\sqrt{\lambda}}{d\gamma}\right)\right) \sinh(d_2), \\ \alpha_2 =& \frac{1}{\sqrt{\lambda}} \left(c_1 \sinh\left(\frac{p_0\sqrt{\lambda}}{d\gamma} + d_2\right) + c_2 \cosh\left(\frac{p_0\sqrt{\lambda}}{d\gamma} + d_2\right)\right) \\ & - \frac{d\gamma}{p_0\lambda} \left(c_1 \cosh\left(\frac{p_0\sqrt{\lambda}}{d\gamma}\right) + c_2 \sinh\left(\frac{p_0\sqrt{\lambda}}{d\gamma}\right)\right) \cosh(d_2). \end{aligned}$$

Using the expressions of the coefficients c_1, c_2 found before, we obtain

$$\begin{aligned} & c_1 \cosh\left(\frac{p_0\sqrt{\lambda}}{d\gamma} + d_2\right) + c_2 \sinh\left(\frac{p_0\sqrt{\lambda}}{d\gamma} + d_2\right) = \\ & = \frac{d\gamma}{p_0} c \left[-\sinh(\rho) \sinh\left(\theta - \frac{p_0\sqrt{\lambda}}{d\gamma} - d_2\right) + \theta \sinh\left(\rho - \theta + \frac{p_0\sqrt{\lambda}}{d\gamma} + d_2\right)\right], \end{aligned}$$

and

$$\begin{aligned} & c_1 \sinh\left(\frac{p_0\sqrt{\lambda}}{d\gamma} + d_2\right) + c_2 \cosh\left(\frac{p_0\sqrt{\lambda}}{d\gamma} + d_2\right) = \\ & \quad = \frac{d\gamma}{p_0} c \left[\sinh(\rho) \cosh\left(\theta - \frac{p_0\sqrt{\lambda}}{d\gamma} - d_2\right) + \theta \cosh\left(\rho - \theta + \frac{p_0\sqrt{\lambda}}{d\gamma} + d_2\right)\right], \\ & c_1 \cosh\left(\frac{p_0\sqrt{\lambda}}{d\gamma}\right) + c_2 \sinh\left(\frac{p_0\sqrt{\lambda}}{d\gamma}\right) = \end{aligned}$$

$$= \frac{d\gamma}{p_0} c \left[-\sinh(\rho) \sinh\left(\theta - \frac{p_0\sqrt{\lambda}}{d\gamma}\right) + \theta \sinh\left(\rho - \theta + \frac{p_0\sqrt{\lambda}}{d\gamma}\right)\right].$$

We recall that

$$\rho = d - d_1.$$

Furthermore, the equalities $\theta = \frac{p_0 a(p_1)}{d\gamma}$, $\quad d_1 - d_2 = \frac{p_0}{d\gamma}(a(p_2) - a(p_1))$ imply that $\theta - \frac{p_0\sqrt{\lambda}}{d\gamma} = \frac{p_0}{d\gamma}(a(p_1) - a(p_2)) = d_2 - d_1$. We are now able to rewrite the coefficients α_1, α_2 as

$$\begin{aligned}
\alpha_1 =& \frac{1}{\sqrt{\lambda}} \left(\frac{d\gamma}{p_0} c \left[\sinh(d - d_1) \sinh(d_1) + \theta \sinh(d) \right] \right) \\
& - \frac{d\gamma}{p_0 \lambda} \left(\frac{d\gamma}{p_0} c \left[-\sinh(d - d_1) \sinh(d_2 - d_1) + \theta \sinh(d - d_2) \right] \right) \sinh(d_2), \\
\alpha_2 =& \frac{1}{\sqrt{\lambda}} \left(\frac{d\gamma}{p_0} c \left[\sinh(d - d_1) \cosh(d_1) + \theta \cos(d) \right] \right) \\
& - \frac{d\gamma}{p_0 \lambda} \left(\frac{d\gamma}{p_0} c \left[-\sinh(d - d_1) \sinh(d_2 - d_1) + \theta \sinh(d - d_2) \right] \right) \cosh(d_2).
\end{aligned}$$

We exploit now the surface boundary condition given by (19). After subbing the solution (21) into the surface boundary condition, the latter particularises to

$$\lambda \alpha_2 = \frac{g d^2}{p_0^2} \alpha_1.$$

Replacing α_1, α_2 we obtain the following

$$\begin{aligned}
& \lambda^{\frac{3}{2}} \left[\theta \cosh(d) + \sinh(d - d_1) \cosh(d_1) \right] \\
& \quad + \frac{d\gamma}{p_0} \cosh(d_2) \left[-\theta \sinh(d - d_2) + \sinh(d - d_1) \sinh(d_2 - d_1) \right] \lambda \\
=& \sqrt{\lambda} \frac{g d^2}{p_0^2} \left[\theta \sinh(d) + \sinh(d - d_1) \sinh(d_1) \right] \\
& \quad + \gamma g \sinh(d_2) \frac{d^3}{p_0^3} \left[-\theta \sinh(d - d_2) + \sinh(d - d_1) \sinh(d_2 - d_1) \right].
\end{aligned}$$

Substituting θ with $\frac{p_0\sqrt{\lambda}}{d\gamma} + d_2 - d_1$ and dividing the result by $\frac{p_0}{d\gamma}$ we obtain the condition

$$\begin{aligned}
&\cosh(d)\lambda^2 + \left[(d_2-d_1)\cosh(d) - \sinh(d_1-d_2)\cosh(d-d_2-d_1)\right]\frac{d\gamma}{p_0}\lambda^{\frac{3}{2}}\\
&+\Big[\left((d_1-d_2)\sinh(d-d_2)+\sinh(d-d_1)\sinh(d_2-d_1)\right)\cosh(d_2)\gamma^2\\
&-g\sinh(d)\Big]\frac{d^2}{p_0^2}\lambda - \left[(d_2-d_1)\sinh(d) - \sinh(d_2-d_1)\sinh(d-d_2-d_1)\right]g\gamma\frac{d^3}{p_0^3}\sqrt{\lambda}\\
&-\left[(d_1-d_2)\sinh(d-d_2)+\sinh(d-d_1)\sinh(d_2-d_1)\right]g\sinh(d_2)\gamma^2\frac{d^4}{p_0^4} = 0.
\end{aligned} \tag{31}$$

The existence of a unique and positive solution of the equation (31) is a necessary and sufficient condition for local bifurcation to occur. Hence, by the means of the relation (13) we obtain the dispersion relation for small-amplitude water waves over flows with a fixed mean-depth, displaying a piecewise constant vorticity with a rotational layer separated by two irrotational ones. Furthermore, the condition (31) can be reexpressed by the substitution

$$x = (c-u)(0) = -\frac{p_0}{d}\sqrt{\lambda}, \tag{32}$$

whereupon, we obtain a quartic equation $p(x) = 0$ where

$$\begin{aligned}
p(x) &= x^4\cosh(d) + \left[(d_1-d_2)\cosh(d) + \sinh(d_1-d_2)\cosh(d-d_2-d_1)\right]\gamma x^3\\
&+\Big[\left((d_1-d_2)\sinh(d-d_2)+\sinh(d-d_1)\sinh(d_2-d_1)\right)\gamma^2\cosh(d_2)\\
&-g\sinh(d)\Big]x^2 - \left[(d_1-d_2)\sinh(d) + \sinh(d_2-d_1)\sinh(d-d_2-d_1)\right]g\gamma x\\
&-\left[(d_1-d_2)\sinh(d-d_2)+\sinh(d-d_1)\sinh(d_2-d_1)\right]g\gamma^2\sinh(d_2).
\end{aligned} \tag{33}$$

We will investigate in the next section the problem of existence and uniqueness of positive solutions to the quartic polynomial equation $p(x) = 0$. The fact that, in the fixed mean-depth scenario, we obtain the same polynomial equation as in the fixed mass flux setting is an indication that the differences between the two approaches manifest in waves of large-amplitude.

3.1 Limiting cases of the vorticity layer

Before we focus our attention on the condition (33) we analyze two limiting cases. We consider the layer of vorticity being extended either to the surface or to the bed. It will turn out that (31) particularises in the limits $d_2 = 0, d_1 = d$ to the corresponding relations from [57, 59].

Vorticity layer adjacent to the surface

In the first case we take $d_2 = 0$ which results in the vorticity layer being adjacent to the surface. Therefore, the equation (31) becomes, after division by $\sqrt{\lambda}$

$$\cosh(d)\lambda^{\frac{3}{2}} + \left[-d_1\cosh(d) - \sinh(d_1)\cosh(d-d_1)\right]\frac{d\gamma}{p_0}\lambda + \left[\left(d_1\sinh(d) - \sinh(d-d_1)\sinh(d_1)\right)\gamma^2 - \frac{d^2}{p_0^2}g\sinh(d)\right]\frac{d^2}{p_0^2}\sqrt{\lambda} - \left[-d_1\sinh(d) + \sinh(d_1)\sinh(d-d_1)\right]g\frac{d^3\gamma}{p_0^3} = 0,$$

which yields

$$\lambda^{\frac{3}{2}} - \gamma\left[d_1 + \frac{\sinh(d_1)\cosh(d-d_1)}{\cosh(d)}\right]\frac{d}{p_0}\lambda - \tanh(d)\left[g - \gamma^2\left(d_1 - \frac{\sinh(d-d_1)\sinh(d_1)}{\sinh(d_1)}\right)\right]\frac{d^2}{p_0^2}\sqrt{\lambda} + \frac{gd^3\gamma}{p_0^3}\tanh(d)\left[d_1 - \frac{\sinh(d_1)\sinh(d-d_1)}{\sinh(d)}\right] = 0.$$

In the case of a vorticity layer extending to the surface, the condition (31) particularises to the relation in [59].

Vorticity layer adjacent to the bed

We set now $d_1 = d$, that is, we extend the rotational layer up to the bed. By setting $d_1 = d$ in the equation (31) we get the following expression

$$\cosh(d)\lambda^{\frac{3}{2}}\left(\sqrt{\lambda} + \frac{d\gamma}{p_0}(d_2-d)\right) + \left(\sqrt{\lambda} + \frac{d\gamma}{p_0}(d_2-d)\right)\lambda\frac{d\gamma}{p_0}\sinh(d_2-d)\cosh(d_2) - \left(\sqrt{\lambda} + \frac{d\gamma}{p_0}(d_2-d)\right)\frac{gd^2}{p_0^2}\sinh(d)\sqrt{\lambda} + \left(\sqrt{\lambda} + \frac{d\gamma}{p_0}(d_2-d)\right)\frac{gd^3\gamma}{p_0^3}\sinh(d_2)\sinh(d-d_2) = 0.$$

Dividing by $\sqrt{\lambda} + \frac{d\gamma}{p_0}(d_2-d)$ we recover the formula

$$\lambda^{\frac{3}{2}}p_0^3 - \frac{p_0^2 d\gamma}{2}\left(\tanh(d) + \frac{\sinh(d-2d_2)}{\cosh(d)}\right)\lambda - gd^2p_0\tanh(d)\sqrt{\lambda} + \frac{gd^3\gamma}{2}\left(1 - \frac{\cosh(d-2d_2)}{\cosh(d)}\right) = 0,$$

which is the condition obtained for a rotational layer adjacent to the bottom in [57].

4 Existence of a unique positive root of the polynomial $p(x)$

In this section we prove that there exists a unique positive root of (33). The existence of such solution leads through (32) to the dispersion relation for small-amplitude waves. To perform the necessary analysis we follow the arguments from [104]. However, we need to make necessary adjustments for the different physical constants, which appear in the different definition of the bifurcation parameter and in the transformation (32). In order to prove the existence of the real positive root of the equation $p(x) = 0$ we have to consider two separate cases, according to the sign of the (constant) vorticity γ.

Case I: Positive vorticity $\gamma > 0$

The analysis follows similarly as in [104]. For the sake of self-contained study we include a brief outline of the main arguments. We note that

$$\begin{aligned} p(0) &= -\left[(d_1 - d_2)\sinh(d - d_2) + \sinh(d - d_1)\sinh(d_2 - d_1)\right] g\gamma^2 \sinh(d_2) = \\ &= -H(d_1) g\gamma^2 \sinh(d_2), \end{aligned}$$

where H denotes the function $d_1 \to (d_1 - d_2)\sinh(d - d_2) + \sinh(d - d_1)\sinh(d_2 - d_1)$, $\quad d_1 \in (d_2, d)$. It is easy to check that $H(d_1)|_{d_1:=d_2} = 0$ and

$$H'(d_1) = 2\cosh(d - d_1)\sinh(d_1 - d_2) > 0, \quad \text{for} \quad d_1 > d_2$$

which implies that $H(d_1) > 0$ for $d_1 \in (d_2, d)$. Therefore, we have that $p(0) < 0$. Since $\lim_{x\to+\infty} p(x) = +\infty$ there must be at least one positive root of p in $(0, \infty)$.

We study in the sequel the number of positive roots of $p(x)$ with the help of an analysis of the polynomial $p'(x)$, which is

$$\begin{aligned} p'(x) &= 4x^3\cosh(d) + 3x^2\left[(d_1 - d_2)\cosh(d) + \sinh(d_1 - d_2)\cosh(d - d_2 - d_1)\right]\gamma \\ &+ 2x\left[\left((d_1 - d_2)\sinh(d - d_2) + \sinh(d - d_1)\sinh(d_2 - d_1)\right)\gamma^2\cosh(d) - g\sinh(d)\right] \\ &- \left[(d_1 - d_2)\sinh(d) + \sinh(d_2 - d_1)\sinh(d - d_2 - d_1)\right] g\gamma. \end{aligned}$$

The intersection of the polynomial $p'(x)$ with the y-axis is given by

$$\begin{aligned} p'(0) &= -\left[(d_1 - d_2)\sinh(d) + \sinh(d_2 - d_1)\sinh(d - d_2 - d_1)\right] g\gamma = \\ &= -G(d_1) g\gamma, \qquad d_1 \in (d_2, d), \end{aligned}$$

where G is the function $d_1 \to (d_1 - d_2)\sinh(d) + \sinh(d_2 - d_1)\sinh(d - d_2 - d_1)$, $\qquad d_1 \in (d_2, d)$. We can check that $G(d_1)\Big|_{d_1:=d_2} = 0$, and the derivative of $G(d_1)$ is given by

$$G'(d_1) = 2\cosh(d - d_1)\sinh(d_1) > 0,$$

which implies that $G(d_1) > 0$ for $d_1 \in (d_2, d)$ and, therefore, $p'(0) < 0$. The latter and the positivity of the highest order coefficient of $p'(x)$ imply that the polynomial $p'(x)$ has at least one positive root. To find the exact number of roots of $p'(x)$ we use Viète's formulas for the sum and the product of roots [123]

$$x_1 \cdot x_2 \cdot x_3 = -\frac{p'(0)}{4\cosh(d)} > 0, \tag{34}$$

$$\begin{aligned} x_1 + x_2 + x_3 &= -\frac{3\left[(d_1 - d_2)\cosh(d) + \sinh(d_1 - d_2)\cosh(d - d_2 - d_1)\right]\gamma}{4\cosh(d)} = \\ &= -\frac{3\gamma F(d_1)}{4\cosh(d)}, \qquad d_1 \in (d_2, d). \end{aligned} \tag{35}$$

We determine now the sign of the numerator of (35). Introducing the function $d_1 \to F(d_1) := (d_1 - d_2)\cosh(d) + \sinh(d_1 - d_2)\cosh(d - d_2 - d_1), d_1 \in (d_2, d)$, we see that $F(d_1)\Big|_{d_1 := d_2} = 0$ when $d_1 \in (d_2, d)$. Moreover,

$$F'(d_1) = 2\cosh(d - d_1)\cosh(d_1) > 0,$$

which yields $F(d_1) > 0$ for $d_1 \in (d_2, d)$ and

$$x_1 + x_2 + x_3 < 0. \tag{36}$$

The relations (34) and (36) together with $p'(0) < 0$ imply that there exists exactly one positive root x_0 of p', which, additionally, satisfies $p'(x) < 0$ in $(0, x_0)$ and $p'(x) > 0$ in (x_0, ∞). Therefore $p(x)$ is strictly decreasing on $(0, x_0)$ and increasing on (x_0, ∞), Figure 4. Since $p(0) < 0$ we can conclude that there indeed exist a unique positive root $x_+ > x_0$ giving the dispersion relation by means of the substitution $x = -\frac{p_0}{d}\sqrt{\lambda}$.

Estimation of the bifurcation parameter when $\gamma > 0$

We provide in the following estimates for the positive root of the polynomial $p(x)$ in terms of the physical quantities involved in the flow. To this end, we notice that equation (31) can be rearranged in the form

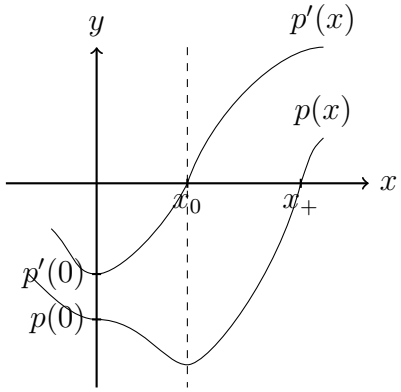


Figure 4: The schematic figure for the unique positive root of polynomial $p(x)$.

$$\begin{aligned}
&\left(\lambda + (d_2 - d_1)\frac{d\gamma}{p_0}\sqrt{\lambda}\right)\left[\cosh(d)\lambda - g\frac{d^2}{p_0^2}\sinh(d)\right] \\
&+ ((d_1 - d_2)\sinh(d - d_2) + \sinh(d - d_1)\sinh(d_2 - d_1)) \times \\
&\gamma^2\frac{d^2}{p_0^2}\left[\cosh(d_2)\lambda - g\frac{d^2}{p_0^2}\sinh(d_2)\right] \\
&+ \sinh(d_1 - d_2)\frac{d\gamma}{p_0}\sqrt{\lambda}\left[-\cosh(d_1 + d_2 - d)\lambda + g\frac{d^2}{p_0^2}\sinh(d_1 + d_2 - d)\right] = 0.
\end{aligned} \tag{37}$$

We state now the results concerning the estimation of $\sqrt{\lambda}$, for certain choices of the physical parameters of the flow.

Proposition 1. *If $\gamma > 0$ and $d > \dfrac{d_1 + d_2}{2}$ the bifurcation parameter $\sqrt{\lambda}$ belongs to the interval $\left(0, \sqrt{\dfrac{gd^2}{p_0^2}\tanh(d)}\right)$.*

Proof. Let assume, for the sake of contradiction, that

$$\lambda \geq \frac{gd^2}{p_0^2}\tanh(d).$$

The latter inequality implies that

$$\lambda > \frac{gd^2}{p_0^2}\tanh(d_2).$$

Moreover, since $d > \frac{d_1+d_2}{d}$, we also have that

$$\lambda > \frac{gd^2}{p_0^2}\tan(d_1 + d_2 - d).$$

Therefore, using all the above inequalities and, since $H(d_1) > 0$, we conclude that the left-hand side of (37) is strictly positive, which is a contradiction. Thus,

$$\lambda < \frac{gd^2}{p_0^2}\tanh(d),$$

which implies that

$$\sqrt{\lambda} < \sqrt{\frac{gd^2}{p_0^2}\tanh(d)}. \tag{38}$$

□

Proposition 2. *If* $\gamma > 0$ *and* $\frac{d_1 + d_2}{2} < d < d_1 + d_2$ *hold for parameters* d, d_1, d_2 *then* $\sqrt{\lambda} > \sqrt{\frac{gd^2}{p_0^2}\tanh(d_1 + d_2 - d)}$.

Proof. Now we assume, by contradiction, that

$$\lambda \leq \frac{gd^2}{p_0^2}\tanh(d_1 + d_2 - d),$$

which, since $d_1 < d$, implies

$$\lambda < \frac{gd^2}{p_0^2}\tanh(d_2),$$

We see now that the sum of the second and of the third terms of the equation (37) is negative. By necessity, it follows that

$$\cosh(d)\lambda - g\frac{d^2}{p_0^2}\sinh(d) > 0,$$

which implies that

$$\lambda \geq \frac{gd^2}{p_0^2}\tanh(d),$$

which is in contradiction to the already proven inequality (38). Therefore, we obtain

$$\lambda > \frac{gd^2}{p_0^2}\tanh(d_1 + d_2 - d),$$

and it follows

$$0 < \sqrt{\frac{gd^2}{p_0^2}\tanh(d_1 + d_2 - d)} < \sqrt{\lambda}.$$

□

Subsequently, summarizing the above propositions we obtain the statement

Proposition 3. *If* $\gamma > 0$ *and* $\dfrac{d_1+d_2}{2} < d < d_1+d_2$ *then*

$$\sqrt{\lambda} \in \left(\sqrt{\frac{gd^2}{p_0}\tanh(d_1+d_2-d)}, \sqrt{\frac{gd^2}{p_0}\tanh(d)} \right).$$

Proof. The proof follows from Proposition 1 and Proposition 2. □

Case II: Negative vorticity $\gamma < 0$

Proposition 4. *Under the assumptions*

$$\frac{g}{\gamma^2} > (d_1-d_2)^2 \frac{(d_1-d_2)\cosh(d_1)+\sinh(d_2-d_1)\cosh(d_2)}{(d_1-d_2)\sinh(d_1)+\sinh(d_2-d_1)\sinh(d_2)}, \tag{39}$$

and

$$\begin{aligned} \frac{g}{\gamma^2} &> \frac{(d_1-d_2)^2\Big[\cosh(d)(d_1-d_2)-3\sinh(d_1-d_2)\cosh(d-d_2-d_1)\Big]}{(d_1-d_2)\sinh(d)+\sinh(d_1-d_2)\sinh(d-d_2-d_1)} \\ &+\frac{2(d_1-d_2)\cosh(d_2)\Big[(d_1-d_2)\sinh(d-d_2)+\sinh(d-d_1)\sinh(d_2-d_1)\Big]}{(d_1-d_2)\sinh(d)+\sinh(d_1-d_2)\sinh(d-d_2-d_1)}. \end{aligned} \tag{40}$$

the equation (31) *has a unique positive root.*

Proof. The substitution

$$\sqrt{\lambda} = \frac{d\gamma}{p_0}(x+d_1-d_2)$$

allows to perform the proof of the sufficiency of (39) and (40) for local bifurcation to occur as in [104] to which we refer the interested reader. □

5 Stability of the laminar solutions

We present here a stability criterion (in a sense to be defined below) of the laminar solutions (given previously in the paper) for our scenario of an isolated layer of vorticity situated between two irrotational layers in the case of the fixed mean-depth formulation. A similar stability analysis was presented in [34] and in [105] for flows exhibiting a piecewise constant distribution of vorticity, but in the context of the fixed mass flux approach. We start with some preliminary notation. With the help of the stream function $\psi(x,y)$ we define the functional

$$\mathcal{F}(\psi) = \iint_{\overline{D_\eta}} \frac{1}{d}\left[\frac{1}{2}\left|\nabla\left(\frac{\psi(x,y)}{p_0}\right)\right|^2 + \frac{Q}{2p_0^2} + \frac{\Gamma\left(\frac{\psi(x,y)}{p_0}\right)}{2d^2}\right] dxdy \tag{41}$$
$$- \iint_{\overline{D_\eta}} \frac{g}{p_0^2}\left(\frac{y}{d} - \frac{\psi(x,y)}{p_0} + 1\right)\left(1 - d\frac{\partial}{\partial y}\left(\frac{\psi(x,y)}{p_0}\right)\right) dxdy.$$

defined on the fluid domain

$$\overline{D_\eta} = \{(x,y) \in \mathbb{R}^2 : 0 \le x \le L, -d \le y \le \eta(x)\}$$

with an unknown free surface.

Remark. *Note that the multiplication of the first integral in* (41) *with the quantity* dp_0^2 *represents a suitable modification of the kinetic energy by terms related to the head,* Q*, and to the vorticity. Moreover, the second integral in* (41) *multiplied with* dp_0^2 *represents a modification of the potential energy by the factor* $1 - d\frac{\partial}{\partial y}\left(\frac{\psi(x,y)}{p_0}\right)$.

We will argue in the sequel along the lines of [31]. The change of variables

$$q = x, \qquad p = \frac{\psi(x,y)}{p_0},$$

transforms the fluid domain into the fixed domain $R = [0, L] \times [-1, 0]$, where $L > 0$ is the wave period. We introduce the modified-height function

$$h(q,p) = \frac{y}{d} - p,$$

where

$$h_q = -\frac{\psi_x}{d\psi_y}, \qquad h_p = \frac{p_0}{d\psi_y} - 1.$$

Given $\alpha \in (0,1)$ we obtain, by means of Theorem 2.1 from [111], a real-analytic curve in $C^{1,\alpha}(R)$ consisting of solutions to (7)

$$h(q,p) := \begin{cases} h_1(q,p), & (q,p) \in [0,L] \times [-1,p_1], \\ h_2(q,p), & (q,p) \in [0,L] \times [p_1,p_2], \\ h_3(q,p), & (q,p) \in [0,L] \times [p_2,0], \end{cases} \tag{42}$$

with the property

$$h_1 \in C^{2,\alpha}\left([0,L] \times [-1,p_1]\right) \cap C^\infty\left([0,L] \times (-1,p_1)\right),$$
$$h_2 \in C^{2,\alpha}\left([0,L] \times [p_1,p_2]\right) \cap C^\infty\left([0,L] \times (p_1,p_2)\right),$$

$$h_3 \in C^{2,\alpha}\left([0,L]\times[p_2,0]\right)\cap C^{\infty}\left([0,L]\times(p_2,0)\right).$$

The functions (42) satisfy along the interfaces $p=p_1$ and $p=p_2$ the compatibility conditions,

$$\begin{array}{ll} h_1(q,p_1)=h_2(q,p_1), & h_2(q,p_2)=h_3(q,p_2),\\ h_{1p}(q,p_1)=h_{2p}(q,p_1), & h_{2p}(q,p_2)=h_{3p}(q,p_2), \end{array} \qquad q\in[0,L], \tag{43}$$

while obeying, as before, the bottom boundary condition $h(q,-1)=0$, and the no stagnation condition $h_p+1>0$. After the change of variables the functional $\mathcal{F}(\psi)$ takes the form

$$\begin{aligned}\mathcal{L}(h)=\iint_R\left[\frac{1+d^2h_q^2}{2d^2(1+h_p)^2}+\frac{Q}{2p_0^2}+\frac{\Gamma(p)}{2d^2}\right](1+h_p)dpdq\\ -\iint_R\frac{gd}{p_0^2}(1+h)h_p dpdq.\end{aligned}$$

To compute variations of $\mathcal{L}$ we will use test functions L-periodic and even in q, defined by

$$k(q,p):=\begin{cases} k_1(q,p), & (q,p)\in[0,L]\times[-1,p_1],\\ k_2(q,p), & (q,p)\in[0,L]\times[p_1,p_2],\\ k_3(q,p), & (q,p)\in[0,L]\times[p_2,0], \end{cases} \tag{44}$$

with

$$\begin{array}{l} k_1\in C^{2,\alpha}([0,L]\times[-1,p_1]),\\ k_2\in C^{2,\alpha}([0,L]\times[p_1,p_2]),\\ k_3\in C^{2,\alpha}([0,L]\times[p_2,0]), \end{array}$$

which satisfy

$$\begin{array}{ll} k_1(q,p_1)=k_2(q,p_1), & k_2(q,p_2)=k_3(q,p_2),\\ k_{1p}(q,p_1)=k_{2p}(q,p_1), & k_{2p}(q,p_2)=k_{3p}(q,p_2), \end{array} \qquad q\in[0,L] \tag{45}$$

and

$$\int_0^L k_3(q,0)dq=0. \tag{46}$$

We compute now the first variation of the functional $\mathcal{L}$, cf. [51], for functions h satisfying (42) and (43). Making use of (43), (45), (46) we get

$$\langle \delta\mathcal{L}(h), k\rangle = \lim_{\varepsilon\to 0}\frac{\mathcal{L}(h+\varepsilon k)-\mathcal{L}(h)}{\varepsilon} =$$
$$= \lim_{\varepsilon\to 0}\iint_R \frac{1}{\varepsilon}\left[\frac{1+d^2h_q^2}{2d^2(1+h_p+\varepsilon k_p)^2} - \frac{1+d^2h_q^2}{2d^2(1+h_p)^2}\right](1+h_p)dqdp$$
$$+ \lim_{\varepsilon\to 0}\iint_R \frac{1}{\varepsilon}\left[\frac{2\varepsilon h_q k_q+\varepsilon^2 k_q^2}{2(1+h_p+\varepsilon k_p)^2}\right](1+h_p+\varepsilon k_p)dqdp$$
$$+ \lim_{\varepsilon\to 0}\iint_R \frac{1}{\varepsilon}\left[\frac{1+d^2h_q^2}{2d^2(1+h_p+\varepsilon k_p)^2} + \frac{Q}{2p_0^2} + \frac{\Gamma(p)}{2d^2}\right]\varepsilon k_p dqdp$$
$$- \lim_{\varepsilon\to 0}\iint_R \frac{1}{\varepsilon}\frac{gd}{p_0^2}(1+h)\varepsilon k_p dqdp - \lim_{\varepsilon\to 0}\iint_R \frac{1}{\varepsilon}\frac{gd}{p_0^2}\varepsilon k(h_p+\varepsilon k_p)dqdp =$$
$$= -\iint_R \frac{1+d^2h_q^2}{d^2(1+h_p)^2}k_p dqdp$$
$$+ \iint_R \left[\frac{1+d^2h_q^2}{2d^2(1+h_p)^2} + \frac{Q}{2p_0^2} + \frac{\Gamma(p)}{2d^2} - \frac{gd}{p_0^2}(1+h)\right]k_p dqdp$$
$$+ \iint_R \frac{h_q}{1+h_p}k_q dqdp - \iint_R \frac{gd}{p_0^2}h_p k dqdp.$$

Using integration by parts we get

$$\langle \delta\mathcal{L}(h), k\rangle =$$
$$= -\int_{p=0}\frac{1+d^2h_q^2}{d^2(1+h_p)^2}kdq + \iint_R\left[\frac{2h_q h_{qp}}{(1+h_p)^2} - \frac{2(1+d^2h_q^2)h_{pp}}{d^2(1+h_p)^3}\right]kdqdp$$
$$+ \int_{p=0}\left[\frac{1+d^2h_q^2}{2d^2(1+h_p)^2} + \frac{Q}{2p_0^2} + \frac{\Gamma(p)}{2d^2} - \frac{gd}{p_0^2}(1+h)\right]kdq$$
$$- \iint_R\left[-\frac{(1+d^2h_q^2)h_{pp}}{d^2(1+h_p)^3} + \frac{h_q h_{qp}}{(1+h_p)^2} + \frac{\gamma(p)}{p_0} - \frac{gd}{p_0^2}h_p\right]kdqdp$$
$$- \iint_R\left[\frac{h_{qq}}{1+h_p} - \frac{h_q h_{qp}}{(1+h_p)^2}\right]kdqdp - \iint_R\frac{gd}{p_0^2}h_p k dqdp =$$
$$= -\iint_R \mathcal{G}_1(h)\frac{k}{(1+h_p)^3}dqdp - \frac{1}{2}\int_{p=0}\mathcal{G}_2(h_3,Q)\frac{k_3}{(1+h_{3p})^2}dq.$$

Where the operators $\mathcal{G}_1, \mathcal{G}_2$ are defined as

$$\mathcal{G}_1(h)(q,p) :=$$
$$= \begin{cases} (\frac{1}{d^2} + h_{1q}^2)h_{1pp} + h_{1qq}(1+h_{1p})^2 - 2h_{1q}h_{1qp}(1+h_{1p}) + \frac{\gamma(p)}{p_0}(1+h_{1p})^3, \\ \qquad\qquad (q,p) \in (0,L) \times (-1,p_1), \\ (\frac{1}{d^2} + h_{2q}^2)h_{2pp} + h_{2qq}(1+h_{2p})^2 - 2h_{2q}h_{2qp}(1+h_{2p}) + \frac{\gamma(p)}{p_0}(1+h_{2p})^3, \\ \qquad\qquad (q,p) \in (0,L) \times (p_1,p_2), \\ (\frac{1}{d^2} + h_{3q}^2)h_{3pp} + h_{3qq}(1+h_{3p})^2 - 2h_{3q}h_{3qp}(1+h_{3p}) + \frac{\gamma(p)}{p_0}(1+h_{3p})^3, \\ \qquad\qquad (q,p) \in (0,L) \times (p_2,0), \end{cases}$$

and

$$\mathcal{G}_2(h_3,Q) := \frac{1}{d^2} + h_{3q}^2 + \frac{(1+h_{3p})^2}{p_0^2}\left(2gd(h_3+1) - Q\right).$$

One notices immediately that any critical point $h = (h_1, h_2, h_3)$ of the functional $\mathcal{L}$ solves the equations

$$\begin{aligned} &\mathcal{G}_1(h) = 0 \qquad \text{in } R \\ &\mathcal{G}_2(h_3,Q) = 0 \qquad \text{on } p = -1, \end{aligned} \tag{47}$$

which shows that critical points of $\mathcal{L}$ are solutions to the water wave equation.

Utilizing (47) we find that the second variation of the functional $\mathcal{L}$ (cf. [51]) at a critical point h is given by

$$\begin{aligned} \left\langle \delta^2\mathcal{L}(h)l,k \right\rangle = &- \iint_R \mathcal{G}_{1h}(h,Q)\frac{lk}{(1+h_p)^3}dqdp \\ &- \frac{1}{2}\int_{p=0} \mathcal{G}_{2h_3}(h_3,Q)\frac{l_3 l_3}{(1+h_{3p})^2}dq. \end{aligned} \tag{48}$$

Thus, we see from (48) that $\delta^2\mathcal{L}(h)$ represents the linearized operator $(\mathcal{G}_{1h}, \mathcal{G}_{2h})$ around the solution h. Moreover, $\delta^2\mathcal{L}(h)$ is a symmetric bilinear form on the space of all functions $k \in H^1(\overline{R})$ which are 2π-periodic and even in q and which satisfy $\int_{-\pi}^{\pi} k(q,0)dq = 0$ and $k(q,-1) = 0$. Therefore, it is justified to introduce the following definition.

Definition 1. *We say that h is formally stable if $\langle \delta^2\mathcal{L}(h)k, k\rangle \geq 0$ for all test functions k such that* (44)*,* (45) *and* (46) *hold.*

We will prove in the sequel that the laminar flow solutions, $\overline{h}(\cdot,\lambda)$, are formally stable for certain values of λ that will be made precise below. To this end, let

$$\overline{h}(p,\lambda) = \begin{cases} \overline{h}_1(p,\lambda), & p \in [-1,p_1], \\ \overline{h}_2(p,\lambda), & p \in [p_1,p_2], \\ \overline{h}_3(p,\lambda), & p \in [p_2,0], \end{cases}$$

denote a laminar solution. Therefore, $\overline{h}$ satisfies the system

$$\begin{cases} \overline{h}_{1pp} = 0, & p \in (-1, p_1), \\ \overline{h}_{2pp} = -\dfrac{d^2\gamma(p)}{p_0}(\overline{h}_{2p}+1)^3, & p \in (p_1, p_2), \\ \overline{h}_{3pp} = 0, & p \in (p_2, 0), \\ \overline{h}_1 = 0, & p = -1, \\ \dfrac{1}{d^2} + \dfrac{(\overline{h}_{3p}+1)^2}{p_0^2}\Big(2gd(\overline{h}_3+1) - Q\Big) = 0, & p = 0, \\ \overline{h}_1(p_1) = \overline{h}_2(p_1), \\ \overline{h}_2(p_2) = \overline{h}_3(p_2), \\ \overline{h}_{1p}(p_1) = \overline{h}_{2p}(p_1), \\ \overline{h}_{2p}(p_2) = \overline{h}_{3p}(p_2). \end{cases} \tag{49}$$

The family of solutions of the system (49) is given by

$$\begin{aligned} \overline{h}_1(p) = \overline{h}_1(p,\lambda) &= \int_{-1}^{p} \frac{ds}{\sqrt{\Gamma(s)+\lambda}} - (p+1), \quad p \in [-1, p_1], \\ \overline{h}_2(p) = \overline{h}_2(p,\lambda) &= \int_{-1}^{p} \frac{ds}{\sqrt{\Gamma(s)+\lambda}} - (p+1), \quad p \in [p_1, p_2], \\ \overline{h}_3(p) = \overline{h}_3(p,\lambda) &= \int_{-1}^{p} \frac{ds}{\sqrt{\Gamma(s)+\lambda}} - (p+1), \quad p \in [p_2, 0], \end{aligned}$$

with $Q > \lambda > -\Gamma_{min}$ and

$$Q = Q(\lambda) = 2gd\int_{-1}^{0} \frac{ds}{\sqrt{\lambda+\Gamma(s)}} + \frac{p_0^2}{d^2}\lambda, \tag{50}$$

where the parameter λ is related to the speed at the flat surface by the relation

$$\sqrt{\lambda} = \frac{1}{\overline{h}_{3p}(0)+1} = \frac{d(u-c)}{p_0}\bigg|_{y=0}.$$

We state now (and subsequently we prove) the main result of this section.

Theorem. *The laminar solutions $\overline{h}(\cdot,\lambda)$ are formally stable if and only if $\lambda \geq \lambda^*$, where λ^* is the certain value for which local bifurcation occurs, cf. the results in Section 4.*

Proof. A routine computation reveals that

$$\mathcal{G}_{1h}(\overline{h})l = \lim_{\varepsilon\to\infty} \frac{\mathcal{G}_1(\overline{h}+\varepsilon l) - \mathcal{G}_1(\overline{h})}{\varepsilon} = \frac{1}{d^2}l_{pp} + l_{qq}(1+\overline{h}_p)^2 + 3\frac{\gamma(p)}{p_0}(1+\overline{h}_p)^2 l_p,$$

and

$$\mathcal{G}_{2h_3}(\overline{h}_3, Q)l_3 = \frac{2(1+\overline{h}_{3p})l_{3p}}{p_0^2}[2gd(\overline{h}_3+1) - Q] + \frac{2(1+\overline{h}_{3p})^2}{p_0^2}gdl_3,$$

where the function

$$l(q,p) := \begin{cases} l_1(q,p), & (q,p) \in [0,L] \times [-1,p_1], \\ l_2(q,p), & (q,p) \in [0,L] \times [p_1,p_2], \\ l_3(q,p), & (q,p) \in [0,L] \times [p_2,0], \end{cases}$$

satisfies (44), (45) and (46). This enables us to find the second variation of the functional $\mathcal{L}$ in $\overline{h}$ as

$$\begin{aligned} \left\langle \delta^2 \mathcal{L}(\overline{h})k, k \right\rangle = &- \iint_R \left[\frac{1}{d^2(1+\overline{h}_p)^3} k k_{pp} + \frac{1}{1+\overline{h}_p} k k_{qq} + 3\frac{\gamma(p)}{p_0(1+\overline{h}_p)} k k_p \right] dqdp \\ &- \frac{1}{2}\int_{p=0} \left[2\frac{gd}{p_0^2}k_3^2 + 2\frac{1}{p_0^2(1+\overline{h}_{3p})} \left[2gd(\overline{h}_3+1) - Q \right] k_3 k_{3p} \right] dq. \end{aligned}$$

Using integration by parts and the matching conditions from (49), satisfied by $\overline{h}_1, \overline{h}_2, \overline{h}_3$ across the interfaces $p = p_1$ and $p = p_2$, we have

$$\int_{-1}^{0} \frac{1}{d^2(1+\overline{h}_p)^3} k k_{pp} dp = \frac{k_3 k_{3p}}{d^2(1+\overline{h}_{3p})^3}\bigg|_{p=0} - \int_{-1}^{0} \frac{k_p^2}{d^2(1+\overline{h}_p)^3} dp + 3\int_{-1}^{0} \frac{k k_p \overline{h}_{pp}}{d^2(1+\overline{h}_p)^4} dp.$$

From the system of equations (49) we know

$$\overline{h}_{pp} = -\frac{d^2\gamma(p)}{p_0}(\overline{h}_p + 1)^3, \tag{51}$$

where $\gamma(p) = 0$ for $p \in [-1, p_1] \cup [p_2, 0]$ and $\gamma(p) \neq 0$ for $p \in [p_1, p_2]$. By (51) we have

$$3\int_{-1}^{0} \frac{k k_p \overline{h}_{pp}}{d^2(1+\overline{h}_p)^4} dp = -3\int_{-1}^{0} \frac{\gamma(p) k k_p}{p_0(1+\overline{h}_p)} dp.$$

Additionally, from (50) we use

$$Q - 2gd(\overline{h}_3(0)+1) = \frac{p_0^2}{d^2(1+\overline{h}_{3p}(0))^2},$$

to infer that

$$\left\langle \delta^2 \mathcal{L}(\overline{h})k, k \right\rangle = - \iint_R \left[\frac{k k_{qq}}{1+\overline{h}_p} - \frac{k_p^2}{d^2(1+\overline{h}_p)^3} \right] dqdp - \int_0^L \frac{gd}{p_0^2} k_3^2(q,0) dq.$$

Next we consider the Fourier series expansion of k

$$k(q,p) = \sum_{n=0}^{\infty} k_n(p) \cos\left(\frac{2\pi n q}{L}\right),$$

where

$$k_n(p) := \begin{cases} k_{1n}(p), & p \in [-1, p_1], \\ k_{2n}(p), & p \in [p_1, p_2], \\ k_{3n}(p), & p \in [p_2, 0], \end{cases}$$

satisfy

$$\begin{array}{lll} k_{1n}(p_1) = k_{2n}(p_1), & k_{2n}(p_2) = k_{3n}(p_2), & k_{30}(0) = 0, \\ \frac{\partial k_{1n}}{\partial p}(p_1) = \frac{\partial k_{2n}}{\partial p}(p_1), & \frac{\partial k_{2n}}{\partial p}(p_2) = \frac{\partial k_{3n}}{\partial p}(p_2). & \end{array}$$

The condition $k_{30}(0) = 0$ arises from (46). Then we obtain that the second variation of $\mathcal{L}$ is given as

$$\begin{aligned} \left\langle \delta^2 \mathcal{L}(\overline{h})k, k \right\rangle = L \left[\int_{-1}^{0} \frac{k_0'^2(p)}{d^2(1+\overline{h}_p)^3} dp - \frac{gd}{p_0^2} k_{30}^2(0) \right] \\ + \frac{L}{2} \sum_{n=1}^{\infty} \left[\int_{-1}^{0} \left(\frac{k_n'^2(p)}{d^2(1+\overline{h}_p)^3} + \left(\frac{2\pi n}{L}\right)^2 \frac{k_n^2(p)}{1+\overline{h}_p} \right) dp - \frac{gd}{p_0^2} k_n^2(0) \right]. \end{aligned}$$

Therefore, the necessary and sufficient condition for the second variation of the functional $\mathcal{L}$ to be non-negative is

$$\int_{-1}^{0} \left(\frac{k_n'^2(p)}{d^2(1+\overline{h}_p)^3} + \left(\frac{2\pi n}{L}\right)^2 \frac{k_n^2(p)}{1+\overline{h}_p} \right) dp \geq \frac{gd}{p_0^2} k_n^2(0).$$

On the other hand we know from section 3 of [76] that

$$\inf_k \frac{-gd^3 k^2(0) + p_0^2 \int_{-1}^{0} a^3 (k')^2(p) dp}{p_0^2 d^2 \int_{-1}^{0} a k^2(p) dp} \geq -\left(\frac{2\pi}{L}\right)^2 \text{ if and only if } \lambda \geq \lambda^*,$$

where $a = \frac{1}{1+\overline{h}_p}$. The above characterization yields that the second variation of the functional $\mathcal{L}$ in $\overline{h}$, $\left\langle \delta^2 \mathcal{L}(\overline{h}) l, k \right\rangle$, is non-negative and the laminar solution $\overline{h}(\cdot, \lambda)$ is formally stable if and only if $\lambda \geq \lambda^*$. The latter finishes the proof. □

Conclusion

The thesis presents research on explicit and exact solutions of the nonlinear Euler equations together with a study of small-amplitude gravity waves. The exact solutions serve as a window to a more complete understanding of geophysical flows occurring on Earth. They generalise to some extent the famous and remarkable solutions derived by Gerstner and Pollard and the complicated extension of these solutions describe three-dimensional waves. With the increase in structural complexity of the geophysical governing equations, it is startling that such exact and explicit solutions exist at all.

This thesis outlines that exact and explicit solutions, besides being mathematically elegant, have also proven to be surprisingly adaptable in modelling a variety of physical scenarios. In particular, in this thesis, these solutions prescribe surface and internal water waves in the equatorial region and internal water waves at an arbitrary latitude. A model of surface water waves in presence of an underlying zonal current and variable meridional current was analysed. Subsequently, a nonhydrostatic model of internal water waves was constructed to describe the oscillation of a thermocline. Both of the solutions derived in these models are Gerstner-like and are applicable in the vicinity of the equator. Consequently, a hydrostatic and nonhydrostatic model at an arbitrary latitude were presented to prescribe internal wave motion outside the equatorial region. Apart from the geophysical models, a model of small-amplitude surface gravity wave is introduced with discontinuous vorticity and an analysis of this scenario in fact describe the wave-current interactions.

In each model a dispersion relation arises as a product of proving the validity of the solutions. The dispersion relation is rich in information describing the resultant flow and gives the phase speed of the wave for fixed physical parameters, which is important as it provides a valuable insight into the physical properties of the wave. We showed that in the model describing equatorial waves the dispersion relation takes the form of a quadratic equation and is dependent on various geophysical variables, in particular the Coriolis force and an underlying current. Moreover, by taking a different type of approximation, a limitation in the number of roots of the dispersion relation is forced. In contrast to that, the dispersion relation in the Pollard-like solution after a non-dimensional change of variables is a polynomial of at least fourth order. Given the order of the polynomial it has only two roots representing standard internal gravity waves in the hydrostatic model. In the nonhydrostatic model a simple inclusion of the transitional layer allows for the existence of an additional root representing a new type of a slow wave mode called an inertial Gerstner wave. The existence of small-amplitude gravity waves in the presence of an isolated layer of constant non-zero vorticity was proved by showing that the dispersion relation has a unique positive solution. The dispersion relation in this case takes the form of a complicated polynomial of fourth order. The solution is showed in separate cases of positive and negative vorticity. The bifurcation parameter representing the

small-amplitude waves is proved to exist always for positive vorticity and it exist under certain conditions for negative vorticity.

The prescription of the explicit solution in terms of Lagrangian labelling variables allowed for a detailed study of the intricate underlying physical flow properties induced by the nonlinear waves. The analysis showed that currents play a major role in the dynamics of fluid motion and the magnitude of mean velocities and the mass transport is undoubtedly and greatly influenced by the underlying current. However, in the case of vanishing currents and in the case of Pollard-like internal water waves net wave mass transport over a wave period is equal to zero, which is a result of the periodicity of the solution.

Future work

In regards to future work, although these solutions of the geophysical governing equations have a quite rigid mathematical description, they have the potential to generate more solutions. The solutions are exact and explicit, therefore a composition and further generalisation of these solutions may represent new physically compound flows. The solutions presented as a part of this thesis still require detailed attention in terms of global dynamics and a stability analysis indicating future work to be done. The Pollard-like internal wave solution in the nonhydrostatic model still can be studied in order to consider the physical flow properties, which is undoubtedly a complicated endeavour given the transitional layer introduced in the model. The presence of currents in the ocean is well-documented, therefore it is justified to extend the Pollard-like internal water wave by the admission of an underlying current. As the complexity of the dispersion relation increases when new layers in the model are introduced, we predict that the inclusion of a current may lead to a polynomial representing the dispersion relation of order higher than sixth with a potential to generate new types of waves. Pollard-like surface waves also require some attention as the physical flow properties have not been investigated in this case yet. Moreover, a latitudinally-trapped Pollard-like solution would be a valuable achievement in the description of the ocean dynamics. In addition to that, a linear Lagrangian theory can be employed in order to find a linear solution in spirit of Pollard solution as it is still unexplored area of the geophysical governing equations, which can be subsequently compared with a well-established Eulerian theory. Moreover, the limiting case of solutions with peaks in the crest of an inverted trochoid representing a surface wave can be analyzed. This peculiar phenomenon is lost in the classical approximation of the governing equations. A similar analysis can be employed for internal water waves, but this time investigating the peaks in the trough of the waves, which have a trochoidal shape. In spite of the special character of the Gerstner and Pollard solution, they present features of general interest and certain values that are in reasonable agreement with experiments.

Bibliography

[1] G. K. Batchelor. *An Introduction to Fluid Dynamics*. Cambridge University Press, Cambridge, UK, 1967.

[2] A. Bennett. *Lagrangian Fluid Dynamics*. Cambridge Monographs on Mechanics. Cambridge University Press, Cambridge, UK, 2006.

[3] J. P. Boyd. *Dynamics of the Equatorial Ocean*. Springer-Verlag Berlin Heidelberg, Berlin, Germany, 2018.

[4] A. Constantin. Edge waves along a sloping beach. *Journal of Physics A: Mathematical and General*, 34:9723–9731, 2001.

[5] A. Constantin. On the deep water wave motion. *Journal of Physics A: Mathematical and General*, 34:1405–1417, 2001.

[6] A. Constantin. The trajectories of particles in Stokes waves. *Inventiones Mathematicae*, 166:523–535, 2006.

[7] A. Constantin. *Nonlinear Water Waves with Applications to Wave-Current Interactions and Tsunamis*, volume 81. Society for Industrial and Applied Mathematics, Philadelphia, USA, 2011. CBMS-NSF Regional Conference Series in Applied Mathematics.

[8] A. Constantin. Dispersion relations for periodic traveling water waves in flows with discontinuous vorticity. *Communications on Pure & Applied Analysis*, 11:1397–1406, 2012.

[9] A. Constantin. An exact solution for equatorially trapped waves. *Journal of Geophysical Research: Oceans*, 117:1–8, 2012.

[10] A. Constantin. On the modelling of equatorial waves. *Geophysical Research Letters*, 39:1–4, 2012.

[11] A. Constantin. Particle trajectories in extreme Stokes waves. *IMA Journal of Applied Mathematics*, 77:293–307, 2012.

[12] A. Constantin. Some three-dimensional nonlinear equatorial flows. *Journal of Physical Oceanography*, 43:165–175, 2013.

[13] A. Constantin. Some nonlinear, equatorially trapped, nonhydrostatic internal geophysical waves. *Journal of Physical Oceanography*, 44:781–789, 2014.

[14] A. Constantin, M. Ehrnström, and G. Villari. Particle trajectories in linear deep-water waves. *Nonlinear Analysis: Real World Applications*, 9(4):1336–1344, 2008.

[15] A. Constantin, M. Ehrnström, and E. Wahlén. Symmetry of steady periodic gravity water waves with vorticity. *Duke Mathematical Journal*, 140:591–603, 2007.

[16] A. Constantin and J. Escher. Symmetry of steady deep-water waves with vorticity. *European Journal of Applied Mathematics*, 15:755—-768, 2004.

[17] A. Constantin and J. Escher. Symmetry of steady periodic surface water waves with vorticity. *Journal of Fluid Mechanics*, 498:171—181, 2004.

[18] A. Constantin and J. Escher. Analyticity of periodic traveling free surface water waves with vorticity. *Annals of Mathematics*, 173:559–568, 2011.

[19] A. Constantin and P. Germain. Instability of some equatorially trapped waves. *Journal of Geophysical Research: Oceans*, 118:2802–2810, 2013.

[20] A. Constantin and R. I. Ivanov. A Hamiltonian approach to wave-current interactions in two-layer fluids. *Physics of Fluids*, 27:1–8, 2015.

[21] A. Constantin, R. I. Ivanov, and C.-I. Martin. Hamiltonian formulation for wave-current interactions in stratified rotational flows. *Archive for Rational Mechanics and Analysis*, 221:1417–1447, 2016.

[22] A. Constantin, R. I. Ivanov, and E. M. Prodanov. Nearly-Hamiltonian structure for water waves with constant vorticity. *Journal of Mathematical Fluid Mechanics*, 10:224–237, 2008.

[23] A. Constantin and R. S. Johnson. The dynamics of waves interacting with the Equatorial Undercurrent. *Geophysical & Anstrophysical Fluid Dynamics*, 109:311–358, 2015.

[24] A. Constantin and R. S. Johnson. Current and future prospects for the application of systematic theoretical methods to the study of problems in physical oceanography. *Physics Letters, Section A: General, Atomic and Solid State Physics*, 380:3007–3012, 2016.

[25] A. Constantin and R. S. Johnson. An exact, steady, purely azimuthal equatorial flow with a free surface. *Journal of Physical Oceanography*, 46:1935–1945, 2016.

[26] A. Constantin and R. S. Johnson. An exact, steady, purely azimuthal flow as a model for the Antarctic Circumpolar Current. *Journal of Physical Oceanography*, 46:3585–3594, 2016.

[27] A. Constantin and R. S. Johnson. A nonlinear, three-dimensional model for ocean flows, motivated by some observations of the Pacific Equatorial Undercurrent and thermocline. *Physics of Fluids*, 29:1–21, 2017.

[28] A. Constantin and R. S. Johnson. Steady large-scale ocean flows in spherical coordinates. *Oceanography*, 31:42–50, 2018.

[29] A. Constantin and E. Kartashova. Effect of non-zero constant vorticity on the nonlinear resonances of capillary water waves. *EPL (Europhysics Letters)*, 86:1–6, 2009.

[30] A. Constantin and S. G. Monismith. Gerstner waves in the presence of mean currents and rotation. *Journal of Fluid Mechanics*, 820:511–528, 2017.

[31] A. Constantin, D. Sattinger, and W. A. Strauss. Variational formulations for steady water waves with vorticity. *Journal of Fluid Mechanics*, 548:151–163, 2006.

[32] A. Constantin, W. Strauss, and E. Vărvărucă. Global bifurcation of steady gravity water waves with critical layers. *Acta Mathematica*, 217:195—-262, 2014.

[33] A. Constantin and W. A. Strauss. Exact steady periodic water waves with vorticity. *Communications on Pure and Applied Mathematics*, 57:481–527, 2004.

[34] A. Constantin and W. A. Strauss. Stability properties of steady water waves with vorticity. *Communications on Pure and Applied Mathematics*, 60:911–950, 2007.

[35] A. Constantin and W. A. Strauss. Pressure beneath a Stokes wave. *Communications on Pure and Applied Mathematics*, 63:533–557, 2009.

[36] A. Constantin and W. A. Strauss. Periodic traveling gravity water waves with discontinuous vorticity. *Rational Mechanics and Analysis*, 202:133–175, 2011.

[37] A. Constantin and E. Vărvărucă. Steady periodic water waves with constant vorticity: regularity and local bifurcation. *Archive for Rational Mechanics and Analysis*, 199:33–67, 2011.

[38] T. Cromwell. Circulation in a meridional plane in the central equatorial Pacific. *Journal of Marine Research*, 12:196–213, 1953.

[39] B. Cushman-Roisin and J.-M. Becker. *Introduction to Geophysical Fluid Dynamics. Physcial and Numerical Aspects*. Academic Press, Waltham, USA, 2011.

[40] M.-L. Dubreil-Jacotin. Sur les ondes de type permanent dans les liquides hétérogenes. *Atti della Accademia nazionale dei Lincei*, 15:814—-819, 1932.

[41] M. Ehrnström, J. Escher, and E. Wahlén. Steady water waves with multiple critical layers. *SIAM Journal on Mathematical Analysis*, 43:1436–1456, 2011.

[42] J. Escher. Regularity of rotational travelling water waves. *Philosophical Transactions of the Royal Society of London A: Mathematical, Physical and Engineering Sciences*, 370:1602–1615, 2012.

[43] J. Escher, A.-V. Matioc, and B.-V. Matioc. On stratified steady periodic water waves with linear density distribution and stagnation points. *Journal of Differential Equations*, 251:2932–2949, 2011.

[44] J. Escher and B.-V. Matioc. On the analyticity of periodic gravity water waves with integrable vorticity function. *Differential Integral Equations*, 27:217–232, 2013.

[45] L. Euler. Principes généraux du mouvement des fluides. *Mémoires de l'académie des sciences de Berlin*, 11:274—315, 1757.

[46] L. Fan, H. Gao, and Q. Xiao. An exact solution for geophysical trapped waves in the presence of an underlying current. *Dynamics of Partial Differential Equations*, 15:201–214, 2018.

[47] A. V. Fedorov and J. Brown. Equatorial waves. In J. E. Steel, S. A. Thorpe, and K. K. Turekian, editors, *Encyclopedia of Ocean Sciences*, volume 2, pages 271–287. Academic Press, London, UK, 2009.

[48] I. Gallagher and L. Saint-Raymond. On the influence of the Earth's rotation on Geophysical Flows. In S. Friedlander and D. Serre, editors, *Handbook of Mathematical Fluid Dynamics*, volume 4, pages 201–329. North-Holland, 2007.

[49] T. Garrison and R. Ellis. *Oceanography: An Invitation to Marine Science*. Cengage Learning, Boston, USA, 2014.

[50] F. Genoud and D. Henry. Instability of equatorial water waves with an underlying current. *Journal of Mathematical Fluid Mechanics*, 16:661–667, 2014.

[51] M. Giaquinta and S. Hildebrandt. *Calculus of Variations I.* Springer-Verlag Berlin Heidelberg, New York, USA, 2004.

[52] D. Gilbarg and N. S. Trudinger. *Elliptic partial differential equations of the second order, Second edition.* Springer-Verlag Berlin Heidelberg, Berlin, Germany, 2001.

[53] A. E. Gill. *Atmosphere-Ocean Dynamics.* Academic Press, San Diego, USA, 1982.

[54] D. Henry. On Gerstner's water wave. *Journal of Nonlinear Mathematical Physics*, 15:87–95, 2008.

[55] D. Henry. On the deep-water Stokes wave flow. *International Mathematics Research Notices*, 2008:1–7, 2008.

[56] D. Henry. Analyticity of the streamlines for periodic travelling free surface capillary-gravity water waves with vorticity. *SIAM Journal on Mathematical Analysis*, 42:3103–3111, 2010.

[57] D. Henry. Dispersion relations for steady periodic water waves of fixed mean-depth with an isolated bottom vorticity layer. *Journal of Nonlinear Mathematical Physics*, 19:58–71, 2012.

[58] D. Henry. Regularity for steady periodic capillary water waves with vorticity. *Philosophical Transactions of the Royal Society of London A: Mathematical, Physical and Engineering Sciences*, 370:1616–1628, 2012.

[59] D. Henry. Dispersion relations for steady periodic water waves with an isolated layer of vorticity at the surface. *Nonlinear Analysis: Real World Applications*, 14:1034–1043, 2013.

[60] D. Henry. An exact solution for equatorial geophysical water waves with an underlying current. *European Journal of Mechanics, B/Fluids*, 38:18–21, 2013.

[61] D. Henry. Large amplitude steady periodic waves for fixed-depth rotational flows. *Communications in Partial Differential Equations*, 38:1015–1037, 2013.

[62] D. Henry. Steady periodic waves bifurcating for fixed-depth rotational flows. *Quarterly of Applied Mathematics*, 71:455–487, 2013.

[63] D. Henry. Internal equatorial water waves in the f-plane. *Journal of Nonlinear Mathematical Physics*, 22:499–506, 2015.

[64] D. Henry. Equatorially trapped nonlinear water waves in a β-plane approximation with centripetal forces. *Journal of Fluid Mechanics*, 804:1–11, 2016.

[65] D. Henry. Exact equatorial water waves in the f-plane. *Nonlinear Analysis: Real World Applications*, 28:284–289, 2016.

[66] D. Henry. On three-dimensional Gerstner-like equatorial water waves. *Phylosophical Transactions of the Royal Society of London A: Mathematical, Physical and Engineering Sciences*, 376:1–16, 2017.

[67] D. Henry and H. C. Hsu. Instability of equatorial water waves in the f-plane. *Discrete & Continuous Dynamical Systems - A*, 35:909–916, 2015.

[68] D. Henry and H. C. Hsu. Instability of internal equatorial water waves. *Journal of Differential Equations*, 258:1015–1024, 2015.

[69] D. Henry, C.-I. Martin, and S. Sastre-Gómez. Large amplitude steady periodic water waves for fixed-depth flows with discontinuous vorticity. *submitted*.

[70] D. Henry and A.-V. Matioc. Global bifurcation of capillary–gravity-stratified water waves. *Proceedings of the Royal Society of Edinburgh: Section A Mathematics*, 144:775—-786, 2014.

[71] D. Henry and A.-V. Matioc. On the symmetry of steady equatorial wind waves. *Nonlinear Analysis: Real World Applications*, 18:50–56, 2014.

[72] D. Henry and B.-V. Matioc. On the regularity of steady periodic stratified water waves. *Communications on Pure & Applied Analysis*, 11:1453–1464, 2012.

[73] D. Henry and B.-V. Matioc. On the existence of steady periodic capillary-gravity stratified water waves. *Annali della Scuola Normale Superiore di Pisa*, 12:955–974, 2013.

[74] D. Henry and B.-V. Matioc. Aspects of the mathematical analysis of nonlinear stratified water waves. In J. Escher, E. Schrohe, and J. Seiler, editors, *Elliptic and Parabolic Equations*. Springer International Publishing, 2015.

[75] D. Henry and S. Sastre-Gómez. Mean flow velocities and mass transport for equatorially-trapped water waves with an underlying current. *Journal of Mathematical Fluid Mechanics*, 18:795–804, 2016.

[76] D. Henry and S. Sastre-Gómez. Steady periodic water waves bifurcating for fixed-depth rotational flows with discontinuous vorticity. *Differential Integral Equations*, 31:1–26, 2018.

[77] H.-C. Hsu. An exact solution for nonlinear internal equatorial waves in the f-plane approximation. *Journal of Mathematical Fluid Mechanics*, 16:463–471, 2014.

[78] H.-C. Hsu. Some nonlinear internal equatorial flows. *Nonlinear Analysis: Real World Applications*, 18:69–74, 2014.

[79] H.-C. Hsu. Some nonlinear internal equatorial waves with a strong underlying current. *Applied Mathematics Letters*, 34:1–6, 2014.

[80] H.-C. Hsu. An exact solution for equatorial waves. *Monatshefte für Mathematik*, 176:143–152, 2015.

[81] D. Ionescu-Kruse. An exact solution for geophysical edge waves in the f-plane approximation. *Nonlinear Analysis: Real World Applications*, 24:190–195, 2015.

[82] D. Ionescu-Kruse. On Pollard's wave solution at the equator. *Journal of Nonlinear Mathematical Physics*, 22:523–530, 2015.

[83] D. Ionescu-Kruse. Instability of Pollard's exact solution for geophysical ocean flows. *Physics of Fluids*, 28:1–10, 2016.

[84] D. Ionescu-Kruse. On the short-wavelength stabilities of some geophysical flows. *Phylosophical Transactions of the Royal Society of London A: Mathematical, Physical and Engineering Sciences*, 376:1–21, 2017.

[85] D. Ionescu-Kruse. A three-dimensional autonomous nonlinear dynamical system modelling equatorial ocean flows. *Journal of Differential Equations*, 264(7):4650–4668, 2018.

[86] D. Ionescu-Kruse and C.-I. Martin. Periodic equatorial water flows from a Hamiltonian perspective. *Journal of Differential Equations*, 262:4451–4474, 2017.

[87] T. Izumo. The equatorial undercurrent, meridional overturning circulation, and their roles in mass and heat exchanges during El Niño events in the tropical Pacific ocean. *Ocean Dynamics*, 55:110–123, 2005.

[88] G. C. Johnson, M. J. McPhaden, and E. Firing. Equatorial pacific ocean horizontal velocity, divergence, and upwelling*. *Journal of Physical Oceanography*, 31:839–849, 2001.

[89] R. S. Johnson. *A Modern Introduction to the Mathematical Theory of Water Waves*. Cambridge University Press, Cambridge, UK, 1997.

[90] R. S. Johnson. Application of the ideas and techniques of classical fluid mechanics to some problems in physical oceanography. *Phylosophical Transactions of the Royal Society of London A: Mathematical, Physical and Engineering Sciences*, 376:1–19, 2017.

[91] I. G. Jonsson. Wave-current interactions. In B. Le Méhauté and D. M. Hanes, editors, *The Sea: Ocean Engineering Science*, volume 9, pages 65–120. Wiley, 1990.

[92] P. Karageorgis. Dispersion relation for water waves with non-constant vorticity. *European Journal of Mechanics, B/Fluids*, 34:7–12, 2012.

[93] W. S. Kessler and M. J. McPhaden. Oceanic equatorial waves and the 1991-93 El Niño. *Journal of Climate*, 8:1757–1774, 1995.

[94] B. Kinsman. *Wind Waves: Their Generation and Propagation on the Ocean Surface*. Dover Publications, Mineola, New York, USA, 2002.

[95] M. Kluczek. Exact and explicit internal equatorial water waves with underlying currents. *Journal of Mathematical Fluid Mechanics*, 19:305–314, 2017.

[96] M. Kluczek. Equatorial water waves with underlying currents in the f-plane approximation. *Applicable Analysis*, 97:1867–1880, 2018.

[97] M. Kluczek. Exact Pollard-like internal water waves. *Journal of Nonlinear Mathematical Physics*, 26:133–146, 2019.

[98] V. Kozlov, N. Kuznetsov, and E. Lokharu. Steady water waves with vorticity: An analysis of the dispersion equation. *Journal of Fluid Mechanics*, 751:1–13, 2014.

[99] J. Lighthill. *Waves in Fluids*. Cambridge University Press, Cambridge, UK, 1978.

[100] M. S. Longuet-Higgins. Mass transport in water waves. *Phylosophical Transactions of the Royal Society of London A: : Mathematical, Physical and Engineering Sciences*, 245:535–581, 1953.

[101] M. S. Longuet-Higgins. On the transport of mass by time-varying ocean currents. *Deep-Sea Research*, 16:431–447, 1969.

[102] J. R. Luyten and J. C. Swallow. Equatorial undercurrents. *Deep-Sea Research*, 23:999–1001, 1976.

[103] C.-I. Martin. Dispersion relations for periodic water waves with surface tension and discontinuous vorticity. *Discrete & Continuous Dynamical Systems - A*, 34:3109–3123, 2014.

[104] C.-I. Martin. Dispersion relations for rotational gravity water flows having two jumps in the vorticity distribution. *Journal of Mathematical Analysis and Applications*, 418:595–611, 2014.

[105] C.-I. Martin. Dispersion relations for gravity water flows with two rotational layers. *European Journal of Mechanics, B/Fluids*, 50:9–18, 2015.

[106] C.-I. Martin. On the existence of free-surface azimuthal equatorial flows. *Applicable Analysis*, 96:1207–1214, 2017.

[107] C.-I. Martin. Resonant interactions of capillary-gravity water waves. *Journal of Mathematical Fluid Mechanics*, 19:807–817, 2017.

[108] C.-I. Martin. Surface tension effects in the equatorial ocean dynamics. *Monatshefte für Mathematik*, 182:675–682, 2017.

[109] C.-I. Martin. On periodic geophysical water flows with discontinuous vorticity in the equatorial f-plane approximation. *Philosophical Transactions of the Royal Society of London A: Mathematical, Physical and Engineering Sciences*, 376, 2018.

[110] C.-I. Martin. On the vorticity in mesoscale ocean currents. *Oceanography*, 31:28–35, 2018.

[111] C.-I. Martin and B.-V. Matioc. Existence of capillary-gravity water waves with piecewise constant vorticity. *Journal of Differential Equations*, 256:3086–3114, 2014.

[112] C.-I. Martin and B.-V. Matioc. Gravity water flows with discontinuous vorticity and stagnation points. *Communications in Mathematical Sciences*, 14:415–441, 2015.

[113] C.-I. Martin and A. Rodríguez-Sanjurjo. Dispersion relations for steady periodic water wavec of fixed mean-depth with two rotational layer. *Discrete & Continuous Dynamical Systems, accepted.*

[114] A.-V. Matioc. An exact solution for geophysical equatorial edge waves over a sloping beach. *Journal of Physics A: Mathematical and Theoretical*, 45:1–10, 2012.

[115] A.-V. Matioc. Exact geophysical waves in stratified fluids. *Applicable Analysis*, 92:2254–2261, 2013.

[116] A.-V. Matioc and B.-V. Matioc. On the symmetry of periodic gravity water waves with vorticity. *Differential Integral Equations*, 26:129–140, 2013.

[117] S. G. Monismith, E. A. Cowen, H. M. Nepf, J. Magnaudet, and L. Thais. Laboratory observations of mean flows under surface gravity waves. *Journal of Fluid Mechanics*, 573:131–147, 2018.

[118] J. N. Moum, J. D. Nash, and W. D. Smyth. Narrowband oscillations in the upper equatorial ocean. Part I: Interpretation as shear instabilities. *Journal of Physical Oceanography*, 41:397–411, 2011.

[119] A. Nachbin and R. Ribeiro-Junior. Capturing the flow beneath water waves. *Philosophical Transactions of the Royal Society of London A: Mathematical, Physical and Engineering Sciences*, 376:1–17, 2018.

[120] J. Pedlosky. *Geophysical Fluid Dynamics*. Springer-Verlag Berlin Heidelberg, Virginia, USA, 1987.

[121] R. T. Pollard. Surface waves with rotation: An exact solution. *Journal of Geophysical Research*, 75:15–32, 1970.

[122] M. C. Potter, D. C. Wiggert, and B. H. Ramadan. *Mechanics of Fluids*. Cengage Learning, Stamford, USA, 2012.

[123] V. V. Prasolov. *Polynomials*. Springer-Verlag Berlin Heidelberg, Berlin, Germany, 2004.

[124] W. J. M. Rankine. On the exact form of waves near the surface of deep water. *Philosophical Transactions of the Royal Society of London*, 153:127–138, 1863.

[125] A. Rodríguez-Sanjurjo. Global diffeomorphism of the Lagrangian flow-map for equatorially-trapped internal water waves. *Nonlinear Analysis*, 149:156–164, 2017.

[126] A. Rodríguez-Sanjurjo. Global diffeomorphism of the Lagrangian flow-map for Pollard-like solutions. *Annali di Matematica Pura ed Applicata (1923–)*, 197:1787–1797, 2018.

[127] A. Rodríguez-Sanjurjo. Internal equatorial water waves and wave–current interactions in the f-plane. *Monatshefte für Mathematik*, 186:685–701, 2018.

[128] A. Rodríguez-Sanjurjo and M. Kluczek. Mean flow properties for equatorially trapped internal water wave–current interactions. *Applicable Analysis*, 96:2333–2345, 2017.

[129] S. Sastre-Gómez. Global diffeomorphism of the Lagrangian flow-map defining equatorially trapped water waves. *Nonlinear Analysis, Theory, Methods and Applications*, 125:725–731, 2015.

[130] S. Sastre-Gómez. Equivalent formulations for steady periodic water waves of fixed mean-depth with discontinuous vorticity. *Discrete & Continuous Dynamical Systems - A*, 37:2669–2680, 2017.

[131] G. G. Stokes. On the theory of oscillatory waves. In *Mathematical and Physical Papers*, pages 197—-229. Cambridge University Press, Cambridge, UK, 2009.

[132] R. Stuhlmeier. On edge waves in stratified water along a sloping beach. *Journal of Nonlinear Mathematical Physics*, 18:127–137, 2011.

[133] R. Stuhlmeier. Internal Gerstner waves: Applications to dead water. *Applicable Analysis*, 93:1451–1457, 2014.

[134] G. P. Thomas and G. Klopman. Wave-current interactions in the nearshore region. In J. N. Hunt, editor, *Gravity Waves in Water of Finite Depth, Computational Mechanics Publications*, pages 255–319. WIT, Southampton, UK, 1997.

[135] G. K. Vallis. *Atmospheric and Oceanic Fluid Dynamics: Fundamentals and Large-Scale Circulation*. Cambridge University Press, New York, USA, 2006.

[136] F. J. von Gerstner. Theorie der Wellen samt einer daraus abgeleiteten Theorie der Deichprofile. *Annalen der Physik*, 32:412–445, 1809.

[137] E. Wahlén. Steady water waves with a critical layer. *Journal of Differential Equations*, 246:2468–2483, 2009.

[138] S. Walsh. Stratified steady periodic water waves. *SIAM Journal on Mathematical Analysis*, 41:1054–1105, 2009.

[139] S. Walsh. Steady stratified periodic gravity waves with surface tension I: Local bifurcation. *Discrete & Continuous Dynamical Systems - A*, 34:3241–3285, 2014.

[140] J. E. H. Weber. Do we observe Gerstner waves in wave tank experiments? *Wave Motion*, 48:301–309, 2011.